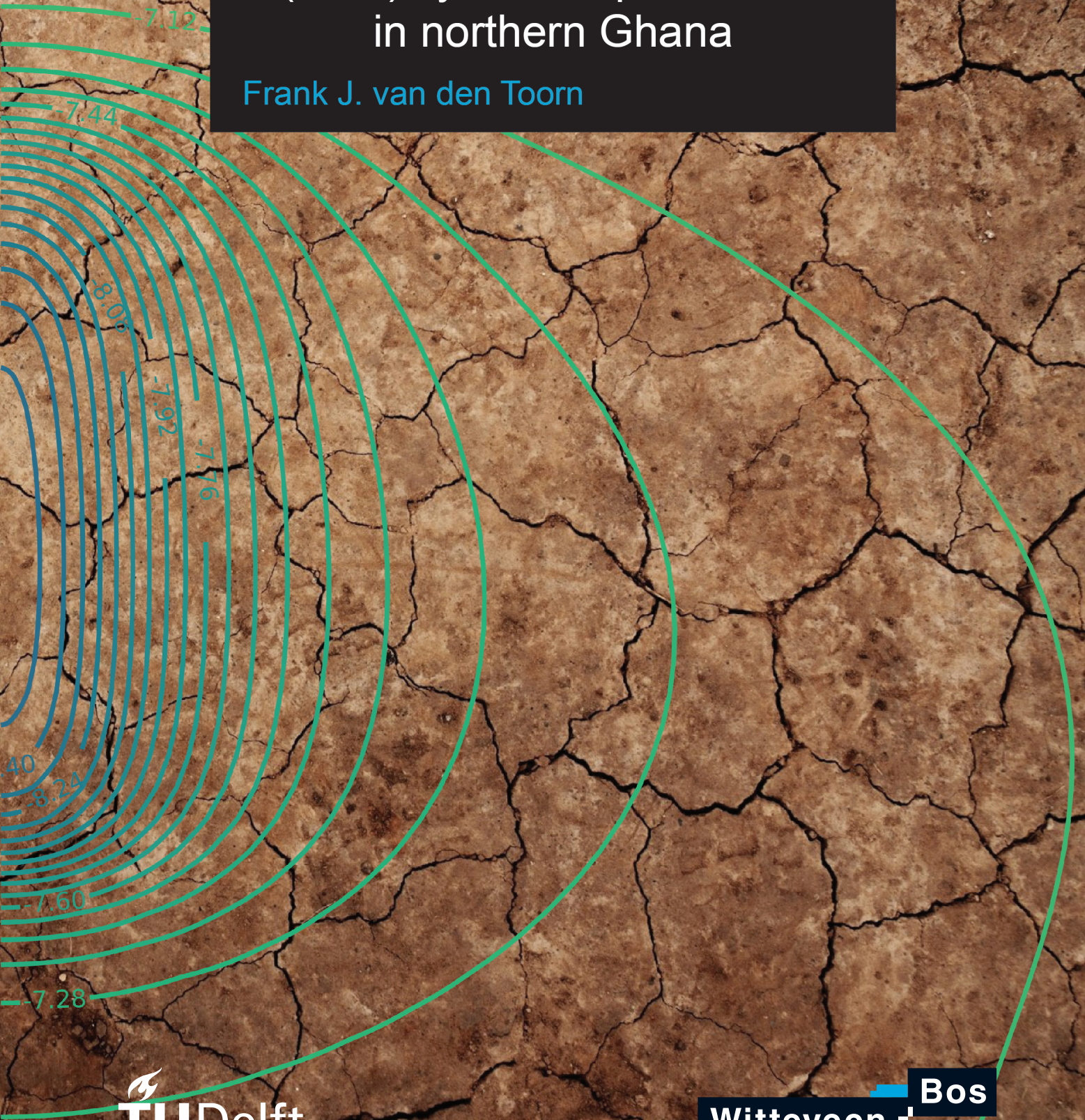


Aquifer Storage & Recovery (ASR) system improvement in northern Ghana

Frank J. van den Toorn



Aquifer Storage & Recovery (ASR) system improvement in northern Ghana

by

Frank J. van den Toorn

to obtain the degree of Master of Science
at the Delft University of Technology,
to be defended publicly on Friday September 7th, 2018 at 11:00 a.m.

Student number: 4179404
Project duration: September 18, 2017 – September 7, 2018
Thesis committee: Prof. dr. ir. M. Bakker, Delft University of Technology
Prof. dr. ir. N.C. van de Giesen, Delft University of Technology
Dr. ir. J.S. Timmermans, Delft University of Technology
Ir. D.A. Brakenhoff, Witteveen+Bos

An electronic version of this thesis is available at <http://repository.tudelft.nl/>.

Preface

This thesis represents the final product in becoming a Master of Science in Watermanagement at the Delft University of Technology - faculty of Civil Engineering and Geosciences. I would like to acknowledge all the people who contributed to my graduation. Some deserve special emphasis. First of all, I would like to thank the entire committee for assessing my thesis. Subsequently, I would like to give a word of gratitude to Witteveen+Bos - Herman Mondeel & David Brakenhoff - for the research facilities and daily supervision. And, last but not least, I owe Conservation Alliance (CA) - Paa Kofi Osei-Owusu - a special gratitude. Without the cooperation of CA, the geohydrological data collection within the northern Ghana local communities would not have been possible.

*Frank J. van den Toorn
Delft, September 2018*



Summary

The northern Ghana climatological conditions are favourable for agricultural production. The annual average precipitation of 800-1250 mm/y is theoretically sufficient for farmers to be year-round self-sufficient. However, the majority of precipitation falls in a 4-month wet season spanning from late May to October. As a consequence, the region is subjected to both seasonal flooding and long periods of drought. The dry season agriculture is of moderate intensity, takes place at small-scale and is groundwater dependent. In the near future it is not unthinkable that extraction exceeds natural recharge and groundwater withdrawal is no longer sustainable in the northern Ghana regions. The small-holder farmers' use of Aquifer Storage and Recovery (ASR) systems can potentially contribute to the continued sustainable use of groundwater in northern Ghana. An ASR system acts as a seasonal bridge. The system recharges flood water and extracts groundwater in periods of drought. A feasibility study on the sustainable use of an ASR system in northern Ghana has been performed by taking present conditions and multiple system improvements into account.

Aquifer tests are carried out at five study sites in northern Ghana to determine local geohydrological conditions. The TTim analytic element modelling environment is used to analyse the obtained groundwater drawdown data and derive parameters for subsurface characteristics. TTim allows for the inclusion of additional model parameters (e.g. borehole storage, well skin resistance and multiple model layers) and outperforms the analytic Theis method in this research. Although some uncertainties are present in the derived subsurface parameters, plausible values for transmissivity (T) and storativity (S) are suggested to be present in the ranges of respectively 1 to 100 (m^2/d) and $1\text{e-}3$ to $1\text{e-}2$ (-).

The year-round performance of a northern Ghana single ASR system is studied with a MODFLOW model. The potential types of ASR system improvements that are examined are (a) the extension of daily pumping time, (b) the enlargement of the borehole diameter, and (c) the reduction of the well skin resistance. The ASR systems sensitivities to changing environmental conditions are explored by (a) the degradation of well depth by clogging, (b) the shortening of the wet season inundation time, and (c) the reduction of the wet season inundation levels. Research results show that well maintenance is key for the performance of existing (and new) ASR systems. The recharge and discharge volumes can be improved by cleaning of the borehole depth and well screen. In the case of a new ASR system, the performance can positively be influenced by an enlargement of the borehole diameter. Furthermore, the construction of a proper permeable well skin (screen and gravel-pack around the well) can also result in increased system capacities. Despite the imposed options of system modifications, the geographic position of an ASR system remains of utmost importance for system performance. The construction of an ASR system at a location sensitive to flooding (riverbank overtopping or rainfall based) can be beneficial from a sustainable perspective. Recharge (volumes) are normative for the sustainable use of an ASR system. The recharges are (approximately linear) dependent on the time-span and levels of inundation. Moreover, the research contains soil scenarios, and demonstrates that the ASR system performs significantly better in regions with higher transmissivity (T) values.

To give insight on some financial aspects of an operational ASR system, the obtained (improved) ASR system discharge capacities are transformed to agricultural and financial yields. A subdivision of the dry season into a tomato and a groundnut cropping season demonstrates that financial yields are crop type dependent. The ASR system revenues are dominantly affected by the choice in crop type(s) and crop-specific market prices. The yields are compared to the ASR system pumping costs. The importance of pump selection is demonstrated by the implementation of the Pedrollo 4" submersible pump efficiencies. The use of a pump that is tuned to local conditions can be beneficial for the operational costs of an ASR system. Although no distinctive conclusion on the financial feasibility can be drawn, the examined system improvements are substantially beneficial for the revenues of a northern Ghana ASR system.

Contents

List of Figures	ix
List of Tables	xi
1 Introduction	1
2 Aquifer test	5
2.1 Research locations in northern Ghana	5
2.2 Methods - Set-up & analysis	6
2.2.1 Measurement set-up	6
2.2.2 Data analysis	8
2.3 Data processing	10
2.3.1 Location Bingo	10
2.3.2 Location Nungo.	11
2.3.3 Location Nyong Nayili	11
2.3.4 Location Janga (1/2)	13
2.3.5 Location Janga (2/2)	14
2.3.6 Location Ziong (monitoring)	14
2.4 Results & conclusions	15
3 ASR system - Improvements & sensitivities	19
3.1 Methods - ASR system simulation.	19
3.1.1 Soil scenarios	19
3.1.2 Base ASR system model definition (reference)	19
3.1.3 System improvements	21
3.1.4 System sensitivities.	22
3.1.5 Sustainability definition	22
3.2 ASR system base model performance.	23
3.2.1 Wet season	23
3.2.2 Dry season	24
3.2.3 Recovery ratio $R_{\%}$	25
3.3 ASR system improvements	26
3.3.1 Extension of daily pumping time	26
3.3.2 Enlargement of borehole diameter	27
3.3.3 Reduction of well skin resistance	27
3.4 ASR system sensitivities	29
3.4.1 Degradation of well depth by clogging	29
3.4.2 Shortening wet season inundation time	30
3.4.3 Reduction wet season inundation level.	30
3.5 Results & Conclusions	32
4 ASR system - Business case	33
4.1 Methods - From water volume to financial considerations	33
4.1.1 Yield - crops of interest.	33
4.1.2 Costs - water withdrawal.	35
4.2 Financial yield	36
4.3 Pumping costs	37
4.4 Results & conclusions	39

5 Discussion & Recommendations	41
5.1 Farmer's guide - ASR system implementation	41
5.2 Research recommendations.	45
5.2.1 Aquifer test	45
5.2.2 ASR system - Improvements & sensitivities.	46
5.2.3 ASR system - Business case	47
6 Conclusions	49
Bibliography	51
Appendices	53
A Borehole log-sheets	55
B Aquifer test - Equipment	61
C Aquifer test - Factsheets measurement results	65
D Aquifer test - Data analysis overview	73
E MODFLOW - Radial conversion	87
F MODFLOW - Model definition	97
G MODFLOW - TTim model validation	101
H Additional model results	103
I Pedrollo 4" submersible pump - product specifications	109

List of Figures

1.1	Example of the northern Ghana climatological conditions:(a) a flooding near Weisi, Upper West Region and (b) the consequences of drought near Nungo, Upper East Region	1
1.2	The year-round principal functions of an Aquifer Storage & Recovery (ASR) system	2
1.3	A simplified visualization of the desired results of ASR system improvements	3
2.1	The geographic positioning of the northern Ghana research locations	5
2.2	The in-field aquifer test (measurement) set-up (a) general, (b) simplistic	7
2.3	Schematic cross-sectional view of (a) the generalized northern Ghana soil stratification and simplified representations: (b) a single layer system, (c) a double layer system, and (d) a system with two layers and partial penetration of the well	8
2.4	The aquifer test data best curve fits for the different simplified models - location Bingo	11
2.5	The aquifer test data best curve fits for the different simplified models - location Nyong Nayili	12
2.6	The aquifer test data best curve fits for the different simplified models - Janga (1/2)	13
2.7	The aquifer test data best curve fits for the different simplified models - location Janga (2/2)	14
2.8	The aquifer test data best curve fits for the different simplified models - location Ziong	15
2.9	Transmissivity (T) & storativity (S) bandwidth selection	17
3.1	Schematic base ASR system model & soil scenario definition	20
3.2	Base ASR system model, the soil scenario 3 cross-sectional head contour plot after (a) five days and (b) 122 days of infiltration	23
3.3	Base ASR system model, the soil scenario 3 discharge performance for (a) the first five days and (b) the last five days of dry season	24
3.4	Base ASR system model, the soil scenario 3 cross-sectional head contour plot after four hours of pumping on (a) the first day (day 123) and (b) the last day (day 365) of dry season	24
3.5	Schematic extension daily pumping time	26
3.6	Results of the yearly total recharge volumes, discharge volumes and recovery ratios - by extension of the daily pumping time	26
3.7	Schematic enlargement borehole diameter	27
3.8	Results of the yearly total recharge volumes, discharge volumes and recovery ratios - by enlargement of the borehole diameter	27
3.9	Schematic reduction well skin resistance	28
3.10	Results of the yearly total recharge volumes, discharge volumes and recovery ratios - by reduction of the well skin resistance	28
3.11	Schematic degradation well depth by clogging	29
3.12	Results of the yearly total recharge volumes, discharge volumes and recovery ratios - by degradation of the well depth	29
3.13	Schematic shortening wet season inundation time	30
3.14	Results of the yearly total recharge volumes, discharge volumes and recovery ratios - by shortening the wet season inundation time	30
3.15	Schematic reduction wet season inundation level	31
3.16	Results of the yearly total recharge volumes, discharge volumes and recovery ratios - by reduction of the wet season inundation level	31
4.1	Crops of interest: (a) Tomatoes and (b) Groundnuts	33
4.2	ASR system operational pumping costs impression	35
4.3	Financial yields for the three types of ASR system improvement, based on a Tomato single cropping season	37

4.4	Financial yields for the three types of ASR system improvement, based on a Groundnut single cropping season	37
4.5	Pumping costs for the three types of ASR system improvement, based on 8 months dry season system use	38
4.6	Pumping costs for the three types of ASR system improvement, based on 8 months dry season system use and a maximum pump efficiency	39
5.1	Farmer's impression	41
B.1	Comparable example of the submersible pump used in aquifer test practise	61
B.2	Comparable example of the generator used in aquifer test practise	62
B.3	The hose & bucket used in aquifer test practise	62
B.4	Comparable examples of Van Essen TD- & Baro-Divers used in aquifer test practise	63
B.5	Comparable examples of In-Situ TD- & Baro-Divers used in aquifer test practise	63
B.6	Comparable example of the water tape used in aquifer test practise	64
C.1	Factsheet of the aquifer test - location Bingo	66
C.2	Factsheet of the aquifer test - location Nungo	67
C.3	Factsheet of the aquifer test - location Nyong Nayili	68
C.4	Factsheet of the aquifer test - location Janga (1/2)	69
C.5	Factsheet of the aquifer test - location Janga (2/2)	70
C.6	Factsheet of the aquifer test - location Ziong (monitoring ASR system practical use)	71
D.1	Overview of the aquifer test data curve fitting analysis - location Bingo	75
D.2	Overview of the derived optimal geohydrological parameter values - location Bingo	76
D.3	Overview of the aquifer test data curve fitting analysis - location Nyong Nayili	78
D.4	Overview of the derived optimal geohydrological parameter values - location Nyong Nayili	79
D.5	Overview of the aquifer test data curve fitting analysis - location Janga (1/2)	80
D.6	Overview of the derived optimal geohydrological parameter values - location Janga (1/2)	81
D.7	Overview of the aquifer test data curve fitting analysis - location Janga (2/2)	82
D.8	Overview of the derived optimal geohydrological parameter values - location Janga (2/2)	83
D.9	Overview of the aquifer test data curve fitting analysis - location Ziong	84
D.10	Overview of the derived optimal geohydrological parameter values - location Ziong	85
E.1	Schematic of an axially symmetric model (Langevin, 2008)	87
E.2	A top view visual impression of the test example grid structures for: (a) a rectangular MODFLOW model, (b) a rectangular round MODFLOW model and (c) a radial scaled (single row) MODFLOW model	89
E.3	MODFLOW radial scaling - schematic test 1: steady flow to a fully penetrating well in a confined aquifer	90
E.4	MODFLOW radial scaling - (relative) groundwater head and drawdown results test 1	91
E.5	MODFLOW radial scaling - schematic test 2: steady flow to a fully penetrating well in an unconfined aquifer	92
E.6	MODFLOW radial scaling - (relative) groundwater head and drawdown results test 2a	93
E.7	MODFLOW radial scaling - (relative) groundwater head and drawdown results test 2b	94
E.8	MODFLOW radial scaling - schematic test 3: unsteady flow to a partially penetrating well in a confined/unconfined aquifer	95
E.9	MODFLOW radial scaling - Cross-sectional head contour plot after 1 day	95
E.10	MODFLOW radial scaling - (relative) groundwater head and drawdown results test 3	96
G.1	TTim validation of the ASR system MODFLOW model infiltration results for soil scenario 3 - Enlargement well diameter	101
G.2	TTim validation of the ASR system MODFLOW model infiltration results for soil scenario 3 - Reduction well skin resistance	101

G.3	TTim validation of the ASR system MODFLOW model infiltration results for soil scenario 3 - Degradation well depth by clogging	102
G.4	TTim validation of the ASR system MODFLOW model infiltration results for soil scenario 3 - Shortening the wet season inundation time	102
G.5	TTim validation of the ASR system MODFLOW model infiltration results for soil scenario 3 - Reduction wet season inundation level	102
H.1	Base ASR system model infiltration performance for soil scenario 3 - Head in representative layers after (a) five days and (b) 122 days of infiltration	103
H.2	Base ASR system model extraction performance for soil scenario 3 - Head in representative layers after four hours of pumping on (a) the first day (day 123) and (b) the last day (day 365) of dry season	103
H.3	Results of the ASR system year-round performance (total inflow, outflow and recovery ratio) by the extension of the daily pumping time - relative to the base ASR system	104
H.4	Results of the ASR system year-round performance (total inflow, outflow and recovery ratio) by the enlargement of the well diameter - relative to the base ASR system	104
H.5	Results of the ASR system year-round performance (total inflow, outflow and recovery ratio) by the reduction of the well skin resistance - relative to the base ASR system	104
H.6	Results of the ASR system year-round performance (total inflow, outflow and recovery ratio) by the degradation of the well depth - relative to the base ASR system	105
H.7	Results of the ASR system year-round performance (total inflow, outflow and recovery ratio) while shortening the wet season inundation time - relative to the base ASR system	105
H.8	Results of the ASR system year-round performance (total inflow, outflow and recovery ratio) by the reduction of the wet season inundation level - relative to the base ASR system	105
H.9	The ASR system total recharge volume by model layers (1m) for soil scenario 3 - when the well depth decreases	106
H.10	The ASR system recharge rates over time for soil scenario 3 - while shortening the wet season inundation time	107
H.11	The ASR system recharge rates over time for soil scenario 3 - while reducing the wet season inundation level	107
H.12	The ASR system year-round net financial returns for the explored three types of system improvement	108
H.13	The ASR system year-round net financial returns for the explored three types of system improvement - while maximum pump efficiency (58%) considered	108

List of Tables

2.1	The derived optimal geohydrological parameter values for the different simplified models - location Bingo	11
2.2	The derived optimal geohydrological parameter values for the different simplified models - location Nyong Nayili	12
2.3	The derived optimal geohydrological parameter values for the different simplified models - location Janga (1/2)	13
2.4	The derived optimal geohydrological parameter values for the different simplified models - location Janga (2/2)	14
2.5	The derived optimal geohydrological parameter values for the different simplified models - location Ziong	15
3.1	Base ASR system model, wet season recharge volumes for the different soil scenarios	23
3.2	Base ASR system model, dry season discharge volumes for the different soil scenarios	25
3.3	Base ASR system model, recovery ratios $R_{\%}$ for the different soil scenarios	25
5.1	The indicative capabilities of groundwater extraction volumes obtained by a basic ASR system in northern Ghana	43
5.2	The ASR system design & operation chart - the relation between system modifications and changing water extraction volumes - applicable for adequate and good soil conditions (soil scenario 3-5)	44
D.1	Schematic overview of the distinctive simulation approaches in aquifer test data analysis	74
E.1	An overview of the obtained leakage factors (λ) (m)	100
H.1	The ASR system screen average specific recharge and discharge volumes (m^3/m) for soil scenario 3 - when the well depth decreases	106
H.2	The ASR system total recharge and discharge volumes specific reduction (m^3/m) for soil scenario 3 - when the well depth decreases	106

Introduction

'End Hunger' is one of the Sustainable Development Goals stated by the United Nations (United Nations, 2018). Currently, 815 million people on earth suffer from hunger. In coherence with the prospects of the world population (growth up-to 10 billion people by the year 2050) hunger is likely to increase (United Nations, 2018). The UN Food and Agricultural Organisation (FAO) expects that a doubling of the global food production will be necessary to feed the world population (FAO, 2018d). Due to strong patterns of urbanization and changing diets, the nutrition necessities are even higher in Sub-Saharan Africa (SSA). Local agricultural sectors within SSA can benefit from inevitable rising food demands (Ministry of Foreign Affairs et al., 2018). The present gap between the actual and potential yield can be bridged by small-scale agricultural innovations. Smallholder farmers can increase productivities by the implementation of more resource-efficient techniques. This bottom-up development approach is supported by the government of the Netherlands (SBIR program) (Ministry of Foreign Affairs et al., 2018).

Water availability is key in food production. 70 percent of the entire humanitarian fresh water-use serves agricultural purposes (United Nations, 2014). Within SSA, the northern Ghana region has favourable agricultural climatological conditions (semi-arid). The Ghana Meteorological Services Department (MSD) measured annual average precipitation of 800-1250 mm/y (1971-2007) (Canadian International Development Agency, 2011). This amount of rainfall is theoretically sufficient for farmers to be self-sufficient (Ministry of Foreign Affairs et al., 2018). However, precipitation is unevenly spread over the year. The majority of precipitation falls in a 4-month wet season spanning from late May to October. As a consequence, northern Ghana is subjected to both seasonal flooding and long periods of drought (Figure 1.1).



(a)



(b)

Figure 1.1: Example of the northern Ghana climatological conditions: (a) a flooding near Weisi, Upper West Region (source: (Owusu et al., 2017) and (b) the consequences of drought near Nungo, Upper East Region

Northern Ghana's food production is predominantly cultivated during the wet season. Dry season (irrigation based) agriculture takes place at small-scale. Only limited quantities of groundwater are used in the irrigation process. Currently, local groundwater use is estimated to be approximately 5% of the annual recharge (2.5-10% of annual precipitation) (Martin, 2008). The amount of water withdrawn is marginal. However, climate change can potentially have a negative influence. Natural recharge could decrease, while governmental policies are more and more pointed towards intensification of dry season agriculture (Wood, 2013). In the near future, it is possible that discharge rates will exceed natural recharge and groundwater extraction is no longer sustainable. Managed Aquifer Recharge (MAR) can potentially contribute to the continued sustainable use of groundwater in northern Ghana.

Aquifer Storage & Recovery (ASR) systems

Water entering a catchment (e.g. precipitation, river or groundwater flow) partially and temporarily contributes to local recharge of groundwater (Fitts, 2012). The natural water cycle can be manipulated by human interventions. Temporarily available water can be directed to the subsurface through creation of preferential flow paths; Managed Aquifer Recharge (MAR) (Dillon et al., 2009). There are different reasons for implementing MAR, e.g. underground water storage to reduce flooding or to counter groundwater shortages. Moreover, implementation can be beneficial for the local retention of water. MAR applications reduce water losses through evaporation and run-off.

There are many different MAR concepts, e.g. surface infiltration basins and sand dams (Dillon et al., 2009). A particular MAR type takes a central stage in this research; Aquifer Storage and Recovery (ASR) systems. Besides the basic MAR principle, groundwater recharge, ASR systems are designed for groundwater withdrawal as well. The principle functions of an ASR system are visualized in Figure 1.2.

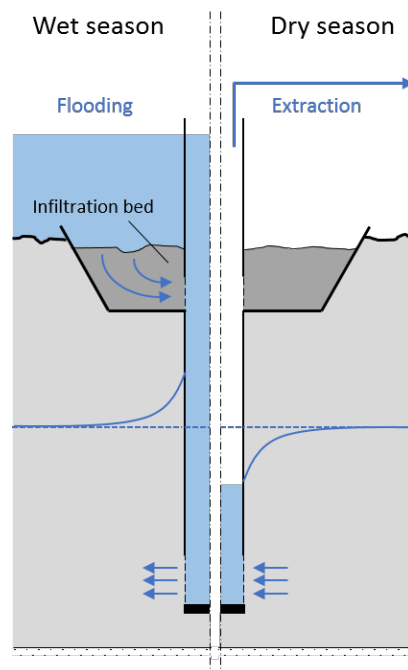


Figure 1.2: The year-round principal functions of an Aquifer Storage & Recovery (ASR) system

An ASR system offers a solution when natural surface infiltration characteristics are insufficient. Wet season water surpluses (e.g. flood and inundation) can be stored in the subsurface through the use of an ASR system. Flood water enters the system under influence of gravity. An infiltration bed around the borehole serves as the preferential path of flow. For purification purposes the bed is designed with a specific soil arrangement (Owusu et al., 2017). Dependent on borehole screen depth the ASR system can be connected to shallow (unconfined) and/or deeper ground layers (unconfined/confined). Dry season water withdrawal takes place by the installation of a submergence pump.

Research questions

ASR systems in northern Ghana make use of natural resources available locally. The system acts as a seasonal bridge, it converts flood water into irrigation water. Little is known about the impact of ASR systems on local geohydrology in northern Ghana (e.g. impact on local nature and agricultural benefits). From a sustainable point of view it is desirable to gain knowledge on year-round ratios between groundwater recharge (wet season) and discharge (dry season). Furthermore, northern Ghana smallholder farmers can potentially benefit from increased system efficiencies, a desired development in the process of becoming a (more) self-sufficient food region (Figure 1.3). The potential impact of ASR systems on water availability in northern Ghana has not been extensively studied. Objective of this research is to conduct a feasibility study on sustainable use of a synthetic ASR system in northern Ghana; taking present conditions and multiple system improvements into account. This research aims to answer the following research question:

How can Aquifer Storage and Recovery (ASR) systems be improved to increase the availability and sustainable use of groundwater for small-scale agriculture in northern Ghana?



Figure 1.3: A simplified visualization of the desired results of ASR system improvements (At present a single tank is filled on daily dry season base). (visual support by Housin Aziz, Jhun Capaya and Nibras@design from Noun Project - <https://thenounproject.com>)

The main research question can be solved in consecutive parts. Three additional research questions are stated that have to be answered:

- *Which range of values for transmissivity (T) and storativity (S) can be obtained from aquifer tests at multiple study sites in northern Ghana?*

It might seem trivial, but the functioning of an ASR system is highly dependent on local (geohydrological) conditions. Locally applicable geohydrological parameters (T and S) have to be determined for the input into the models used to further study ASR system performance. The desired information is obtained through site-specific measurements at multiple locations in northern Ghana.

- *How can ASR system design and operation be improved to increase water supply, while maintaining sustainable system use?*

For northern Ghana smallholder farmers this question is key, but the answer to it is rather challenging. The terms 'how' (types of improvement) and 'to what extent' (limit of sustainability) need further specifications. In order to judge the potential improvements (and sensitivities) of the ASR system, a synthetic northern Ghana base ASR system model is defined as reference.

- *How will the ASR system improvements impact the financial yields and pumping costs?*

The (improved) performance of the synthetic ASR system is expressed in water volumes. Translating water volumes into expected financial returns gives more insight into the impact and feasibility of ASR systems. By considering expected crop yields and pumping costs, the financial feasibility of an operational ASR systems is examined.

Methodology

In northern Ghana, in-field aquifer tests are carried out at five ASR systems. The obtained data is analysed in a transient analytical element modelling environment; TTim (Bakker, 2013a,b). The obtained values for transmissivity (T) and storativity (S), are used as input in the subsequent geohydrological models. Multiple model scenarios are run to study the basic performance of an ASR system, the impact of changes in ASR design parameters, and the system's sensitivity to different/changing natural conditions. The models are created in the finite difference environment for groundwater flow; MODFLOW (Harbaugh, 2005; Niswonger

et al., 2011). The simulated results on the (improved) ASR system performances are expressed in both water volumes and financial returns.

Reader's guide

Chapter 2 presents the measurement locations and describes the derivation (process) of the geohydrological parameter values (T and S). The results of simulated ASR system improvements and the system sensitivities to changes in local natural conditions are explained in Chapter 3. In Chapter 4 a business case is presented, translating the model results from Chapter 3 into operational financial returns. Each of the Chapters 2 - 4 includes an own detailed descriptions of the applied research methods on: aquifer test application (e.g. data generation and processing), synthetic ASR-system model definition and water volume-to-yield transformations (Section 2.2, 3.1 & 4.1). In Chapter 5, a farmer's guideline is written based on the model results, giving recommendations for the design of ASR systems in northern Ghana. This Chapter also discusses the main research limitations and gives recommendations for further research. Chapter 6 contains the research conclusions.

2

Aquifer test

The performance of an ASR system is dependent on the physical properties of its surroundings (Bakker, 2010). In the north of Ghana, subsurface characteristics can vary at short mutual distances (Owusu et al., 2017). Representative information on the local geohydrology is obtained through site-specific measurements. Aquifer tests are performed at multiple locations in northern Ghana.

The research locations are presented in Section 2.1. Section 2.2 describes the aquifer test methodologies in measurement set-up and data analysis. Appendix C contains the raw measurement results. The aquifer test data is analysed in Section 2.3. In Section 2.4 the conclusions on the site visits and the data analysis are described. The chapter concludes with the derivation of locally applicable values for T and S . These parameters are the input for the study on potential ASR system improvements in northern Ghana.

2.1. Research locations in northern Ghana

Multiple ASR systems are present in the Upper East Region (UER) and the Northern Region (NR) of Ghana. Commissioned by the NGO Conservation Alliance (CA), some of these systems are installed in the summer of 2016. Pumping tests are performed at four (CA) ASR systems, located in Bingo; Nungo; Nyong Nayili and Janga. At the location Ziong an ASR system is used for the monitoring of the system practical use by farmers. Figure 2.1 shows a map of the research locations in northern Ghana.

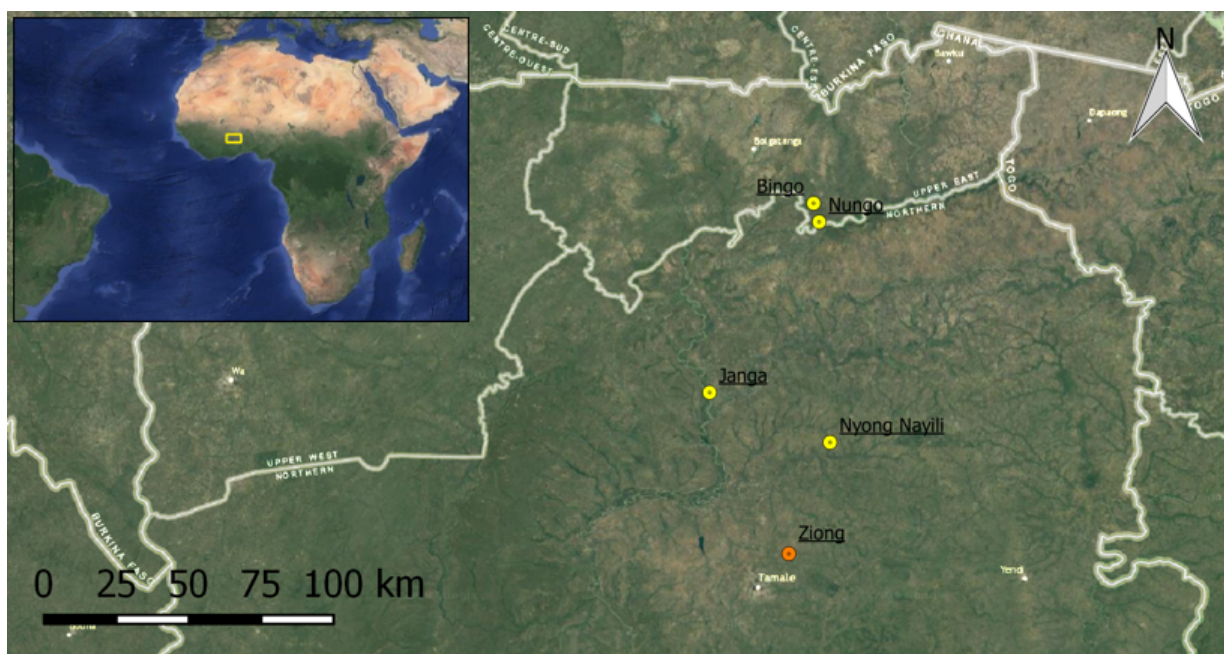


Figure 2.1: The geographic positioning of the northern Ghana research locations

2.2. Methods - Set-up & analysis

The five northern Ghana study sites (Section 2.1) are subjected to aquifer tests. A complete description of the test process (from measurement data generation to geohydrological parameter values derivation) is described below. The raw results (measurement data) can be found in Appendix C. Data analysis (Section 2.3 & 2.4) is possible by the implementation of the here presented methodologies.

2.2.1. Measurement set-up

This section contains the ins and outs of the practical aquifer test set-up. The aquifer tests accommodates both pumping-recovery tests and the monitoring of the system use by farmers. Due to differences in ASR systems encountered, the data collection is designed by a hybrid measurement approach. The stated approach can be used as input for data (re)production (transparency).

Pump installation

Based on the (2016) original log sheets (Appendix A), site-specific borehole depths are known in advance. The ASR system inspection showed, the accumulation of sedimentation at the borehole bottom. To prevent pump damages and make sure properly functioning is maintained, actual borehole depths are measured before pumping tests are executed. Outcomes of the measurements are taken into account for each individual set-up. To prevent the excessive spread of soil particles, the submersible pump is positioned at least 5 m above the measured borehole bottom (sediment). In practice, this resulted in a pump suction depth of approximately 30-35 m.

Pump discharge & measurement

A single 100 m hose is directly connected to the outlet of the submersible pump. Based on the pump position (deep inside borehole), a distance of circa 65 m is applied for the horizontal displacement of water. At this distance, water is discharged on the surface. The head of the hose is equipped with a nozzle to roughly regulate the discharge rate. By the use of this nozzle, discharge rates in the range of 50-75 m³/d are obtained during the pumping tests. Rates are measured by the use of a stopwatch and a 50 l bucket. Starting at the moment of pump operation, the duration of filling is measured twice every 15 minutes. The obtained 15 minute average is used to calculate the time dependent discharge rates. More detailed discharge information can be found in the site-specific fact sheets (Appendix C).

Groundwater table (GWT) measurement

Groundwater level reductions caused by pumping tests are preferably measured in multiple piezometers, located at a certain known horizontal distance from the discharge well (Kruseman and de Ridder, 2000). In the northern Ghana surroundings, close range monitoring options are absent. Due to a lack of time and/or resources these facilities could not be arranged either. Moreover, the implementation of such facilities do not match research nature. Aim of this research is to collect fieldwork data by the use of minimal resources. The absence of widespread measurement options strengthens this approach. As a consequence, the time dependent GWTs (drawdowns) are measured in the discharge well only.

A water tape is used as hand equipment. First of all to determine the initial (static) GWT. Subsequently, the device is applied as a real time indicator of drawdown. During the pumping tests, multiple hand measurements are applied at randomly picked moments to monitor the test progress. Gathered data functions as verification and back-up of the pressure sensors (divers), which are normative.

Two types of divers (different brands) are used as GWT measurement devices. Product specifications show that these divers can respectively measure pressures up to 10 m (Van Essen) and 9 m (In-Situ) water column (Appendix B). The northern Ghana regional subsurface is characterized as highly heterogeneous. The pumping test GWT drawdown magnitude is therefore unpredictable. To prevent the occurrence of missing drawdown data, the single borehole is equipped with multiple divers at ascending depths. The water column between the initial static water table and pump position is filled with about four divers, with a mutual distance that meets the divers range specifications. To make sure the divers stay in position they are leashed to a rope which runs from well top to pump. This measurement set-up forms a robust network for the collection of drawdown data (figure 2.2a).

However, practical circumstance can cause the application of a more simplistic set-up (figure 2.2b). One can think of a situation in which the pump is already installed and/or will not be removed at the end of

the pumping test. In this case, the (rope) attachment of the divers to the pump is not possible. Adverse effect of the simplistic set-up is a more vulnerable data collection. To prevent the occurrence of undesired diver movement, a minimum distance of 5-10 m between the pump and lowest diver is implemented in this set-up. A complete overview of the borehole measurement set-up (general and simplistic) can be found in figure 2.2.

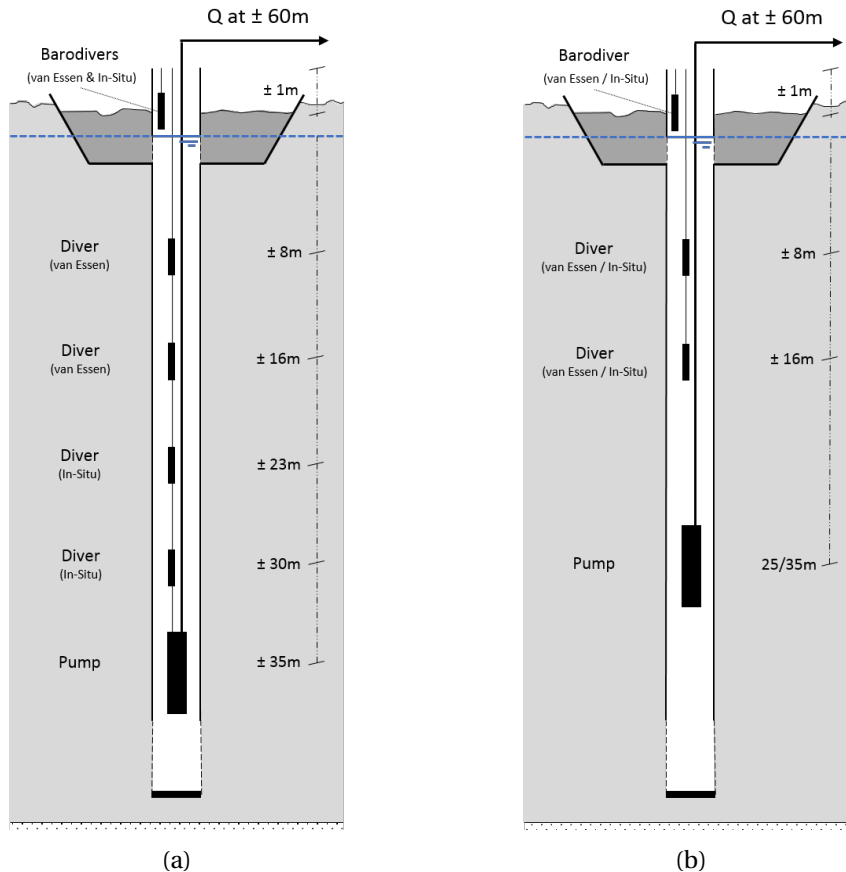


Figure 2.2: The in-field aquifer test (measurement) set-up (a) general, (b) simplistic

Besides the divers, the measurement set-up also accommodates two baro-divers (van Essen & In-Situ). The baro-divers are positioned in the borehole top section. Drawdown is by definition expressed as time dependent GWT reductions relative to the initial status. Short-term atmospheric fluctuations in pressure are compared to the water pressures negligible small. Nonetheless, these minor atmospheric influences are also included in the data collection.

Pumping test duration & time measurement

For each individual pumping test the exact start of pump operation could not be determined in advance. As a consequence, the total pumping test duration differs per pumping test as well. In every single measurement, a minimum of four hours of pumping and one hour of recovery is pursued.

To avoid unnecessary risks in missing out on the collection of drawdown data, all pressure sensors are programmed to start logging in time (08:00:00, local time, at pumping test days). All divers are set to log with a similar linear interval of 10 seconds. As a single exception, the In-Situ BaroTROLL is programmed to linear log once a minute (its minimum sample interval).

* An overview of the aquifer test results for each individual research location can be found in Appendix C. More details on the applied equipment can be found in Appendix B.

2.2.2. Data analysis

Raw drawdown time series are the result of in-field measurements. The data sets are more or less meaningless on its own. The methods below describe the required components in analysis to transform the obtained aquifer test data to the desired transmissivity (T) and storativity (S) values.

Simplified theoretical models

The original borehole log sheets (appendix A) are the most reliable source of local geological information available. Although the sheets contain site-specific information, similarities in stratification are present. In each case (2.1) the upper 50 m is divided into two or three layers, consisting of a (semi-)impermeable top layer and below that one or two high(er) permeable layers (aquifers). Groundwater tables are predominantly positioned slightly below the bottom of (semi-)impermeable layer, in the top aquifer (labelled as layer 1 in the figure below). Strictly seen, the conditions are therefore unconfined. But given the small interval (relative to total model thickness) between the the aquifer top and the GWI, the situation is close to confined. Based on the borehole log sheets three simplified theoretical models for the analysis of fieldwork data are proposed, as depicted in Figure 2.3.

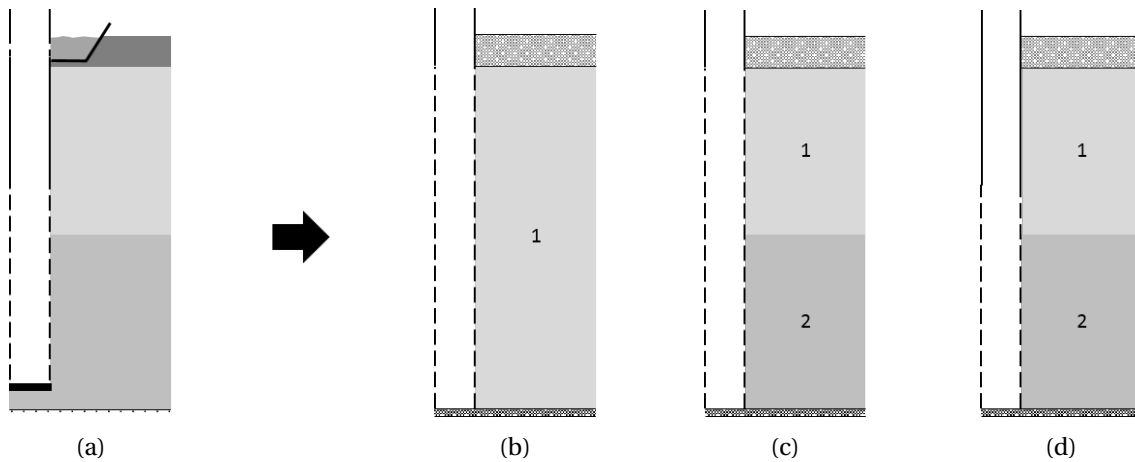


Figure 2.3: Schematic cross-sectional view of (a) the generalized northern Ghana soil stratification and simplified representations: (b) a single layer system, (c) a double layer system, and (d) a system with two layers and partial penetration of the well

These simplified models (Figure 2.3b - 2.3d) mimic local conditions, making the derivation of representative hydraulic subsurface characteristics (T and S) potentially possible (Kruseman and de Ridder, 2000). Double layered models are applied to provide more degrees of freedom, perhaps resulting in more accurate solutions. To limit the chances of equifinality (abundant degrees of freedom) a maximum of two soil layers are implemented in data analysis.

Parameter derivation method's & model environment

It lacks a single best approach in the derivation of the geohydrological parameter values (T and S). A widespread variety of analyses (e.g. analytical and computational) can be applied on the pumping test data. The details of the (analytical) models and methods used in this research are described below.

- Theis's method

Groundwater drawdown due to the withdrawal of water can be determined analytically with Theis's equation (Equation 2.1). Theis's method is applicable on the situation depicted in Figure 2.3b; a constant rate pumping test applied on a well that is fully penetrating a single layer aquifer (Kruseman and de Ridder, 2000). Confined conditions are assumed in Theis's method. Therefore, this analytical solution is suitable for obtaining a first indication (approximation) of the research geohydrological parameters.

$$s = \frac{Q}{4\pi KD} E_1(u) \quad (2.1)$$

$$u = \frac{r^2 S}{4KDt} \quad (2.2)$$

Where s (m) is the drawdown at distance r (m) from the well, Q (m^3) is the constant well discharge, KD (m^2/d) is the aquifer transmissivity ($KD = T$), S (-) is the aquifer storativity, t (d) is the time measured from the start of pumping and E_1 is the exponential integral. The drawdown measurements in this research are limited to in-well measurements. The distance r in Theis's equation is assumed to be the length of the well radius (0.0635 m). Appendix D.1 shows the implementation of Theis's method in Python.

- Analytic Element Modelling in TTim

TTim is a computer program based on analytic elements and designed for the analysis of transient groundwater flow. The analysis can be applied on a single or multiple layer(s). Several analytical elements (and types of elements) can be added to model layers. The use of TTim makes it possible to take additional well characteristics into account. Groundwater heads can be determined inside the well and the model optionally accounts for borehole storage and well skin resistance. Moreover, well discharge can be toggled on and off multiple times. This allows for simulations of both single pumping-recovery tests and long-term well operations (Bakker, 2013a,b).

This research fieldwork data is analysed within the TTim Model3D configuration. A single well (analytical element) is included in the model environment. The groundwater heads are determined inside the well. Aspects as actual borehole storage, optimal borehole storage and/or optimal well resistance are alternately accounted in different compositions of analysis. Moreover, the three types of simplified theoretical models (Figure 2.3) are consecutively considered. A complete overview of all approaches in data analysis (25x) can be found in Appendix D.2.

The top layer (aquifer 1 in Figure 2.3) is configured as being a phreatic layer. In other words, the top layer storage coefficient (S) is a phreatic storage coefficient (S_y). This model assumption is based on the observed initial groundwater tables, which are located below the bottom of the (semi-)impermeable top layer. In analysis, each simplified model layer has a hypothetical thickness of 1 m. The derived hydraulic conductivities (k) can therefore be interpreted as transmissivities (T) and the storage is expressed as the layer storage coefficient (S). This is done to directly derive T and S values. Additionally, this approach automatically corrects for the absence of knowledge on the thickness of the deepest soil layer in which the well is screened. There is no information about soil conditions beyond the bottom of the wells in the borehole log-sheets (Appendix A).

Optimization functions

As a final step in the determination of values for T and S , the analytical solution (Theis's method) and composed TTim models are linked (fitted) to the fieldwork data. Two optimization functions are applied.

- Fmin-RMSE function

Differences between the measured and modelled drawdown (curves) can be expressed by the Root-Mean-Square-Error (RMSE) objective function (Equation 2.3). The Fmin function (part of Python's `scipy.optimize` package) is applied to minimize the RMSE value. In other words, the function is applied to minimize the difference between modelled and observed drawdowns. The optimization results in (RMSE based) optimal T and S values (and optionally values for borehole storage and/or well skin resistance). These values theoretically represent local conditions. An example Python implementation of the Fmin-RMSE optimization function is depicted in Appendix D.1.

$$RMSE = \sqrt{\sum \frac{(s_{mod} - s_{field})^2}{N}} \quad (2.3)$$

Where s_{mod} is the modelled drawdown (m), s_{field} is the observed drawdown (m) and N is the number of data points.

- Calibration function

TTim has a built-in calibration function for the derivation of parameter values. Application of this second method improves the research robustness (reference values). An example of the Python implemented TTim Calibrate optimization function is part of Appendix D.1.

Both optimization methods require initial parameter estimations. More than one suitable solution is possible, which makes the outcome of the optimization dependent on the choice of the initial values. Other studies found that T and S values are commonly low in northern Ghana (e.g. Owusu et al., 2017, 2015). Based on these other studies the following initial conditions are applied: k_{aq0} is 10 (m/d), k_{aq1} is 10 (m/d), S_{aq0} is 0.01 (-), S_{aq1} is 0.001 (-) and well resistance is 0.1 (d). The well radius (measured in-field) is used as the (initial) borehole storage: 0.0635 (m). Boundary conditions are applied to avoid the optimization resulting in physically improbable parameter values, i.e. negative parameter values and unnaturally high storativity values (greater than 0.3 (-)).

2.3. Data processing

The findings of the site visits are described in this section. Moreover, the section contains the analysis of the aquifer test data. The most important outcomes for each of the five locations are discussed below. A complete overview of all simulations in data analysis (25 per location) can be found in Appendix D.

2.3.1. Location Bingo

Site inspection

The surroundings of Bingo are characterized by a mildly sloping landscape. (Bed)rock appears occasionally at the surface. Site inspection showed an abundance of charred vegetation. The area is exposed to bush fires. As a consequence of these bush fires the agricultural field is not in operation. Map inspection shows the presence of the Volta river within several kilometres from Bingo. However, no indications of surface water (water-bodies and/or ponds) were observed. Bingo inhabitants experience inundation levels up to 1-2 m, usually lasting for days. The inhabitants label wet season flooding as high. Flooding is not always directly caused by rain. Sometimes rainfall collects to fill up depressions in the landscape at a certain moment in time. Inspection on the infiltration well revealed the presence of a steel lid. Above surface level no well screen perforations were observed.

Measurement quality

A malfunctioning power converter postponed the pumping test start. Since nightfall was a time limiting factor, the delay resulted in a shortened total test duration. Well turbulence caused the rope to which the divers were tied to tangle, which meant the sensor depths changed over the course of the experiment (see measurement set-up in Appendix B). Additionally, because of the tangle, hand measurements also became unreliable. The direct result is a long-term gap in pumping test drawdown data (yellow dotted line in Figure 2.4). The exact drawdown at the last moment of pumping is missing.

Fit analysis

The absence of data has its effects on the parameter fitting capabilities. As visible in Figure 2.4, Theis's method encounters difficulties here. Drawdown most definitely exceeded the measurement limit of 8 m. This is not reflected in the parameter outcome of Theis's method. Defective fitting capabilities, due to a gap in data, are clearly less emphatically present in the analysis by the use of TTim. Optimal parameter values are found at which drawdown curves exceed the drawdown measurement limit. Taking borehole storage and/or well resistance in consideration may potentially underlie this. This example shows it is not by definition required to feature complete drawdown data. By the use of TTim incomplete time series can result in adequate optimal parameter values. In order size the values found are low but align initial conditions. Furthermore, it can be appointed that the double-layered transmissivity values found, suggest the presence of only one layer of groundwater flow.

Table 2.1: The derived optimal geohydrological parameter values for the different simplified models - location Bingo

	Method	Stor [m]	Res [d]	T1	T2 [m ² /d]	S1	S2 [-]	RMSE [m]
Analytical	fmin	-	-	10.83	-	2.0e-04	-	0.798
1 lay	fmin	0.0647	5.6e-02	26.23	-	6.6e-03	-	0.163
2 lay	fmin	0.0635	-	2.8e-04	8.25	3.0e-03	2.1e-06	0.107
2 lay (pp)	fmin	0.0597	-	8.6e-04	7.44	7.1e-03	6.3e-06	0.078

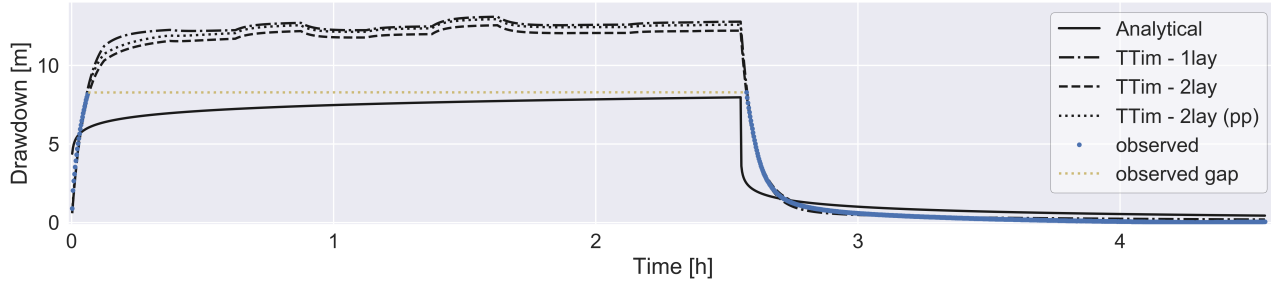


Figure 2.4: The aquifer test data best curve fits for the different simplified models - location Bingo

Effect of model complexity

Both parameter optimization functions (`Fmin` and `Calibrate`) are able to derive reasonable solutions. Results of the `Calibrate` optimization function reveal that an increase in model degrees of freedom does not necessarily lead to better performance (Appendix D). By looking at the `TTim` best fit solutions (Figure 2.4) only minor distinction can be made in the performance between the models with a single layer, double layer or double layer with a partially penetrating well. Overall, model accuracy slightly increases (Root-Mean-Square-Error slightly decreases) with an increase in model complexity. However, this increase is not significant.

2.3.2. Location Nungo

Site inspection

The remote community of Nungo is located in the Upper East Region (UER) of Ghana. Access is only possible by an unpaved road. The landscape is mildly sloping to flat. Low vegetation is interspersed by plains. Adjacent to the village an out of use agricultural field is present. The Volta river is located at approximately 400 m. Wet season flooding occurs due to riverbank over-topping. Inhabitants label inundation levels as extreme. Water levels of 3 m and higher persist for the entire rainy season. The infiltration well has perforations above surface level. At the moment of inspection the top of the well was deformed by heat, which meant it was not possible to close it off by a lid.

Measurement quality

Installation of the test set-up was affected by difficulties with pump immersion. From the first moment of pumping, discharge rates were effectively zero. An inspection revealed the well was filled with a liquid consisting of water, sandy clay and debris. The pumping test was restarted twice with an increased pump elevation. This did not result in an improvement. It was not possible to perform a pumping test at this location.

Remark

The well is clogged and should be cleaned before measurements can be done. No pumping test was performed and no data was acquired.

2.3.3. Location Nyong Nayili

Site inspection

The landscape of Nyong Nayili and its surroundings is mostly flat. A mix of bushes, low vegetation and crop fields is present. During site inspection, no agricultural fields had been delineated. The local community

estimated that wet season inundation levels reach up to 1 m. Throughout the season inundation fluctuations occur, caused by rainfall. No river or water flow was observed in the area. A muddy, stagnant pond is present at close well range (approximately 40 m). The infiltration bed was still inundated (approximately 0.2 m) during the pumping test. Well perforations were observed above the infiltration bed. The presence of water on the infiltration bed definitely had an impact on the measurements of the pumping test.

Measurement quality

The start of the pumping test was delayed because the well could not immediately be located, and because of a clogged discharge hose. Since nightfall was a time limiting factor, the delay resulted in a shortened total test duration. In addition, the inundated infiltration bed affected the pumping test. The first 20 minutes of drawdown measurements are affected by an (unknown) additional inflow (see Appendix C). This period is not taken into account in further analysis. The noise of dripping water during pumping test application suggests the interference of additional inflow even beyond the first 20 minutes.

Fit analysis

Theis's method encounters difficulties in finding parameter values leading to a reasonable good fit. The optimal solution does not result in a reasonable curve fit. The resulting storativity is equal to the predefined upper bound. The solution is unreliable and can be neglected. The use of TTim has a positive impact on the outcome in data analysis. Found transmissivity values are not analogous, but potentially represent nature. The resulting storativity values can be interpreted as low. The obtained optimal borehole storage values are considerably high compared to the initial conditions. Values upto five times the actual borehole storage are encountered. These values potentially reflect the presence of additional inflow. Overall curve fitting performances are moderately good. The absence of a decent fit can potentially be attributed to the data that was left out and/or the unknown additional inflow of water over time.

Table 2.2: The derived optimal geohydrological parameter values for the different simplified models - location Nyong Nayili

	Method	Stor [m]	Res [d]	T1	T2 [m ² /d]	S1	S2 [-]	RMSE [m]
Analytical	fmin	-	-	6.00	-	3.0e-01	-	0.752
1 lay	cal	0.2419	-	13.35	-	7.8e-05	-	0.457
2 lay	cal	0.2436	-	6.95	6.98	4.6e-06	3.6e-05	0.457
2 lay (pp)	fmin	0.2659	1.7e-02	1.7e-04	28.61	1.1e-02	4.4e-06	0.450

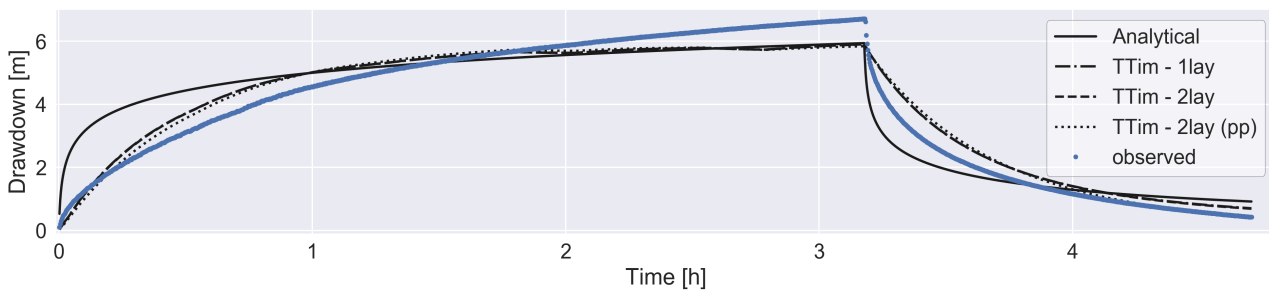


Figure 2.5: The aquifer test data best curve fits for the different simplified models - location Nyong Nayili

Effect of model complexity

The choice of optimization function did not significantly impact the values of the optimized parameters. An increase in the number of parameters did not improve model performance, it even worsens model performance in some cases. In all the model simulations the Root-Mean-Square-Error is substantial. The accuracy of the optimal parameter values is questionable. Further research on the impact of missing starting data and/or the impact of water inflow during a pumping test is recommended.

2.3.4. Location Janga (1/2)

Site inspection

The infiltration system near Janga is located at the bank of a dry river bed. The Volta river is located at approximately 1000 m (see fact-sheet visualisation, Appendix C). A stagnant pond is present at a distance of approximately 70 m from the well. Wet season flooding is caused by the river. The flooding was described as a constant inundation of over 4 m and lasts for the the four months of wet season. During field visit no agricultural farm was seen. The infiltration well above surface level has perforations and is equipped with a plastic/concrete cover.

Measurement quality

Bush fires are frequent occurrences in the region. Due to close range appearance of fire at the time of measurement, the test is aborted early. The duration of the recovery process monitoring is affected. The color change in water discharged during the pumping test was noteworthy. The water switched color from brownish to grey to white to clear several times.

Fit analysis

The magnitude of the parameter is in line with the values found at the other research locations. The RMSE values are significantly larger, indicating the drawdown curve was not correctly modelled. The large RMSE-values can be attributed to the pumping test drawdown part. The shape of the drawdown curve shows an initial lowering of the groundwater level, which becomes more steady as time progresses. But then after approximately 90 minutes, the groundwater level starts dropping more quickly again before levelling off slightly. None of the methods used in the analysis of the pumping test data is able to mimic the behaviour observed during this pumping test.

Table 2.3: The derived optimal geohydrological parameter values for the different simplified models - location Janga (1/2)

	Method	Stor [m]	Res [d]	T1	T2 [m ² /d]	S1	S2 [-]	RMSE [m]
Analytical	fmin	-	-	8.84	-	3.0e-01	-	1.339
1 lay	fmin	0.0635	-9.7e-03	9.09	-	1.6e-02	-	1.382
2 lay	fmin	0.1287	-	12.48	1.3e-04	1.9e-02	1.1e-08	1.445
2 lay (pp)	fmin	0.0635	-	9.1e-05	15.19	4.3e-08	3.1e-03	1.530

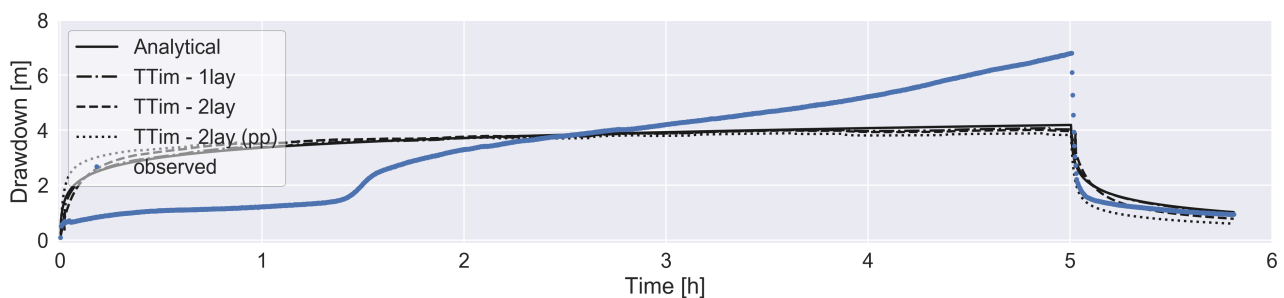


Figure 2.6: The aquifer test data best curve fits for the different simplified models - Janga (1/2)

Effect of model complexity

The shape of the drawdown curve is striking. There is a sudden increase in drawdown after 90 minutes of pumping. Towards the end of pumping period (four to five hours) the curve does not show the characteristic behaviour of reaching a new equilibrium. The variable rates of drawdown observed during the pumping test are not observed during the recovery test. As stated by Kruseman and de Ridder (2000), most of the time there is not a unique theoretical solution for these well-flow problems. This makes the identification of the right (theoretical) system even more difficult. Additional fieldwork could provide more information as to which local characteristics are causing this behaviour. A second pumping test was performed to verify whether the first test was done correctly.

2.3.5. Location Janga (2/2)

Measurement quality

The initial (first two hours) pumping test discharge rates vary slightly (Appendix C). The drawdown curve is potentially affected by these variations. Similar to the first test, the extracted water changed color several times. Compared to the previous research, the recovery period was monitored for longer.

Fit analysis

Despite the application of a pumping test with a lower discharge (compared to first attempt) the drawdown data shows similar behaviour. The lower values in Root-Mean-Square-Error can be attributed to the lower absolute drawdown (test with lower discharge rate) and the increased duration of recovery monitoring. The RMSE values still indicate the models are not able to describe the observed behaviour. The resulting parameters are shown in Table 2.4.

Table 2.4: The derived optimal geohydrological parameter values for the different simplified models - location Janga (2/2)

	Method	Stor [m]	Res [d]	T1	T2 [m ² /d]	S1	S2 [-]	RMSE [m]
Analytical	fmin	-	-	15.97	-	3.0e-01	-	0.571
1 lay	fmin	5.4e-07	-9.7e-03	13.54	-	1.9e-02	-	0.551
2 lay	fmin	0.2228	-2.2e-02	2.05	8.13	2.1e-02	4.1e-04	0.545
2 lay (pp)	fmin	0.2005	-3.1e-02	6.59	0.86	9.4e-05	2.1e-03	0.545

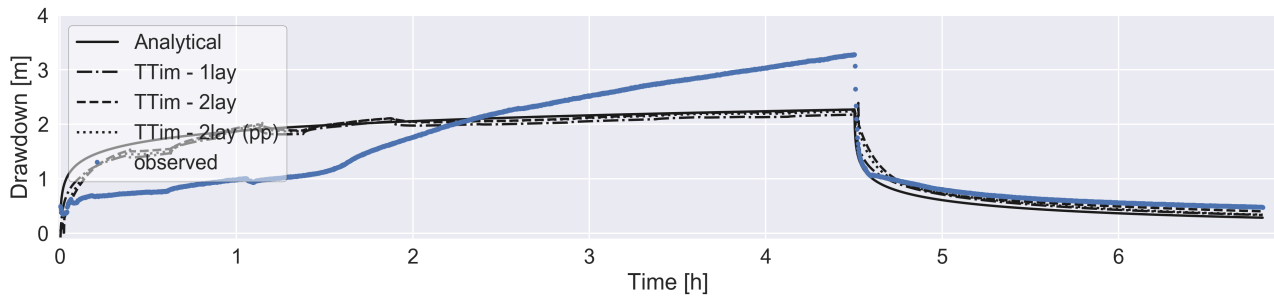


Figure 2.7: The aquifer test data best curve fits for the different simplified models - location Janga (2/2)

Effect of model complexity

The second test confirms the behaviour observed in the first test. There are multiple explanations for this behaviour, i.e. one can think of the subsurface layers that are emptied as pumping continues, hydraulic interaction with the river bed or fracture zones drawdown and more.

2.3.6. Location Ziong (monitoring)

Site inspection

In the study site surroundings of Ziong, no rivers, water flows or ponds were observed. Wet season inundation depths were said to be less than 2 m. Daily level variations occur as flooding is caused by rainfall. The landscape is flat. Occasionally, (bed)rock is observed at the surface. High grasses and bushes are present. There are several crop fields nearby. The infiltration system does not have perforations above surface level. A steel lid is present to cover the top of the well. The agricultural field and the ASR-system were fully operational.

Measurement quality

During the observed period the system was in daily operation. The system was monitored over multiple days. The divers had to be installed above the lowest groundwater levels because of the presence of the pump and the fact that the system was already in operation. This meant that the largest drawdowns could not be measured. The estimated discharge rate of 20 m³/d is based on multiple measurements of the volume meter. In analysis it is assumed to be constant. The exact time at which the recovery starts is unknown because the lowest groundwater levels could not be measured. Based on the comparable test situation at

the location Bingo, it is assumed the recovery starts 4 minutes before the first measurement indicating the recovery has started.

Fit analysis

The analytical Theis method was not applied in this monitoring test situation. Analysis with TTim show reasonable results. The modelled drawdown corresponds closely with the observations. This example shows the advantages of TTim. The obtained transmissivity values of approximately $1 \text{ m}^2/\text{d}$ are low.

Table 2.5: The derived optimal geohydrological parameter values for the different simplified models - location Ziong

	Method	Stor [m]	Res [d]	T1	T2 [m^2/d]	S1	S2 [-]	RMSE [m]
1 lay	fmin	0.0382	-	1.76	-	1.1e-03	-	0.255
2 lay	fmin	0.0635	-0.05	0.38	1.05	2.9e-02	1.2e-03	0.240
2 lay (pp)	fmin	0.0147	-0.08	0.23	0.78	2.6e-02	1.3e-03	0.243

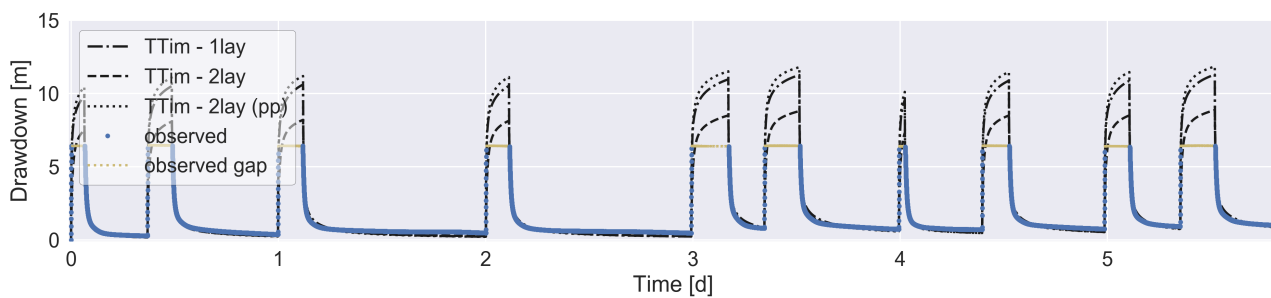


Figure 2.8: The aquifer test data best curve fits for the different simplified models - location Ziong

Effect of model complexity

Both optimization functions (Fmin and Calibrate) yield comparable parameters. When applying a simplified model with an increased number of degrees of freedom, the Fmin optimization function tends to score slightly better on values for the Root-Mean-Square-Error (Appendix D). This however concerns a single measurement analysis, with a single set of predefined initial parameters. No other objective functions are taken into account. The performance of the different models does not show any trend. Models with an increased number of degrees of freedom do not necessarily describe the observed data better. All three theoretical models are able to describe the observed data at Ziong to a certain extent.

2.4. Results & conclusions

This section contains the conclusions that can be drawn from the site visits and the analysis of pumping test data. The final part of this section describes how this data was used to derive parameters for soil scenarios to study potential methods for improvements of ASR systems in northern Ghana.

Maintenance of ASR systems

- ASR-system cleaning

One year after construction (2016) the penetration depth of all five boreholes has decreased (significantly) due to the deposition of sand at the bottom of the well. The impact differs per location, but at each location a minimal depth decrease of 6 m is observed. The most striking example is the borehole at location Nungo, where a complete clogging has occurred (over 40 m decrease in depth). Measures should be taken to prevent the occurrence of clogging. It is recommended to seal off each borehole with a plastic/concrete lid. The tube penetrations above the infiltration bed should be sealed off permanently to avoid inflow of undesired sand and clay. In addition, annual maintenance of the borehole and infiltration bed is desirable.

- Additional research

The results obtained through the analysis of the pumping tests seem to yield plausible estimates of subsurface characteristics. However, the models are not able to closely match the observations in all cases. Additional research could be done to expand the models to include processes that were left out in this analysis, e.g. inflow from the infiltration bed and irregularities (sudden additional decrease) in the drawdown time-series. Methods to deal with missing data (gaps in time series) could also be improved upon.

- Recommendations for future pumping tests

Pumping tests should be performed with at least one (preferably more) observation well at a certain distance from the well (Kruseman and de Ridder, 2000). These tests potentially give insight in well skin behaviour (degree of resistance) and increase the amount of data from which subsurface parameters can be derived. The installation of one or more divers is recommended if complete ASR system understanding is required. This can provide more insight into how these system function throughout the year.

Applicability of methods & models

- Performance (analytical) methods; Theis & TTim

Compared to the simplest pumping test interpretation (Theis's method), TTim offers more model options (borehole storage, well skin resistance, multiple layers) in drawdown data analysis (Bakker, 2013a,b). In this research TTim outperforms Theis's method. However, TTim also encounters limitations, e.g. when there is a variable inflow at the start of a pumping test or when an additional sudden drop in drawdown occurs.

- Performance of optimization functions; Fmin & Calibrate

The obtained geohydrological parameters represent local nature to a certain extend. This is confirmed by the Root-Mean-Square-Error values (objective function). Application of the two optimization functions generates outcomes. The results of different optimization functions can lead to differences in parameter size, while goodness of the fit statistics (RMSE) are comparable. However, the resulting parameters are generally similar. Therefore, it can be concluded that both optimization functions (Fmin and Calibrate) are applicable for the determination of suitable T and S values.

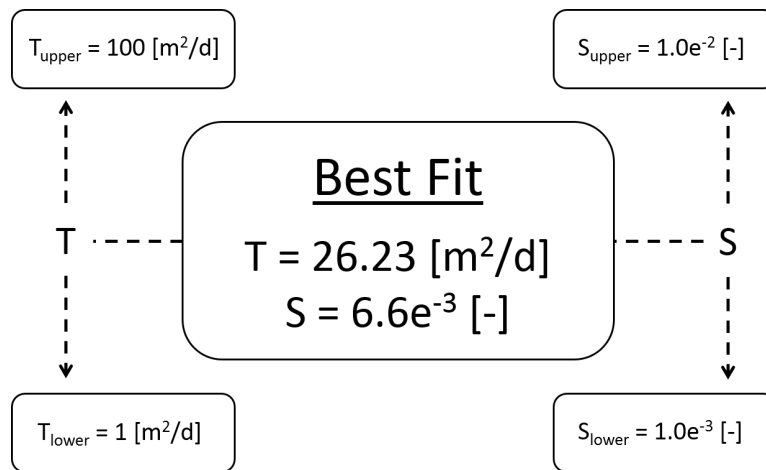
- Performance of proposed subsurface models

Three simplified system models were used: a single layer model, a double layer model and a model with two layers and partial penetration of the well (Figure 2.3b - 2.3d). Based on the Root-Mean-Square-Error objective function, none of these systems performs consistently better or worse than any of the others. Therefore, the most simple (the single layer) model is applied in the rest of this research.

T & S values

Drawdown measurements are taken in the extraction well. This set-up deviates from the desired common standard (Kruseman and de Ridder, 2000). It should be kept in mind that the quality of the data can be questioned. At each location different combinations of parameters yielded similar drawdown curves. This is likely a consequence of only having measurements inside the extraction well. The different models that were applied in the analysis of the data did not yield significantly different results. It is clear that due to the lack of groundwater measurements in the vicinity of the pumping wells, there is some uncertainty in the derived subsurface parameters.

The results from Bingo are used in further analysis. A bandwidth is defined to deal with the uncertainties mentioned in Section 2.3. Upper and lower limits for T and S values are derived. The bandwidth is presented in Figure 2.9. Transmissivity limits are based on the obtained values in Section 2.3 and some factor of safety. For the definition of the storativity values a different approach was used. The parameters limits are based on more commonly found values. The chosen lower limit storativity (S_{lower}) corresponds with the situation of a confined aquifer, while the upper limit (S_{upper}) related more to the specific yield of a phreatic storage (Fitts, 2012; Strack, 1989).

Figure 2.9: Transmissivity (T) & storativity (S) bandwidth selection

3

ASR system - Improvements & sensitivities

In the north of Ghana farmers are in search of sources to increase the water availability during dry season. This chapter investigates to what extent an Aquifer Storage and Recovery (ASR) system, and the potential improvements of the system, can provide solutions. The potential improvements to ASR systems are studied with a geohydrological model of a single ASR system. The geohydrological conditions are derived from field measurements (Chapter 2.4).

In Section 3.1, the different soil scenarios are presented and a base ASR system model is defined. The types of ASR system improvements that are examined, the sensitivity analysis and test criteria are included in this section. The year-round performances of the modelled ASR system are explained in Section 3.2. Section 3.3 contains the results of three types of ASR system improvements; (a) the extension of daily pumping time, (b) the enlargement of the borehole diameter, and (c) the reduction of the well skin resistance. In Section 3.4, the ASR systems interaction with the environment is explored with a sensitivity analysis on; (a) the degradation of well depth by clogging; (b) the shortening of the wet season inundation time, and (c) the reduction of the wet season inundation levels. The chapter ends with conclusions in Section 3.5.

3.1. Methods - ASR system simulation

In this section the model set-up for simulating an ASR system is described. The applied representations of (northern Ghana) natural conditions are defined. The section contains information on soil scenarios, the base ASR system model (reference), the types of ASR system improvements that are studied and a description of the sensitivity analysis. The described methods are implemented in the subsequent parts of this Chapter (Section 3.2 - 3.5). Additional information on the modelling environment (MODFLOW) is included in the Appendices F - E.

3.1.1. Soil scenarios

The geohydrological conditions in northern Ghana are represented by the results from the aquifer test data analysis in Chapter 2. The parameter bandwidth (Figure 2.9) is used to derive model scenarios representative of geohydrological conditions in northern Ghana. Transmissivity (T) values in the range of 1 - 100 (m^2/d) and storativity (S) values between $1\text{e-}3$ - $1\text{e-}2$ (-) are used to define five soil scenarios. An overview of the research soil scenarios is presented in Figure 3.1.

3.1.2. Base ASR system model definition (reference)

The applied geo(hydro)logical conditions in the base model are tailored to results of the northern Ghana study site inspections and the borehole log-sheets (Appendix A). The simplified model represents a hypothetical 'standard' ASR system. The base model is a reference, to which the impact of system improvements can be compared. The overall representation of the base model (e.g. subsurface, well characteristics and simulation time frame) is presented in Figure 3.1. The Figure also contains the different soil scenarios.

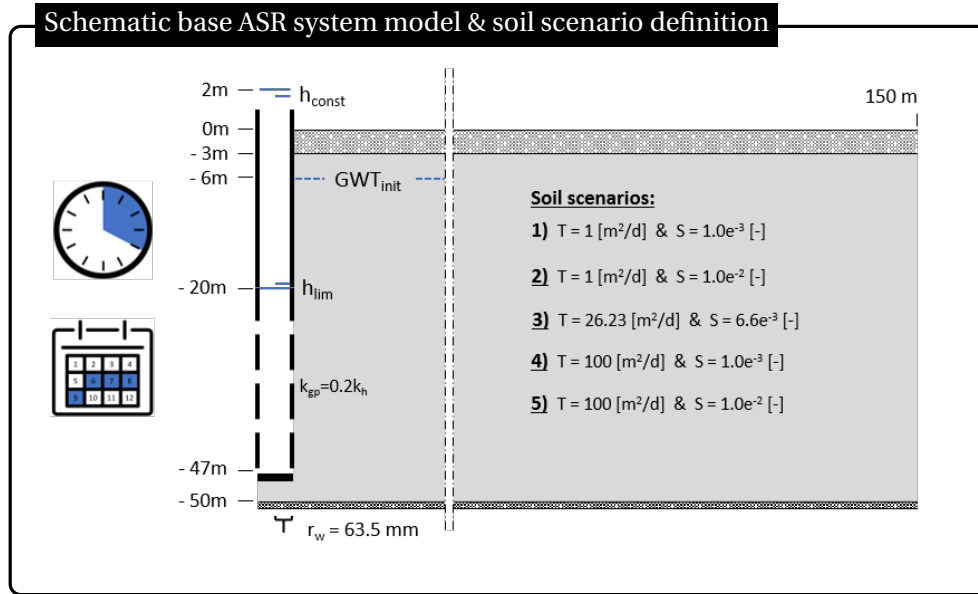


Figure 3.1: Schematic base ASR system model & soil scenario definition

Subsurface

The interaction between the ASR system and the upper 50 m of subsurface is simulated. The model top is bounded by a 3m-thick poorly permeable soil layer. The well penetration (partially) occurs in the underlying 47 m thick aquifer. With an elevation of -6 m the initial groundwater table (GWT) is positioned just under the top of the aquifer, which means the model is unconfined. The T and S values, defined in the soil scenarios of Section 3.1.1 (and Figure 3.1), are applied to this aquifer. The aquifer is assumed to be homogeneous and horizontally isotropic, while the vertical anisotropy is $1/4$ (-). Based on the models used to simulate the pumping tests (Section 2.2.2), the ASR system model boundary is defined at a radial distance of 150 m. The influence of the well is assumed to be negligible at this distance. More information on the derivation of the model extent can be found in Appendix F.2.

Well dimensions & pump placement

The base model contains a single well with a radius of 0.0635 m (2.5 inch) and a total length of 47 m. It is assumed the well (depth) is entirely clean. Well-screen perforations are present from 20 m to 47 m below the model top (screen length 27 m). More details on the hydraulic conductivity of the well screen are described below. Dry season groundwater withdrawal is possible through the installation of a pump. The well contains a submersible pump positioned at an elevation of -30 m. The maximum drop in GWT is limited to an elevation of -20 m (14 m drawdown relative to initial conditions). This prevents the water level from dropping below the well-screen elevation and the pump.

Well hydraulic conductivity

The soil around a well and the well-screen itself have different hydraulic properties than the surrounding aquifer, which is taken into account through the well skin resistance/conductance parameter. In this research the well hydraulic conductance is defined by the use of Equations 3.1 - 3.4.

$$cond = \frac{2\pi r_w b}{c_{skin}} \quad (3.1)$$

$$c_{skin} = \frac{\Delta r_{skin}}{K_{skin}} \quad (3.2)$$

where $cond$ (m^2/d) is the well hydraulic conductance, r_w (m) is the radius of the well, c_{skin} (d) is the well skin resistance, Δr_{skin} (m) is the well skin (radial) length and K_{skin} (m/d) is the well skin hydraulic conductivity.

As stated by Houben (2015), the hydraulic conductivity of a sequence of materials (i.e. well-screen, gravel-pack and aquifer) can be calculated by Equation 3.3 (1D flow). In the research model, the dimension of the cells containing the well is equal to the well radius (Appendices F & E). Therefore, the well skin conductance is assumed to be dependent on the materials of the well-screen and the gravel-pack only. In this case, the well skin hydraulic conductivity corresponds with the simplified variant of Equation 3.3; Equation 3.4.

$$K_{tot} = \frac{\Delta r_{tot}}{\frac{\Delta r_{sc}}{K_{sc}} + \frac{\Delta r_{gp}}{K_{gp}} + \frac{\Delta r_{aq}}{K_{aq}}} \quad (3.3)$$

$$K_{skin} = \frac{\Delta r_{skin}}{\frac{\Delta r_{sc}}{K_{sc}} + \frac{\Delta r_{gp}}{K_{gp}}} \quad (3.4)$$

where K_{tot} , K_{skin} , K_{sc} , K_{gp} and K_{aq} (m/d) are respectively the total, the well skin, the well-screen, the gravel-pack and the aquifer hydraulic conductivities and Δr_{tot} , Δr_{skin} , Δr_{sc} , Δr_{gp} , Δr_{aq} (m) are the corresponding (radial) length intervals of these materials.

The well skin length (Δr_{skin}) equals the sum of the length of the well-screen Δr_{sc} and the gravel-pack Δr_{gp} . An ASR system well-screen length of 0.005 m is measured. The radius of the soil around the well, the gravel-pack, is undetermined. As stated by Bot (2016), for proper installation a minimum radial length of 0,125 m is required. This value is applied in the research.

Like the summed radial lengths, the well skin hydraulic conductivity (K_{skin}) accounts for the combined conductivity of the well-screen (perforations) and the gravel-pack around the well. The hydraulic conductivity of the well screen (K_{sc}) is based on research done by Houben (2015). Perforation sizes (screen slot width) of 2 mm are measured (study site investigation). These screen sizes correspond with a (clean) hydraulic conductivity (K_{sc}) of 1 m/s (Houben, 2015). As stated by Konikow et al. (2009), the well skin hydraulic conductivity (K_{skin}) is typically expected to be lower than the aquifer hydraulic conductivity (K_h). To meet this requirement, the gravel-pack hydraulic conductivity (K_{gp}) is assumed to be 1/5 of the, soil scenario dependent, aquifer hydraulic conductivity (K_h).

Time frame

As stated by the Canadian International Development Agency (2011), the northern Ghana regions encounter a single wet season of approximately four months (dependent on the year and altitude) annually. Interviews with local inhabitants (site visits) confirmed this. Locals indicated inundation levels of 0.5 m - 4 m, with a variable time-span from weeks till the four months of wet season (Appendix C).

Seasonal system performance is simulated by using a model period of one year. In the (simplified) model it is assumed the region encounters flooding for the entire duration of the wet season. A flood duration of four months is taken into account, starting on June 1st and ending on September 30th. The flooding is simulated by adding a constant water level on top of the ASR system. A constant (122 days) 2 m inundation level is assumed (Figure 3.1). In the subsequent eight months of dry season (October-May) no flooding or rainfall is taken into account. In accordance with the data obtained in the ASR system monitoring and interviews with farmers, groundwater withdrawal takes place during 4 hours of pumping every day. For the purposes of this research it is assumed the hypothetical groundwater withdrawal last for as long as the dry season (243 days).

Modelling environment - MODFLOW

The computational modelling of the ASR system is done with Modular Ground-Water Flow Model (MODFLOW), a finite difference model for groundwater flow developed by the U.S. Geological Survey (USGS). MODFLOW is the international standard in groundwater simulation (Harbaugh, 2005; Niswonger et al., 2011). More information on the applied inputs can be found in the Appendices F - E.

3.1.3. System improvements

As stated by Bakker (2010) and Ward et al. (2007), the success and sustainability of an ASR system is amongst others dependent on the length of injection, storage and recovery; the well dimension; and potential clogging of the well screen. Based on these findings, the following three system improvements have been defined:

- a) Extension of daily pumping time:
The base model dry season pumping time (4 hours daily) is increased (by 1 hour steps) up to a maximum daily pump operation of 8 hours.
- b) Enlargement of borehole diameter:
The base model radius (0.0635m) is multiplied by a factor (ranging from 2 to 5) which yields a well radius of up to 0.3175 m.
- c) Reduction of well skin resistance:
The impact of the well skin resistance is studied by altering the hydraulic conductivity of the gravel-pack. In four equal steps, the base model gravel-pack hydraulic conductivity (K_{gp}) is increased to a maximum of $(9/5)*K_h$. Note, well skin hydraulic conductivities larger than the aquifer hydraulic conductivities become part of the research.

3.1.4. System sensitivities

The boundary conditions governing inflow into the aquifer are assumed to be constant. Also the degradation/maintenance of the wells is not taken into account in the simulations. To examine the impact of these approximations on the model results, three types of model modifications are included in a sensitivity analysis:

- a) Degradation of well depth (clogging):
The study site observations suggest that ASR systems in northern Ghana can be vulnerable to the accumulation of sedimentation, effectively causing the well penetrations depth decreases over time. The reduction is simulated by decreasing the well-screen length. An initial screen length of 30 m (longer than base model) is reduced in 5 m steps to a total screen length of 10 m.
- b) Shortening the wet season inundation time:
Within northern Ghana the duration of the wet season is spatially dependent and wet season durations naturally differ between years (Canadian International Development Agency, 2011). The wet season duration is reduced from four months (Jun-Sept) till one (Aug).
- c) Reduction of wet season inundation level:
The impact of lower inundation levels is analysed. Relative to the base model (Δh is 8 m), the difference between flood level and GWT is reduced (in steps of 2 m) to a minimum of Δh is 2 m.

3.1.5. Sustainability definition

As mentioned in Section 3.1.2, the synthetic ASR system performance is simulated for one year. A distinction can be made between the wet and dry season. The wet season ASR system functionality is characterized by the groundwater recharge. The inflow volume is calculated and the impact of this inflow on the GWT is analysed. In the subsequent eight months of dry season, the system works in reverse. In this period, maximum pump discharge and the accompanied impact on GWT is of key interest. The relation between recharge and discharge is considered. This is done by the introduction of the 'Recovery ratio' $R_{\%}$ (Equation 3.5). The recovery ratio is similar to the Recovery Efficiency (RE) applied by Ward et al. (2007). Ward et al. (2007) mentions the RE ($R_{\%}$) is a measure to indicate the degree of recovery, i.e. RE = 1 (-) implies complete recovery.

$$R_{\%} = \frac{V_{out,tot}}{V_{in,tot}} \quad (3.5)$$

Where $R_{\%}$ is the year-round recovery ratio (-), $V_{in,tot}$ (m^3) is the wet season total volume recharged and $V_{out,tot}$ (m^3) is the dry season total volume discharged.

In this research it is assumed the ASR system should be used sustainably. And 'sustainability' is defined as the situation in which the $R_{\%}$ is smaller than or equal to 1 (-). Therefore, a 100% recovery ratio is set as an upper limit in ASR system performance. This means the dry season pumping discharge (upper limit) is determined based on the wet-season inflow.

3.2. ASR system base model performance

This section describes the results obtained with the year-round performance of the ASR system base model for all five soil scenarios.

3.2.1. Wet season

The four months of wet season flooding are simulated with a constant head of 2 m on top of the ASR system. The difference between the level of inundation and the groundwater table (GWT initially -6 m) results in a gravity based groundwater recharge. At the start of the simulation the head difference (hydraulic gradient) is highest, which means the initial inflow is also above average. The recharge causes the GWT to increase and the hydraulic gradient decreases over time. In the first days (approximately five days) the hydraulic gradient declines rapidly. Thereafter, the decline remains present but progresses excessively slow. Although the inflow does not reach a steady state, the rate of recharge is relatively constant over the four month infiltration period. This system recharge performance is (together with different inundation durations en levels) visualized for soil scenario 3 in the Figure H.10 and H.11, but takes place in all soil scenarios.

As an visual example of the impact of wet season flooding on groundwater, the soil scenario 3 radial cross-sectional head contours at the beginning (day 5) and end of wet season (day 122) are presented in Figure 3.2. The (partially aquifer penetrating) well is positioned at the absolute left and the groundwater head contours are presented in a 100 m radial distance (from the well) for the top 50 m of subsurface. A comparison between the Figures 3.2a and 3.2b shows that the impact of inflow on the groundwater heads increases over time, in terms of levels and in radial distance.

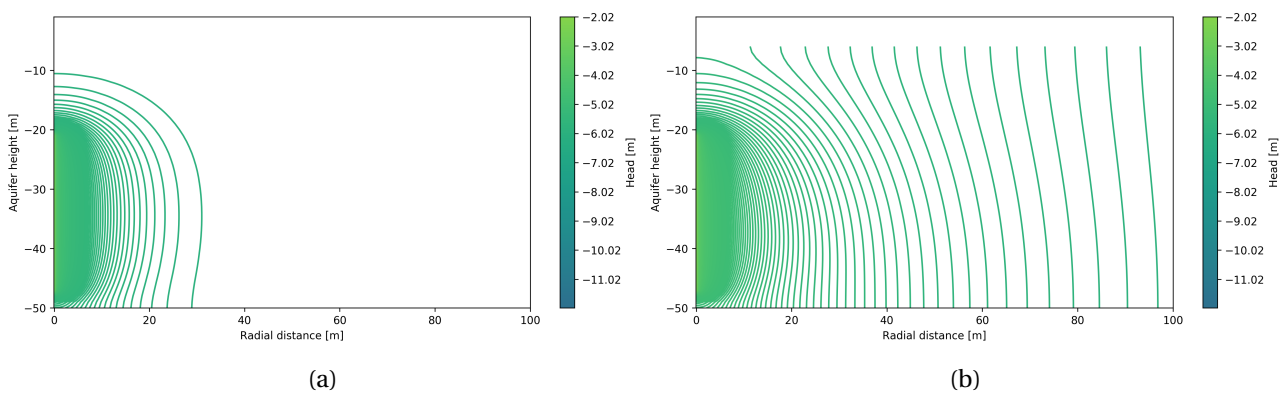


Figure 3.2: Base ASR system model, the soil scenario 3 cross-sectional head contour plot after (a) five days and (b) 122 days of infiltration

The head contour values upto -3 m to -2 m in Figure 3.2a suggests that a significant (more or less instant) head increase is encountered close to the well-screen. The groundwater head does not reach the level of flooding, not even at end of the wet season (Figure 3.2b). The groundwater recharge is hampered by the well skin resistance and soil conditions. In terms of radial distance the impacts on the GWT remain limited (Figure H.1, Appendix H.1). After 122 days of infiltration the increase in groundwater level is little at distances of 60-80 m in all scenarios.

The scenario dependent results on total wet season inflow volumes are shown in Table 3.1. Differences between the soil scenario 1 and 2 as well as the scenarios 4 and 5 are small. These soil scenarios only differ in the applied storativity (S) values. The variance in storativity (defined in bandwidth) appears to have only limited influence on the inflow of water. The differences in inflow volumes between the soil scenarios with different transmissivities is large.

Table 3.1: Base ASR system model, wet season recharge volumes for the different soil scenarios

	Sc 1	Sc 2	Sc 3	Sc 4	Sc 5
Volume in (m ³)	207.57	208.68	5357.45	20330.33	20333.15

3.2.2. Dry season

The simulated well discharge (4 hours of pumping daily) is set to the maximum withdrawal rate such that the ASR system is sustainable. In all soil scenarios, this base model maximum discharge rate cannot be sustained because the maximum allowable drawdown (-14 m) is reached (visualized for soil scenario 3 in Figure 3.3). The head bound (-20 m in well) is reached very quickly after the start of pumping operation. In the subsequent hours of pumping, the head bound continues to limit the discharge rate. In reality, pumping takes place at a more or less constant rate. This means that the modelled outcomes overestimate the discharge volumes slightly. A comparison between pumping rates per day shows a difference in total discharge on day one relative to the other days of pumping. The first day of pumping generates somewhat higher volumes. In the subsequent days discharge volumes are by approximation equal.

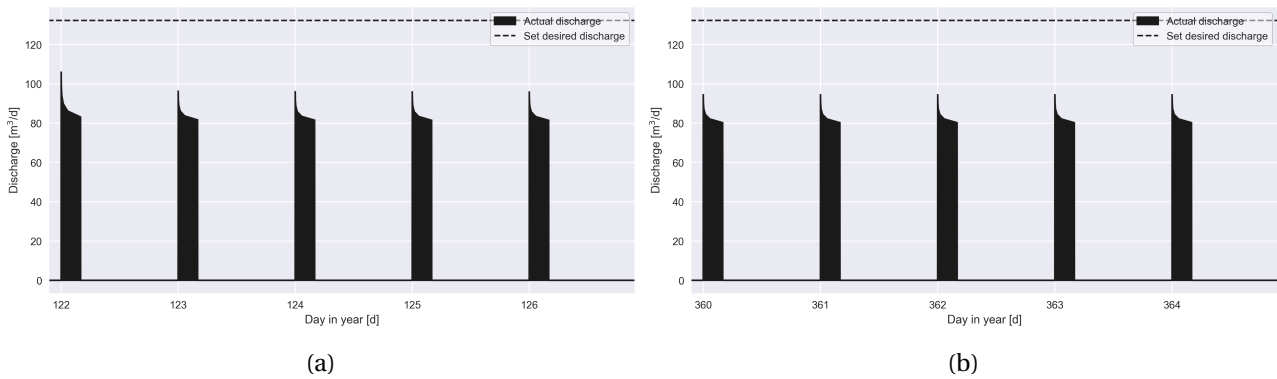


Figure 3.3: Base ASR system model, the soil scenario 3 discharge performance for (a) the first five days and (b) the last five days of dry season

The impact of well discharge on groundwater (example soil scenario 3) is presented in the cross sectional contour plot of Figure 3.4. After the first days of pumping the transition from wet season (recharge) to dry season (discharge) is still observable by the characteristic shape of the head contours (Figure 3.4a). Towards the end of the year this impact is no longer present (Figure 3.4b). Over the entire dry season, the head bound (-20 m) is not observed in the contour plot. This can be justified by the obstructing influence of the well skin resistance and soil conditions on the discharge rates. The maximum allowed drawdown (14 m) is reached in the well, and outside the well the drawdown is lower on account of well-screen resistance. More visualizations on the base model performance can be found in Appendix H.1.

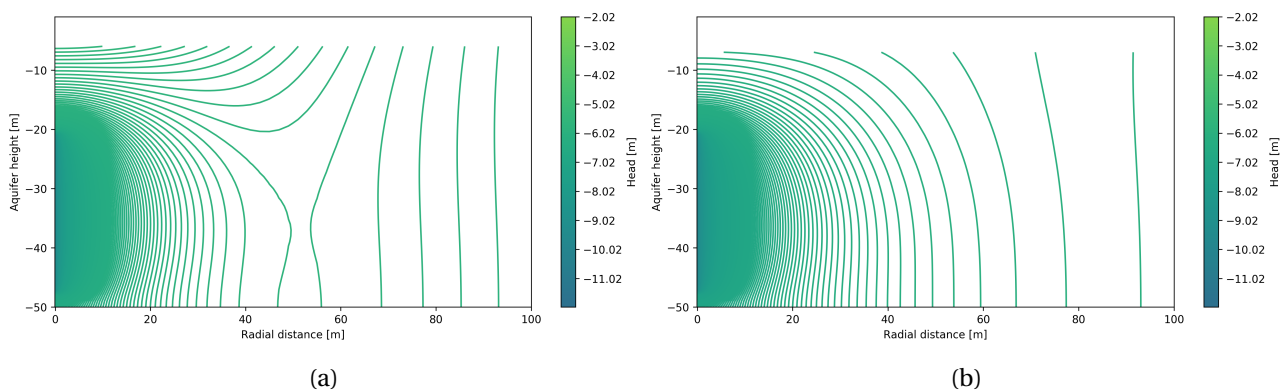


Figure 3.4: Base ASR system model, the soil scenario 3 cross-sectional head contour plot after four hours of pumping on (a) the first day (day 123) and (b) the last day (day 365) of dry season

Unlike the outcomes in recharge, all different soil scenarios show distinctive results in total discharge volumes. The effect of variation of storativity on flow is more pronounced for discharge than for recharge. However, the total volumes withdrawn are still in the same order of magnitude for the soil scenarios 1 and 2, and scenarios 4 and 5. The transmissivity (range) has a stronger impact on discharge variability than

storativity.

Table 3.2: Base ASR system model, dry season discharge volumes for the different soil scenarios

	Sc 1	Sc 2	Sc 3	Sc 4	Sc 5
Volume out (m ³)	129.84	137.76	3299.99	12080.08	12353.58

3.2.3. Recovery ratio $R_{\%}$

The recovery ratios $R_{\%}$ are in the same order of magnitude for all soil scenarios (Table 3.3). In all scenarios the base model recovery ratio stays below 100%. In eight months of pumping 4 hours per day it is not possible to fully recover the volumes infiltrated due to four months of constant inundation (2 meter) on top of the well. A reason for this is that the inflow bubble may level out over the aquifer due to the hydraulic gradient (Bakker, 2010). The discharge water is not by definition the 'original' recharge water. The recovery ratios show that in all cases the base model ASR system use (discharge) is not limited by the boundary of sustainability.

Table 3.3: Base ASR system model, recovery ratios $R_{\%}$ for the different soil scenarios

	Sc 1	Sc 2	Sc 3	Sc 4	Sc 5
$R_{\%}$ (-)	0.626	0.660	0.616	0.594	0.608

3.3. ASR system improvements

This section presents the impact of potential improvements of an ASR-system. The model performances are described by the following criteria: total recharge, discharge and Recovery ratio ($R_{\%}$). The results are compared to the outcomes of the base ASR system model.

3.3.1. Extension of daily pumping time

A simple method to increase discharge from the ASR system is to increase the amount of pumping time. Except from additional fuel and possibly storage requirements (tanks), no further modifications are required. Base model pump operation was set to be 4 hours per day for 243 days. This study is pointed at a maximum time-scope of pumping for 8 hours daily. As visualized in Figure 3.5, the system improvement is implemented in 4 simulation steps.

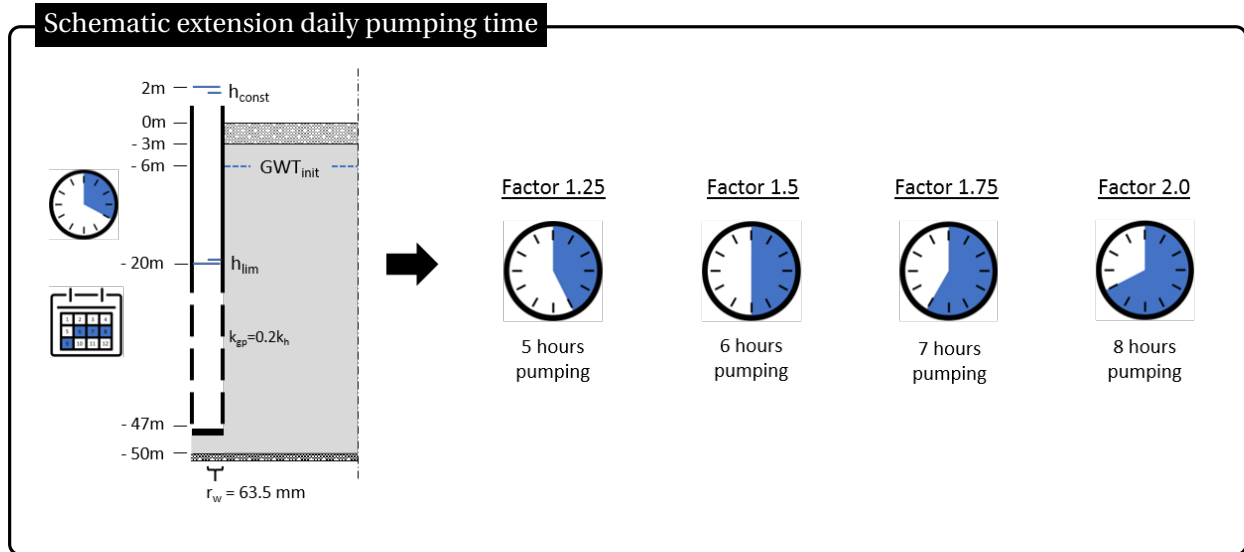


Figure 3.5: Schematic extension daily pumping time

There are no changes in the wet season for this system improvement as pumping operation only applies to the dry season. As visible in Figure 3.6, discharged volumes are affected by the duration of pumping. An approximately linear ascending relation is observed in the obtained total discharge volumes for all soil scenarios. The performance can be justified by the daily discharge performance (Figure 3.3). After four hours of pumping in the dry season the maximum discharge rate (as governed by the drawdown limit of -20 m) is reached. Increasing the amount of operational hours means the total extracted volume of water increases approximately linearly with pumping time.

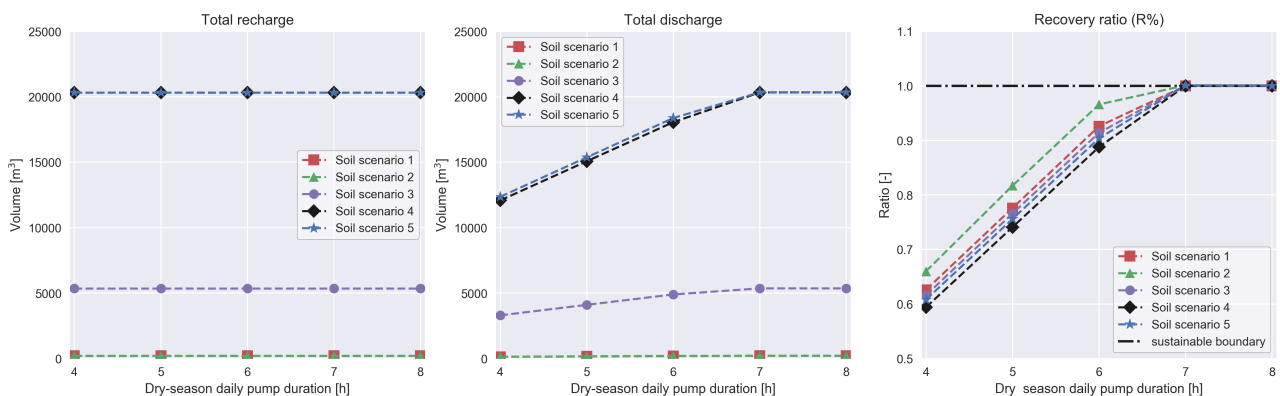


Figure 3.6: Results of the yearly total recharge volumes, discharge volumes and recovery ratios - by extension of the daily pumping time

By the extension of the daily pumping time, the total discharge volumes can equal the total inflow volumes (four months). A 100% recovery is obtained in the situation of 6 till 7 hours of daily pumping in all soil scenarios. When base model conditions (2 m constant inundation for four months) apply, it is advisable pumping time should not exceed 6 till 7 hours per day. This way, the ASR system use will remain sustainable.

3.3.2. Enlargement of borehole diameter

The enlargement of the borehole diameter is an adjustment that can not be applied on existing systems. If the appropriate equipment is present (e.g. drilling machinery), the enlargement can be applied to new constructions. The enlargement is tested by a stepwise (4 steps) increase of the original borehole radius (Figure 3.7).

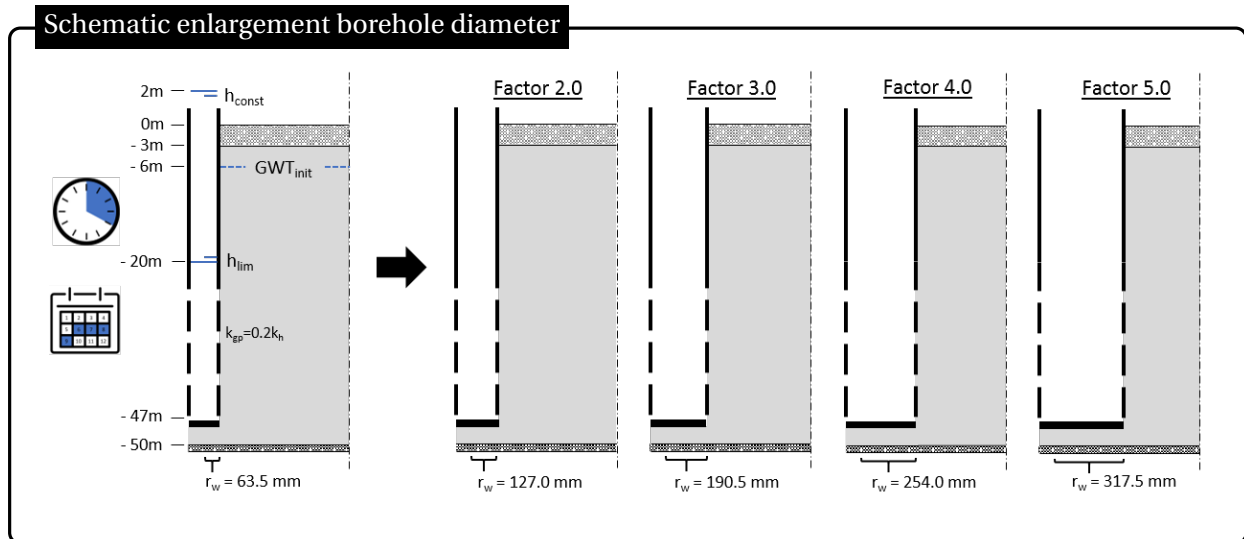


Figure 3.7: Schematic enlargement borehole diameter

The increase of the borehole diameter is beneficial for both groundwater recharge and discharge. In Figure 3.8, it can be seen that a non-linear ascending relation is present between the ASR system diameter and the total inflow, outflow and recovery ratio. Well-size improvement is beneficial, but a decreasing positive effect is obtained. Total recharge and discharge volumes of respectively ~ 2.3 and 2.3 to 2.7 times the base model capacities are obtained in the (diameter enlargement) scope of this research (See also Figure H.4, Appendix H.2).

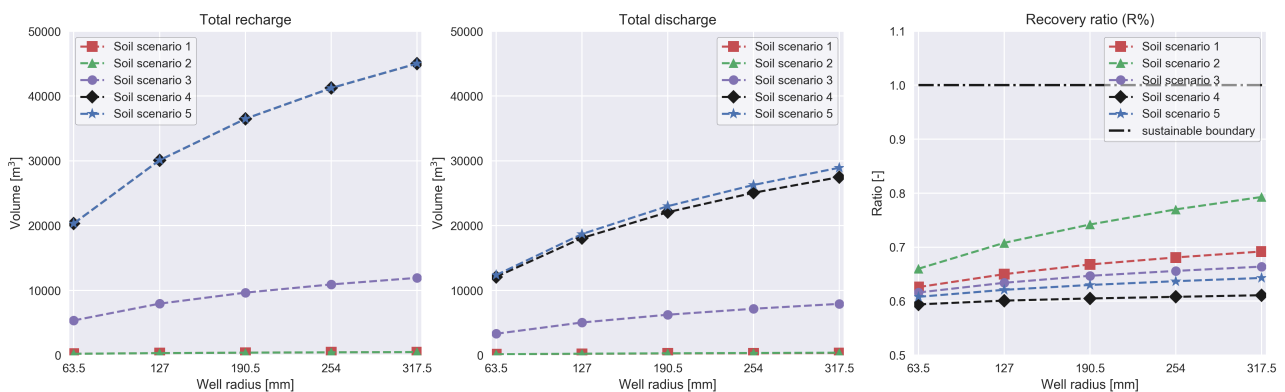


Figure 3.8: Results of the yearly total recharge volumes, discharge volumes and recovery ratios - by enlargement of the borehole diameter

3.3.3. Reduction of well skin resistance

This improvement might possibly be applied to existing systems (think of maintenance of the well-screen) but is also relevant to newly installed systems. Based on the statements done by Konikow et al. (2009) and

Houben (2015), the base model is designed with a gravel-pack that is moderately permeable. The (simulated) improvements are implemented by a stepwise increase of the the gravel-pack hydraulic conductivity. As visible in Figure 3.9, gravel-pack hydraulic conductivities that exceed the soil hydraulic conductivities are considered.

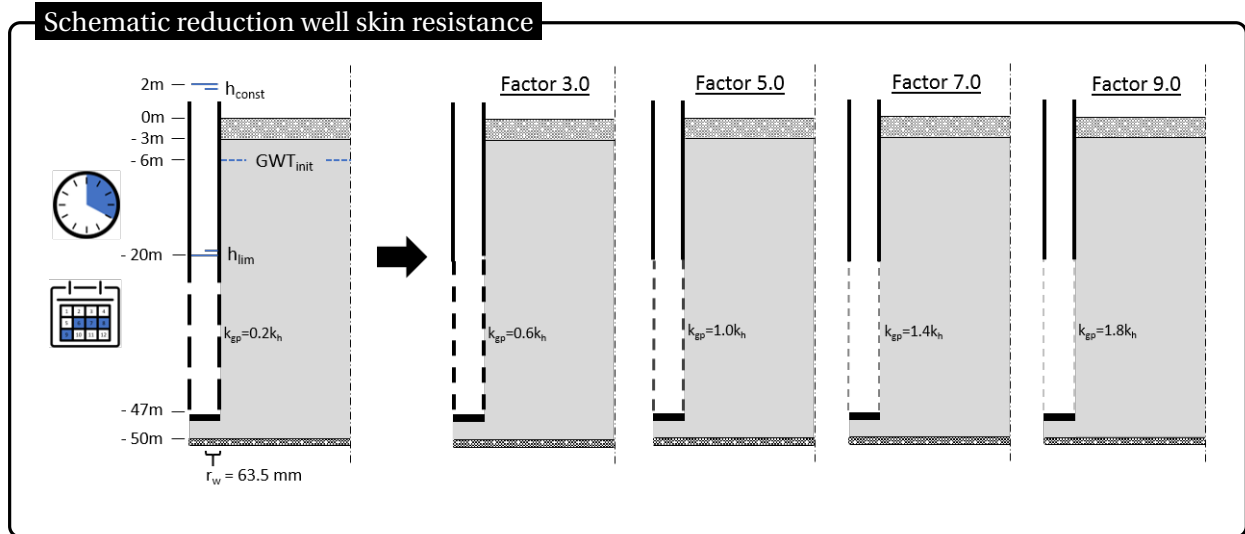


Figure 3.9: Schematic reduction well skin resistance

Figure 3.10 presents the results of the (simulated) improvements of an ASR system by the modification of the gravel-pack hydraulic conductivity. It can be seen that the ASR system capacity (total recharge, discharge and recovery ratio) increases by improved gravel-pack permeabilities. A non-linear ascending relation is present. In the scope of this research (upto nine times the base model gravel-pack permeability), base model inflow and outflow volumes are (slightly) more than doubled (Figure H.5, Appendix H.2). Significant system improvements can be made, especially in conditions with low well-screen permeabilities. When considered from another perspective, these results indicate that system performance can suffer significantly when maintenance (i.e. keeping well skin resistance as low as possible) is lacking.

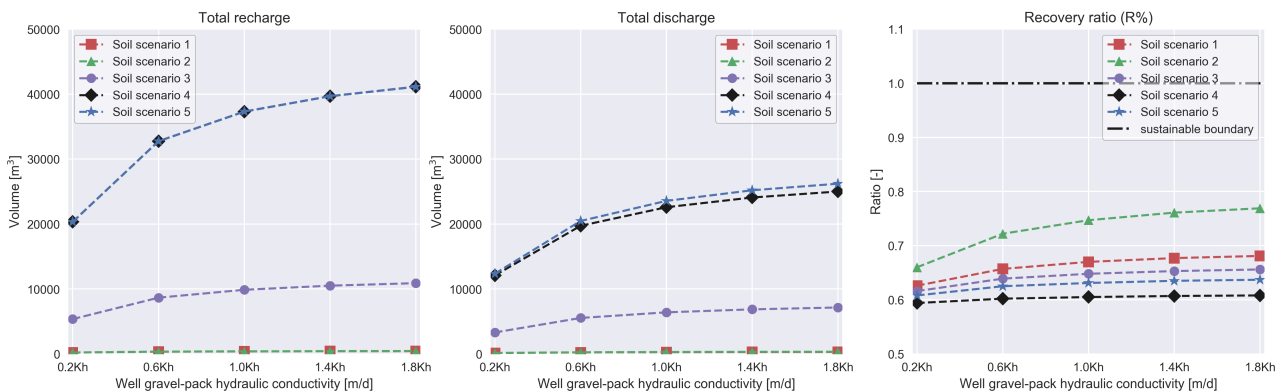


Figure 3.10: Results of the yearly total recharge volumes, discharge volumes and recovery ratios - by reduction of the well skin resistance

Note, the figures in this section show results for all soil scenarios. Due to the differing order of magnitude, the results for the scenarios with low transmissivities are not clearly visible. See the figures of Appendix H.2 for a more detailed look on the impact of system improvements (compared to base model performances).

3.4. ASR system sensitivities

This section explores the impact of changing natural conditions on the system performance. The system sensitivity is examined by looking into: total recharge, discharge and recovery ratio ($R\%$).

3.4.1. Degradation of well depth by clogging

Prior simulations (Section 3.2 - 3.3) were done with a clean borehole (the whole well is capable of infiltrating and extracting groundwater). The northern Ghana fieldwork inspections (site visits) revealed that sand and/or clay can accumulate in the borehole. The presence of soil can reduce the well penetration depth. The effect of borehole clogging is simulated by decreasing the well-screen length (Figure 3.11). In four successive steps the 30 m screen length of an already partially penetrating well is reduced to a minimum of 10 m.

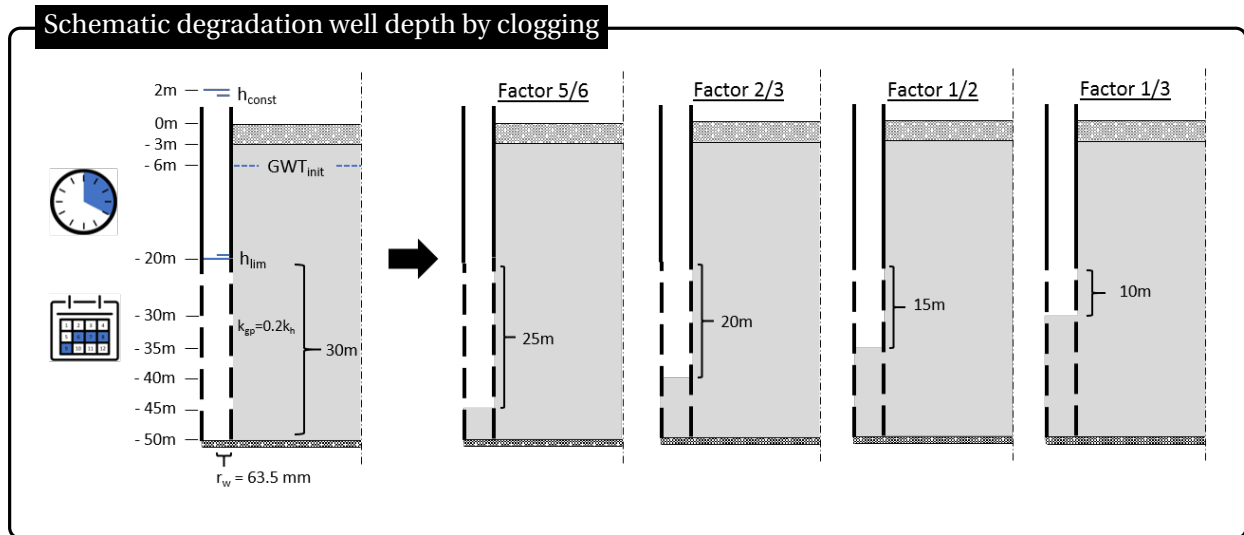


Figure 3.11: Schematic degradation well depth by clogging

Figure 3.12 shows the system performance while the borehole screen length is reduced. For the considered soil scenarios (homogeneous aquifer) and the range of well-screen lengths, the relation between screen-length and inflow, outflow and recovery ratio is nearly linear. It is clearly important to properly maintain the well and ensure the penetration depth is not significantly reduced. This can be done by using a pulse drill to clear out the soil at the bottom of the well.

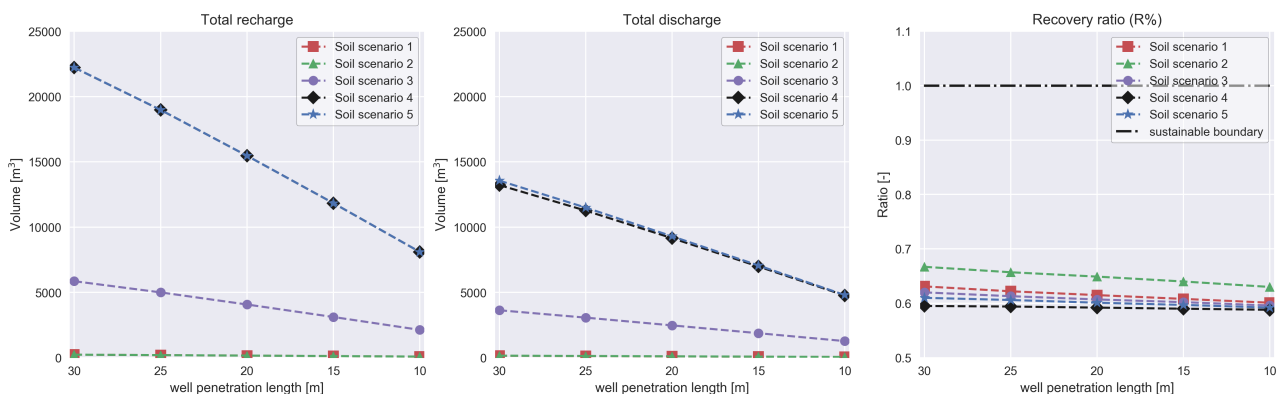


Figure 3.12: Results of the yearly total recharge volumes, discharge volumes and recovery ratios - by degradation of the well depth

The deviation from a linear relation is not significant and difficult to deduce from the figure. See Appendix H for a more detailed perspective. The section contains information on the average specific recharge and discharge volumes (m^3/m screen) for the different well-screen lengths. Moreover, the distribution of the recharge volumes over the (variable) well-screen length is presented for soil scenario 3 (Figure H.9).

3.4.2. Shortening wet season inundation time

Within northern Ghana the duration of the wet season is spatially dependent. At higher latitudes the wet season time-span is generally less than four months (Canadian International Development Agency, 2011). Besides, wet season duration differs annually. The relation between the wet season duration and the ASR system performance is described in this part of the sensitivity analysis. The flood duration is reduced from 4 months (June-September) in the base model to one month (August) in steps of one month.

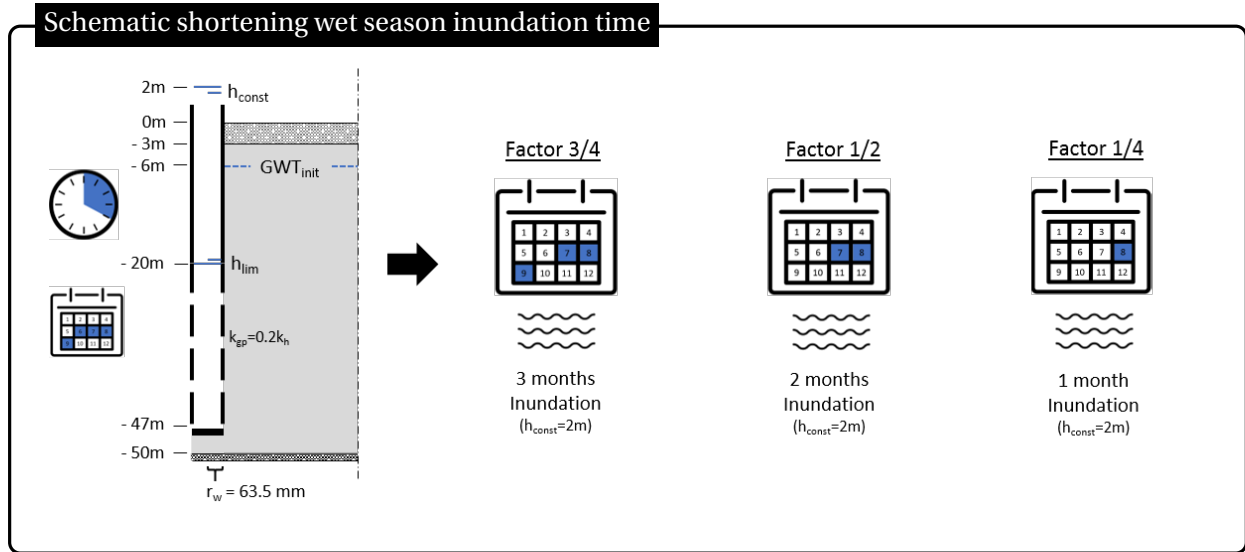


Figure 3.13: Schematic shortening wet season inundation time

Figure 3.14 shows an approximately linear relation between the inundation time and the obtained total recharge volumes. A fractional reduction of the (constant level) flood duration, causes an almost equal fractional decrease in the total volumes recharged. The system performance can be explained by the fact that shortly after the inundation start (after approximately 5 days) the inflow rate is nearly constant (as mentioned in Section 3.2.1). The reduction in total discharge volumes originates from the defined boundary of sustainable system use. In the cases where the inundation time-span is less than 2 months the withdrawal of groundwater is limited by the maximum allowed 100% recovery. More details on the development of inflow volumes over (inundation) time can be found in Figure H.10, Appendix H.3.

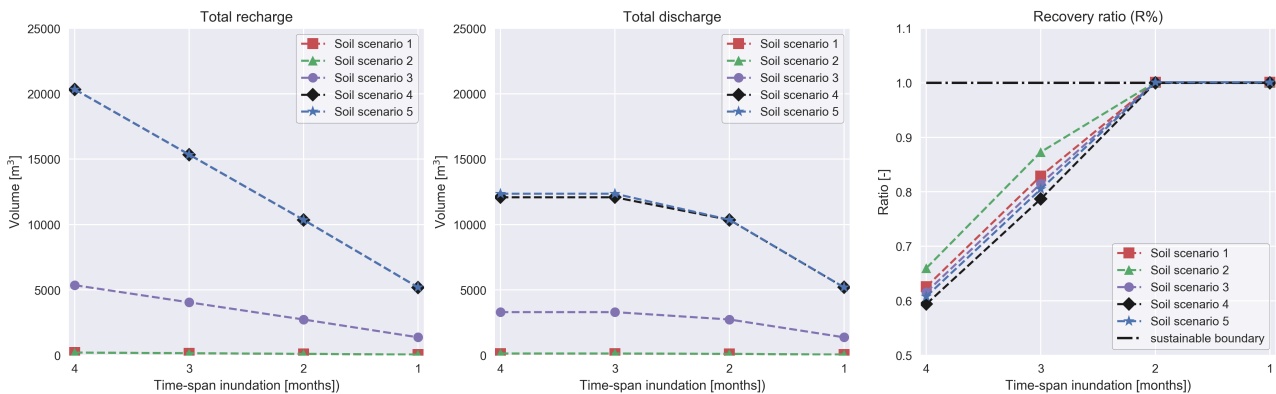


Figure 3.14: Results of the yearly total recharge volumes, discharge volumes and recovery ratios - by shortening the wet season inundation time

3.4.3. Reduction wet season inundation level

In northern Ghana groundwater tables are not fixed and different flood levels are encountered (Appendix C). The impact of lower flood inundation levels is analysed in this research part. Relative to the base model (Δh is 8 m) the difference between flood level and GWT is reduced (in steps of 2 m) to a minimum of Δh is 2 m (Figure 3.15).

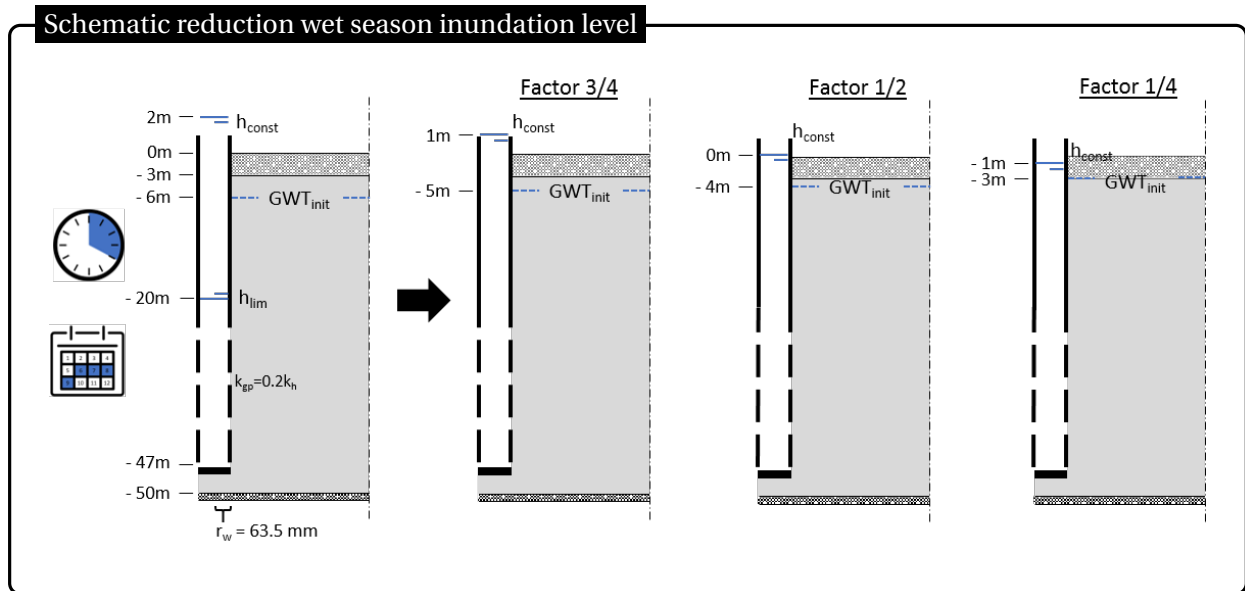


Figure 3.15: Schematic reduction wet season inundation level

Figure 3.16 presents the impact of the (simulated) reduced flood levels. It can be seen that the total recharge volumes corresponds linearly with the constant level of inundation. Shortly after the start of the flooding a constant groundwater head is obtained. As a consequence, the recharge rates become approximately constant over the 4 months of flooding. Due to the defined boundary in sustainable system use (maximum recovery ratio of 100%), a reduction of the total inflow volumes can impose restrictions in discharge volumes. In the research simulations these limitations occur when flood levels (Δh) smaller than 4 m are implemented. More information on the flood level dependent inflow volumes over time can be found in Figure H.11 (Appendix H.3).

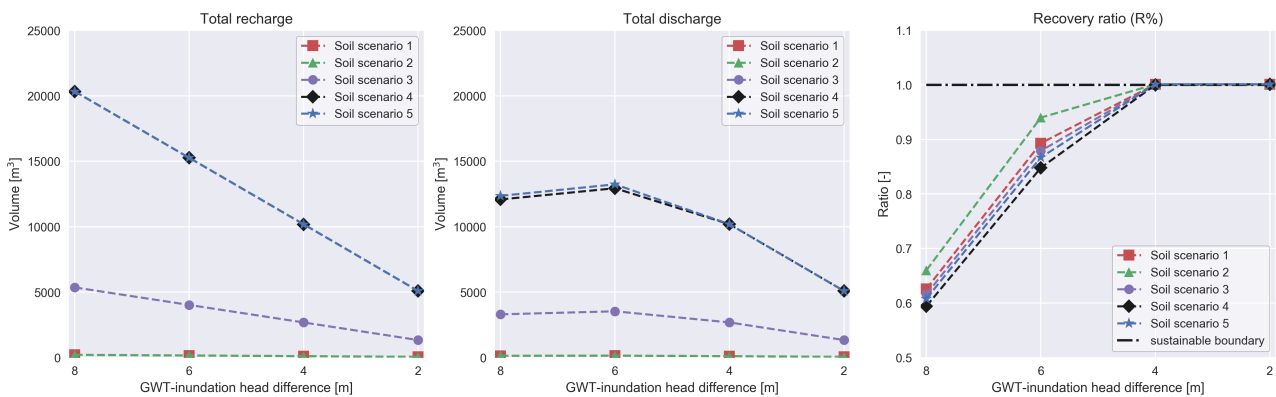


Figure 3.16: Results of the yearly total recharge volumes, discharge volumes and recovery ratios - by reduction of the wet season inundation level

It is worth-mentioning that compared to the base model (Δh is 8 m) the total discharge volumes are slightly higher for the situations with a Δh of 6 m. This is caused by the increase of the level of the GWT to -5 m instead of -6 m. A higher GWT allows for an increased well discharge (drawdown is still limited at the -20 m level).

Note, the figures in this section show results for all soil scenarios. Due to the differing order of magnitude, the results for the scenarios with low transmissivities are not clearly visible. See the figures of Appendix H.3 for a more detailed look on the impact of system sensitivities (compared to base model performances).

3.5. Results & Conclusions

This section contains conclusions on potential improvements in the performance of an ASR system. The conclusions on system performance are drawn from the base model, the simulated ASR system modifications and the system sensitivity analysis.

Performance of an ASR system in northern Ghana

- Recharge & discharge volumes

The total inflow and outflow volumes are both affected by transmissivity. An increase of the transmissivity value, in the range of 1 - 100 (m^2/d), results in recharge and discharge volumes that are significantly higher. The range in storativity values, $1\text{e-}3$ to $1\text{e-}2$ (-), appears to have only limited influence on the recharge volumes, while the discharge volumes increase slightly due to an increased storativity.

- Sustainability

The base ASR system model performances stay within the (defined) limits of sustainable system use. Year-round recovery ratios in the range of 59% to 66% are obtained for the different soil scenarios. In eight months of 4 hours of pumping per day, with a discharge bounded by a maximum drawdown (Δh of 14 m), it is not possible to fully recover the water volumes recharged during four months of constant inundation (Δh is 8 m).

ASR system improvements

- Preservation of sustainable use

Higher total discharge volumes can be obtained by an increase of the daily pumping time. By considering the predefined conditions (e.g. 4 months of flooding, inundation levels of Δh is 8 m), it is recommended to keep daily pumping periods below 6 to 7 hours to ensure sustainable use of the ASR system.

- Increase in total recharge & discharge volumes

In terms of volumes (and recovery ratios), the capacity of an ASR system can be increased by both the enlargement of the borehole diameter and the reduction of the well skin resistance. An increase of the base model well diameter by a factor of 5 results in total recharge and discharge volumes that are respectively ~ 2.3 and 2.3 to 2.7 times the original total volumes. A reduction of well skin resistance by a factor $1/9$ yields approximately twice as much inflow volumes as in the base model, while total available outflow volumes are obtained in the range of 2.1 to 2.4 times the original volumes. The relationship between water availability and the well diameter or well skin resistance is non-linear. The largest gain in system capacities is achieved with the first increase in size or reduction in resistance relative to the base model. Therefore, a significant improvement in system performance can be achieved with relatively small modifications to the ASR reference design.

ASR system sensitivities to nature

- Total recharge volumes

The relation between the partially penetrating well-screen length (ranging from 10 - 30 m) and inflow and outflow is nearly linear for the situations considered in this research. When the active screen length reduces cleaning becomes not only in absolute terms but also relatively (slightly) more important. Within the research time-span, the recharge volumes are linearly related to the inundation period (ranging from 1 - 4 months). Recharge volumes are also linearly related to pressure difference between the inundation level and the groundwater table (Δh ranging from 2 - 8 m).

4

ASR system - Business case

The Aquifer Storage and Recovery (ASR) system performance has thus far been expressed in water volumes. Using simple rules of thumb, the calculated volumes are expressed as financial yield. This chapter offers a rough glimpse to the financial feasibility of an ASR system in northern Ghana.

The methodology of section 4.1 specifies the crops of interest and describes how the pumping costs are derived. Section 4.2 presents the financial yield of respectively the first dry season crop-cycle (tomatoes) and the subsequent crop-cycle (groundnut). In Section 4.3 the ASR system operational pumping costs are discussed. The agricultural yield is compared to the pumping costs in Section 4.4.

4.1. Methods - From water volume to financial considerations

This section contains describes how to make a simplistic financial balance for an operational ASR system. The section is split to two parts. Part one presents information on the crops of interest, the irrigation efficiency and the currency exchange rates. Part two describes operational costs, i.e. how power consumption and costs for groundwater extraction is calculated.

4.1.1. Yield - crops of interest

Some crops need more water than others. Some crops thrive better in northern Ghana climate than others. Some crops are financially more beneficial than others. In other words, many elements are decisive in the process of crop type selection. The focus of this research is not on crop selection. The tomato and groundnut crops (both grown in northern Ghana) have been selected for further analysis. Analysis of the financial considerations of these crops should give an idea of the financial feasibility of ASR systems in northern Ghana.

Crops of interest



Figure 4.1: Crops of interest: (a) Tomatoes and (b) Groundnuts
(visual support by Ben Davis and Lemon Liu from Noun Project - <https://thenounproject.com>)

- Tomato

The second most important vegetable crop worldwide (after the potato) is the tomato. Because of its relatively high (financial) yield, the vegetable is a desired crop for cultivation. After a period of approximately 90 to 120 days the seeds are grown to fully-fledged crops and the tomatoes are ready for harvesting. Over the growth season the crop performs best by the supply of 400 to 600 mm of water (rain-fed). To reduce the chances of diseases (pests and infestations) the crop should be cultivated in rotation with other crops. When irrigation is applied, the tomato yield is approximately 45 to 65 ton/ha (FAO, 2018b). The (direct) derivation of crop agricultural yield is based on the average 'water utilization efficiency' (E_y), which equals 11 kg/m³ in the case of tomatoes. For the transformation of agricultural yield to financial benefits, the Esoko march 2018 Ghana average wholesale price is used. The tomato wholesale price is set at a value ranging from 217.86 to 220.43 GHS for a 52 kg crate (Modern Ghana, 2018). For the purposes of this research the highest average value is applied. To summarize:

- Growth season (rain-fed) water consumption: 400-600 (mm)
- Length growth season: 120 (d)
- Water utilization efficiency: $E_y = 11$ (kg/m³)
- Wholesale price: 4.239 (GHS/kg)

- Groundnut

The groundnut is a crop commonly grown in Ghana. The production is often the responsibility of small-holder farmers in the North. Almost the complete Ghana groundnut production originates here (Ghana-made, nd). The growth season length is dependent on the varieties (sequential or alternating). In general harvesting can take place after a period of 90 to 140 days. For a proper single season production, groundnut crops require approximately 500 to 700 mm of water. Rain-fed crops can produce average yields of 2 to 3 ton/ha unshelled nuts. With irrigation these values even reach 3.5 to 4.5 ton/ha (FAO, 2018a). These yields are not often achieved as can be seen from the average yield in Ghana in 2016 of 1.25 ton/ha (FAO, 2018c). The Food and Agricultural Organisation of the United Nations (2018a) average water utilization efficiency (E_y) of 0.7 kg/m³ is used in the calculations. The financial yield fluctuates highly over time. Market forces are dominant in actual returns. The march Esoko 2018 Ghana average unshelled groundnut wholesale price is set at a value ranging from 247.50 to 282.50 GHS for a 82 kg bag (Modern Ghana, 2018). For the purposes of this research the highest average value is applied and interpreted as the unshelled groundnut price. To summarize:

- Growth season (rain-fed) water consumption: 500-700 (mm)
- Length growth season: 123 (d) (assumed)
- Water utilization efficiency: $E_y = 0.7$ (kg/m³)
- Wholesale price: 3.445 (GHS/kg)

As stated before, the time frame of the simulation consists of 243 days of dry season. It is assumed two consecutive growth seasons fit within this period. The tomato growth season is succeeded by a growth season for the production of groundnut. This approach is in line with the recommendation of rotational crop cultivation.

The previous parameters have been derived from brief research into crop types and financial yield and should be treated as assumptions that warrant further research for an in-depth study into financial feasibility. The obtained (financial) yields should solely be interpreted as indicative. In other words, "All rights reserved".

Irrigation efficiency

The dry season agriculture is assumed to be purely dependent on irrigation for the supply of water. Different types of irrigation are suitable in northern Ghana. One can think of border strip/furrow irrigation; a simplistic but inefficient technique. Higher degrees of efficiency can be achieved with sprinkler irrigation.

However the most water efficient method of irrigation is drip irrigation, which is the type of irrigation considered in this calculation. The ASR systems are normally installed with poly-tank(s), pipes and drip hoses. Distances between the extraction and irrigation are small, resulting in limited losses. However, water losses are present due to pipe connections and potential evaporation. Therefore, an irrigation system efficiency of 0.8 (-) is used. 80% of all water withdrawn is assumed to be net usable for crop growth. An assumption that corresponds with drip irrigation efficiencies described by van de Giesen (2013). Note, this efficiency number also accounts for the required schedule in irrigation water amounts. Over the growth season, the required water volumes are assumed to be equal per day.

Financial yield

The calculated water volumes can be expressed as financial returns using the parameters described above. The agricultural yield (kg/m^3) and the weighted crop prices (GHS/kg) are defined. The financial returns are expressed in US dollars for consistency purposes. The Bloomberg financial exchange rate from July 7th, 2018 is applied: 0.2081 USD/GHS (Bloomberg, 2018).

4.1.2. Costs - water withdrawal

The ASR system profits are accompanied by costs. For this research all Capital Expenditures (CAPEX) are unknown and not considered. The same applies for large parts of the Operating Expenses (OPEX), e.g. wages and fertilizer costs. The only costs accounted for in this research are the costs related to the energy (diesel) consumption due to pumping. Outcomes are purely focused on the feasibility of daily operation.

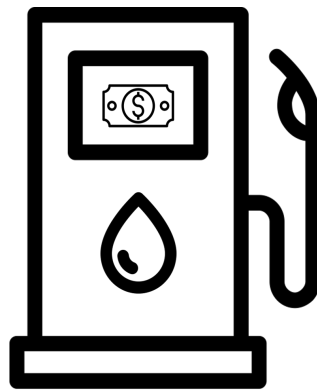


Figure 4.2: ASR system operational pumping costs impression

(visual support by Nociconist, Quan Do and Phonlaphat Thongsriphong from Noun Project - <https://thenounproject.com>)

Pump application

The Pedrollo 4" submergence pump was used during the aquifer tests. The same pump is used as the standard in the subsequent parts of this research. General specifications can be found in Appendix I. The results of the simulations contain time dependent discharge rates (4 hours daily, 243 days). When the discharge rate exceeds the pump capacity an extra identical pump is used. The pumps are operated in parallel ensuring the same heads and efficiencies, while discharge capacities are multiplied (van de Giesen, 2013).

Energy Consumption

The available groundwater has to be lifted to the surface. Depending on the obtained discharges, the lifting action requires a certain magnitude of power (Equation 4.1). For water displacement a distance of 30 m between the pump position and surface level is applied. An extra lift of 15 m is added to account for friction losses and the higher elevation (above the surface) of the poly tank(s). A total head lift of 45 m is applied.

$$N_{net} = g * Q * \Delta H \quad (4.1)$$

Where N_{net} (kW) is the net power required, g (m/s^2) is the gravitational acceleration ($9.81 \text{ m}/\text{s}^2$), Q (m^3/s) is the dry season discharge (time dependent (and in m^3 per second)) and ΔH (m) is the net head (total lift) required. In this equation it is assumed the water has a density of $1000 \text{ kg}/\text{m}^3$.

Equipment that requires power is in use generally accompanied by power losses (for example due to friction and turbulence). Every single power-related equipment works at a certain level of efficiency. The power generator used during fieldwork (Appendix B) was and is used for a period of several years. Due to its age, a generator efficiency of 70% is estimated. The efficiency of the Pedrollo pump(s) is dependent on the discharge rate during dry season operation. An overview of the efficiency curve is present in Appendix I. In this study, the pump efficiencies are related to the time dependent discharges obtained in the model simulations. Besides equipment losses, energy is lost due to mutual transmission. An extra efficiency value of 90% is used (van de Giesen, 2013). The result of these efficiency factors is a variable ASR system efficiency that never exceeds 36.5 % (based on the maximum pump efficiency of 58%).

$$\eta_{total} = \eta_{generator} * \eta_{transmission} * \eta_{pump} \quad (4.2)$$

Where η_{total} (-) is the overall power efficiency, $\eta_{generator}$ (-) is the generator power efficiency, $\eta_{transmission}$ (-) is the transmission power efficiency and η_{pump} (-) is the pump power efficiency.

The combination of total ASR system efficiency and net required power results in a gross power (Equation 4.3). The gross power should be delivered by the generator to supply the desired volumes of water to the agricultural fields. Multiplying the gross power required by the total hours of pump operation returns the total energy consumed (kWh).

$$N_{gross} = \frac{N_{net}}{\eta_{total}} \quad (4.3)$$

Where N_{gross} (kW) is the gross power required, N_{net} (kW) is the net power required and η_{total} (-) is the overall power efficiency.

Energy costs

The Kipor power generator (Appendix B) contains a 15 liter diesel tank. On a fully filled tank the generator can operate for 6.5 hours. A fuel consumption of 2.31 l/h is taken into account. During operation the generator delivers a continuous power capacity of 4.5 kW (TS24, 2018). The Ghana diesel price of 5.03 GHS/l (begin of July 2018) is adopted as normative (GlobalPetrolPrices, 2018). The Bloomberg financial exchange rate (0.2081 USD/GHS) is also applied on the fuel costs for proper financial comparison (Bloomberg, 2018).

$$Cost_{fuel} = \frac{E_{con,gen} * C_{fuel}}{P_{gen}} * \$_{exchange} \quad (4.4)$$

Where $Cost_{fuel}$ (USD/kWh) is the price of fuel, $E_{con,gen}$ (l/h) is the generator fuel consumption, C_{fuel} (GH-S/l) is the fuel price in Ghana, $\$_{exchange}$ (USD/GHS) is the Bloomberg financial currency rate and P_{gen} (kW) is the generator continuous power capacity.

4.2. Financial yield

The impact of the different ASR system improvements are expressed in terms of total volumes discharged (Section 3.1.3). These volumes represent the total water volumes of eight months of daily groundwater withdrawal. The water quantities obtained in the first four months (120 days) are allocated for the production of tomatoes (one cropping season). The groundwater withdrawal of the subsequent 123 days of dry season is allocated to a single cycle of groundnut cultivation. The corresponding financial yields are calculated using the method described in the previous section (Section 4.1.1). The crop-specific financial results are presented in Figure 4.3 (Tomatoes) and Figure 4.4 (Groundnut), for each soil scenario and for each type of ASR system improvement.

The determination of the financial yield is based on relatively simplistic analysis. The obtained revenues are based on the multiplication of calculated discharge volumes with several factors. Therefore, the trends in financial revenue match the change in discharge rates as a result of system improvements. The results show that higher (financial) yield can be expected when the ASR system capacity is improved. Exact revenues are dependent on the type and 'size' of improvement. Within the research scope the financial yield can be more

than double as result of the ASR system capacity improvements.

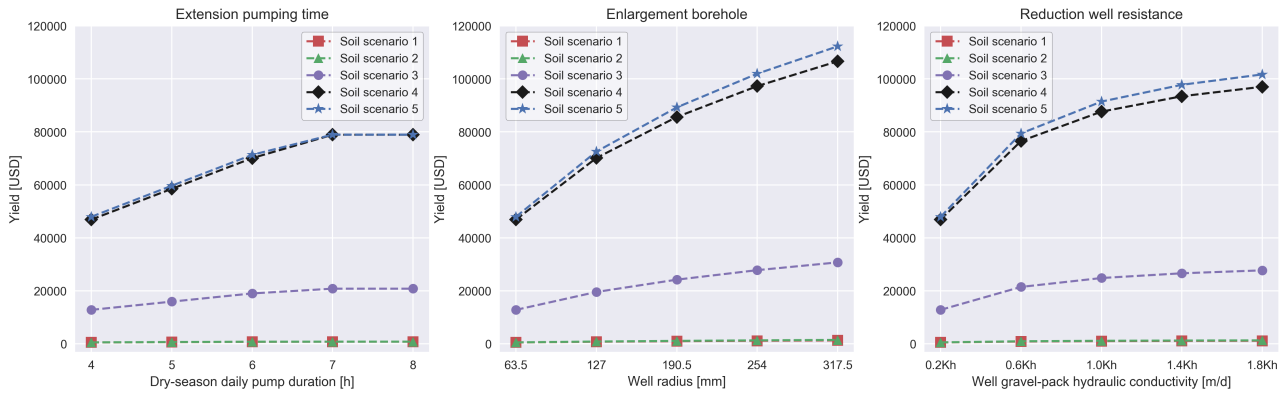


Figure 4.3: Financial yields for the three types of ASR system improvement, based on a Tomato single cropping season

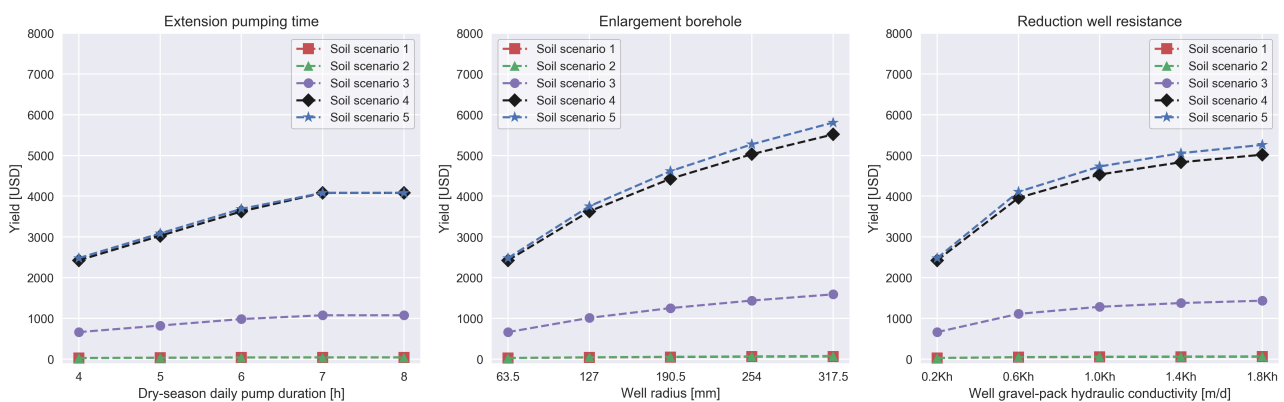


Figure 4.4: Financial yields for the three types of ASR system improvement, based on a Groundnut single cropping season

The water allocation for the cultivation of tomatoes versus groundnuts is comparable. Nonetheless, a comparison between the results presented in Figure 4.3 and Figure 4.4 reveals that the crop-specific revenues differ substantially as a result of differing yield values. Independently of the type of system improvement, the tomato revenues considerably exceed the groundnut revenues (about 15 - 20 times higher). The results show it can pay-off to pick the 'right' crop. The selection of the crop type potentially affects the ASR system financial profits more dominantly than the implementation of one of the system improvements.

It is worth-mentioning that the derivation method of the financial yield is a simple approach that contains some uncertainty. As mentioned in the crop specification (Section 4.1.1), yields can differ both in terms of agriculture (tons per hectare) and financially (GHS per kilogram). The revenues are dependent on aspects as crop quality, shelf life and seasonal crop availability. The market (fluctuation) is decisive in the crop-specific (wholesale) price. Therefore, it is difficult to select the 'right' crop type. The obtained financial results should only be interpreted as indicative. If more detailed information on the combination of crop revenues and ASR system implementation is desired, additional research is recommended.

4.3. Pumping costs

The ASR system operational expenses incurred as a result of fuel consumption are taken into consideration in this section. The remainder of CAPEX (e.g. system installation and pump purchase) and OPEX (e.g. farmer loans and fertilizer costs) are not considered. It is possible that ASR system installation is financed through development funds, making the financial feasibility question more complex. Therefore the focus in this research is only on pumping costs, which gives an indication of the operational feasibility of an (improved) ASR system in northern Ghana.

The costs for the withdrawal of groundwater (total volumes presented in Section 3.1.3) are presented in Figure 4.5, for each soil scenario and for each type of ASR system improvement (multiple steps). The operational costs go from hundreds upto thousands of dollars (dependent on the volumes and conditions). The operational expenses are minor relative to the obtained tomato yields, but comparable with the revenues of a single groundnut cropping season.

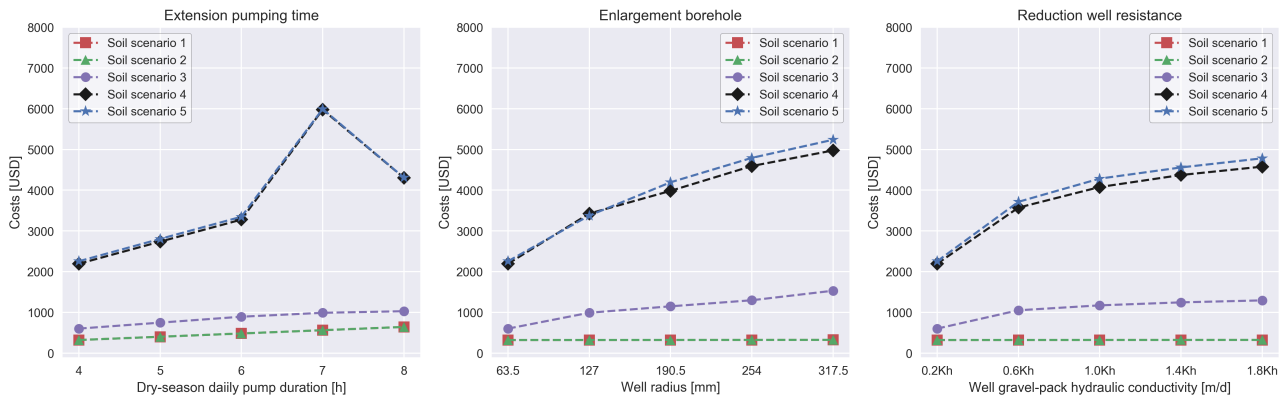


Figure 4.5: Pumping costs for the three types of ASR system improvement, based on 8 months dry season system use

In the comparison of soil scenario 1 and 2 versus soil scenario 3 substantial differences are present in the simulated total volumes discharged (Section 3.1.3). As shown by Figure 4.5, these deviations are less dominantly present in the pumping costs. This is most clearly visible for the base model simulations (absolute left-side of Figures) and the simulations with an ('improved') extension of the daily pumping time. The smaller differences in costs can be attributed to the applied pump efficiencies. The pumping curve of the Pedrollo 4" submersible pump is defined as normative (Appendix I). The discharge rates obtained in the simulations of soil scenarios 1 and 2 do not match the ideal specification of this pump. As a result, low(er) pumping efficiencies are implemented and high(er) discharge costs are obtained.

The ASR system capacities obtained in some cases (higher soil scenarios base model and improvements) exceed the maximum Pedrollo pump capacity. In these situations it is assumed multiple pumps are implemented to supply the water quantities collectively. The specified discharge rates are met by the implementation of this approach. This sometimes leads to relatively low (non ideal) pumping efficiencies. This explains the peak in operation costs for scenarios 4 and 5 when a 7 hour daily pumping schedule is implemented (Figure 4.5).

The installation of an over-dimensioned pump and the use of abundant number of pumps (in parallel) are both situations that are practically unlikely and undesired (low efficiencies and high purchase costs). Figure 4.6 presents the ASR system operational costs for each soil scenario and for each type of improvement (multiple steps), when maximum pumping efficiencies are taken into account. Based on the specifications of the Pedrollo 4" submersible pump a maximum pumping efficiency of 58% is implemented (Appendix I). A comparison of the Figures 4.5 and 4.6 shows that optimal pumping efficiencies can (sometimes) significantly lower the system's operational costs. For efficient use of the ASR system, one should tune the applied pump (pumping curve) to the local circumstances.

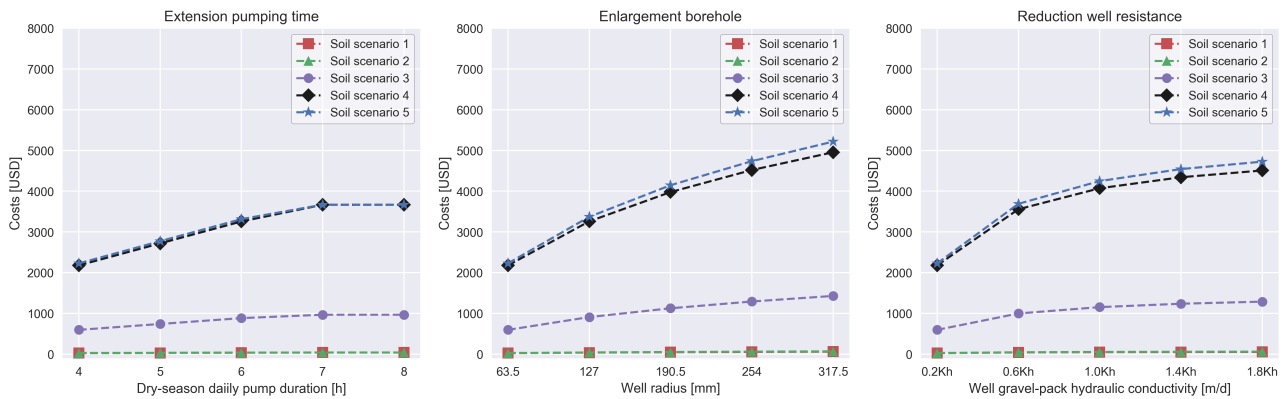


Figure 4.6: Pumping costs for the three types of ASR system improvement, based on 8 months dry season system use and a maximum pump efficiency

An overview of the business case financial returns is presented in Appendix H.4. The ASR system financial returns for both the 'actual' and the optimal pumping efficiency costs are included.

4.4. Results & conclusions

This section contains the conclusions from the ASR system business case and proposes directions for further research.

- Yield increase

The three types of improvements of ASR systems led to increased discharge volumes and higher financial (and agricultural) yields. A crop-specific yield comparison (Tomato versus Groundnut) reveals that the financial yield is more dominantly affected by crop type choice rather than the implementation of one of the investigated system improvements. In the end, the crop-specific market price remains decisive in the ASR system financial feasibility.

- Operational cost reduction

The ASR system operational costs are influenced by the extraction efficiencies. For an efficient use of the ASR system, the applied pump (pumping curve) should be specifically tuned to the local groundwater discharge rates. The natural geohydrological conditions and the design of the system play a role in this process. The selection of the 'right' pump can make a significant difference in the financial feasibility of an ASR system.

- Additional research

The business case contains simplifications, uncertainties and is incomplete. Multiple additional components in CAPEX and OPEX can be added. It is unknown to what extent ASR system components are eligible for funds. For a more detailed financial feasibility of an ASR system implemented in northern Ghana, further financial research is recommended.

5

Discussion & Recommendations

This chapter contains recommendations on the implementation of ASR systems in northern Ghana, which are based on the results of this research. Also, in this section the results obtained in earlier chapters are discussed. The approximations that were made to simplify calculations are analysed, and potential topics or improvements for future research are proposed.

5.1. Farmer's guide - ASR system implementation

Based on the research results, a guide is presented that focuses on the farmer's perspective regarding the implementation of ASR systems in northern Ghana. Multiple distinctive elements are provided with an (expert) interpretation. The information guide offers some simple guidelines for a (more) efficient deployment of an Aquifer Storage and Recovery (ASR) system in northern Ghana.

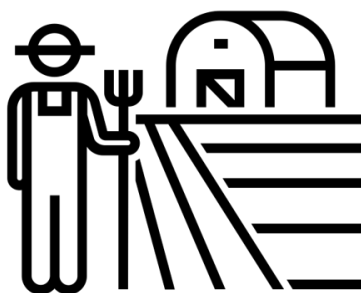


Figure 5.1: Farmer's impression
(visual support by Symbolon from Noun Project - <https://thenounproject.com>)

General considerations

The agricultural purpose and investment plans should be determined in advance to ultimately create a profitable ASR system.

- **Business plan**
Before any actions on the ASR system can be started, a business plan should be defined. The construction of a new ASR system or the use of an existing one should always match the financial capabilities. The system design and potential usage can be tuned to this plan. The presence of a business plan can make the difference in the financial feasibility of the ASR system. The choice in crop type(s) is an element that can be included in the business plan.
- **Determination of crop type(s)**
The research demonstrates that the financial feasibility is dominated by the cultivated crop type rather than the improvement options in ASR system design. The system improvements are beneficial, but a financially viable choice in cultivated crop type(s) is most important. It should be considered

which crop thrives best in northern Ghana (crop quality). The expertise of local farmers can be used in this process. Moreover, the presence of specific market desires should be considered as well. In the end, it is the crop-specific market price that is decisive in the system's financial feasibility.

Geohydrological applicability

It is of key importance to gain knowledge about subsurface characteristics. The local geohydrological conditions determine system performance. An ASR system can not be applied at any location in northern Ghana. The following conditions can be distinguished:

- Inadequate conditions (Soil scenarios 1 & 2)
A low permeable subsurface (T: $1 \text{ m}^2/\text{d}$ and S: $1\text{e-}3 - 1\text{e-}2$) can potentially be encountered in northern Ghana. When encountered, the potential infiltration volumes and discharge rates of an ASR system are insufficient to warrant an investment. One would do well to seize opportunities somewhere else.
- Adequate conditions (Soil scenarios 3)
Within northern Ghana it is possible to encounter subsurface conditions comparable to the location Bingo (T: $26.23 \text{ m}^2/\text{d}$ and S: $6.6\text{e-}3$). Under these geohydrological circumstances, multiple tanks (approximately three tanks of 4500 l) can potentially be filled daily when pumping for four hours per day using the base ASR system as defined in this research. The conditions are favourable for the implementation of groundwater based dry-season (irrigation) crop cultivation. The system can contribute to the farmer(s) (community) self-sufficiency in food production.
- Good conditions (Soil scenarios 4 & 5)
Although not encountered during research aquifer tests, it is not unthinkable a moderately permeable subsurface (T: $100 \text{ m}^2/\text{d}$ and S: $1\text{e-}3 - 1\text{e-}2$) is present in northern Ghana. With these geohydrological conditions, farmers can potentially be supplied with sufficient groundwater for (market-oriented) small-scale agriculture. Based on the (scenario 4 and 5) simulated total volume results (Section 3.2) and the defined crop water consumption (Section 4.1.1), simple calculations suggest one ASR system is sufficient to supply water to up to one hectare for two cropping seasons during the dry period.

ASR system operation

When an existing ASR system is located in an area similar to one of the latter two conditions as described above, the fundamental conditions for successful operation of an ASR system are present. The following aspects are potential improvements for the operation of ASR systems.

- System check & maintenance
Inspect the well before the start of the dry-season groundwater withdrawal. If the borehole depth deviates from the original depth (borehole log-sheets, Appendix A), cleaning is needed. The accumulated sediment (at the bottom) can be removed with a 'pulse drill'. Every bit of sediment that can be removed (increase in active well screen length) will be beneficial for discharge (and recharge) capabilities. Preferably, this check is done once a year.
- Discharge schedule & pump-choice
The next step is to inspect well discharge performance. The performance of an aquifer test (comparable with pumping test applied in this research, see Chapter 2) in the well is sufficient. The test provides information on the (maximum) pumping capacities of the system. If the results are (substantially) worse than in previous years, cleaning measures can be considered. Well-screen maintenance can be applied so that the well skin resistance remains close to the conditions of a clean system. As soon as the discharge capacities are sufficient, a dry-season discharge schedule can be made (based on this discharge capacity). In this financially driven schedule, considerations can be made in:
 - time-span of system use (one or more cropping season(s))
 - the frequency of system use (daily, every other day, etcetera)
 - the discharge rates (volumes for daily requirements or temporal storage in tank(s))

High operational costs can be avoided by the application of a specific pump type (pumping curve) that fits the conditions of the ASR system. Subsequently, the pump should be deployed at its optimal capabilities to guarantee high(er) withdrawal efficiencies.

New ASR system construction

The construction of a new ASR system offers some extra opportunities to improve the ASR system performance.

- **Geographic position**

The determination of an ASR system's location is decisive for system performance. The location should meet the requirements mentioned above for geohydrological applicability. To be used sustainably, the ASR system should be positioned at a location that is subjected to seasonal river flooding or within an area that inundates due to rainfall. The location should be picked strategically, taking aspect as the presence of local communities (villages) and road access into account. A detailed preliminary site investigation is recommended.

- **System design**

In contrast to an existing system, the construction of a new ASR system can to a certain extent be tuned to desired discharges (and recharges). The system performances can further be improved by the extension of the active screen length, the enlargement of the well diameter and the installation of a proper (clean) gravel-pack around the well (minimum of 0.125 m radial-length advised). The impact of these system modifications are discussed below.

A farmers' guidance on ASR system improvement and sensitivity impacts

The interest of farmers is ultimately focused on the absolute impact of the different types of ASR system improvements and sensitivities. This part offers a guide that can be used by farmers themselves to explore the opportunities. The calculated values are indicative and can be used as support in the process of an ASR system design.

Table 5.1 shows extraction volumes per subsurface scenario and translates those to cropping areas and yields. This table is based on the base ASR system as defined in this research (see Chapter 3.1.2). This table can serve as a starting point for research into the improved operation or design of ASR systems. The table contains research results regarding groundwater withdrawal volumes. The base extraction volumes represent the dry season (gross) water quantities that are available for irrigation. Through relatively simple calculations, the (8 months) dry season extraction volumes are transformed to tomato and groundnut single cropping season areal field-sizes and financial yields. The pumping costs are expressed as a percentage of the crop-specific yields. The range of pumping costs is based on the maximum pump efficiency (58%) and the actual discharge dependent efficiencies of the Pedrollo 4" submersible pump. Through the interpretation of agricultural areal-sizes, financial yields and pumping costs it is clear that the application of an ASR system is not feasible for the lower soil scenarios (T: 1 m²/d and S: 1e-3 - 1e-2). When adequate (soil scenario 3) and good (soil scenario 4 and 5) geohydrological conditions are present, the base ASR systems are applicable and improvements (or the impact of sensitivities) can be explored.

Table 5.1: The indicative capabilities of groundwater extraction volumes obtained by a basic ASR system in northern Ghana

Soil condition	Base extraction volume (m ³ / 8-month)	Tomato			Groundnut			Feasible	Improvement
		Areal (ha)	Yield (\$)	Fuel costs (%)	Areal (ha)	Yield (\$)	Fuel costs (%)		
Sc 1	130	0.013	500	2 - 40	0.010	26	45 - »100	No	-
Sc 2	138	0.014	535	2 - 40	0.011	28	45 - »100	No	-
Sc 3	3300	0.33	12810	2 - 3	0.25	660	45 - 48	Yes	See, Table 5.2
Sc 4	12080	1.2	46890	2 - 4	1.0	2420	45 - 73	Yes	See, Table 5.2
Sc 5	12350	1.2	47950	2 - 4	1.0	2480	45 - 73	Yes	See, Table 5.2

The impact of ASR system improvements and sensitivities can (with respect to the basic system performance) be calculated by the use of the 'design and operation chart' (Table 5.2). The chart present a 'base extraction multiplier' for each type and for each step of the proposed ASR system improvements and sensitivities. The multiplier can be applied to the content of Table 5.1. The table serves as a calculation tool to

explore the impact of system modifications in terms of withdrawal volumes, agricultural field-sizes, financial yields and pumping costs.

Table 5.2: The ASR system design & operation chart - the relation between system modifications and changing water extraction volumes - applicable for adequate and good soil conditions (soil scenario 3-5)

Pumping time ($t = 4$ hour)	$1.25t$	$1.5t$	$1.75t$	$2t$
Base extraction multiplier (x)	1.25	1.50	1.70*	1.70*
Borehole diameter ($\varnothing = 5$ inch)	$2\varnothing$	$3\varnothing$	$4\varnothing$	$5\varnothing$
Base extraction multiplier (x)	1.50	1.85	2.10	2.35
Skin resistance (by $k_{gp} = 0.2k_h$)	$3k_{gp}$	$5k_{gp}$	$7k_{gp}$	$9k_{gp}$
Base extraction multiplier (x)	1.60	1.83	1.95	2.05
Screen length ($L = 30$ m)	$0.83L$	$0.67L$	$0.5L$	$0.33L$
Base extraction multiplier (x)	0.85	0.69	0.52	0.35
Flood time ($\Delta t = 4$ months)	Δt	$0.75\Delta t$	$0.5\Delta t$	$0.25\Delta t$
Base extraction multiplier (x)	1.00	1.00	0.84*	0.42*
Flood level ($\Delta h = 8$ m)	Δh	$0.75\Delta h$	$0.5\Delta h$	$0.25\Delta h$
Base extraction multiplier (x)	1.00	1.07	0.81*	0.41*

Note, the multipliers in Table 5.2 are determined in such a way that the extraction volumes will not exceed the infiltration volumes (year-round). The multipliers provided with a * are directly affected by this sustainable boundary condition. Furthermore, the multipliers are solely applicable for the soil scenarios 3 - 5 (range T: 26.23 - 100 m²/d and S: 1e-3 - 1e-2). Beyond these geohydrological ranges, the multiplier can deviate somewhat.

Calculation example

In this example, the impact of an installation of an ASR system with a diameter that is twice the original (base) size is explored. The construction site is characterized by the adequate geohydrological parameters: $T = 26.23$ m²/d and $S = 6.6e-3$ (-). The ASR system business plan prescribes that the ASR system will be used for the the irrigation of single groundnut cropping season (4 months) only.

In this example the single cropping season total (gross) discharge volume can be calculated by using the multiplier presented in Table 5.2 ($2\varnothing \rightarrow 1.50x$). Furthermore, one should account for the 4 months of withdrawal (instead of 8 months). As a result, a total volume of approximately 2475 m³ can be extracted by the new ASR system. This volume roughly corresponds with an agricultural groundnut field of 0.375 ha, a financial yield of \$990 and (minimum) fuel costs of \$445.50.

5.2. Research recommendations

This section describes the limitations for each part of the research. Where applicable, recommendations are provided to overcome the limitations.

5.2.1. Aquifer test

Measurement

- Aquifer test set-up
All aquifer tests are performed by groundwater table (GWT) measurements in the discharge well. This is a relatively low-cost approach that has some general limitations:
 - rope tangle
 - inflow from the infiltration bed
 - potential well turbulence

Some specific limitations can be mentioned as well. The lack of piezometers in the vicinity of the pumping wells results in additional uncertainty in the derived subsurface parameters (T and S). The uncertainty is increased by the (relative) short test durations and incomplete data time-series. Future pumping tests should be performed with at least one (preferably more) observation well(s). The pumping tests should obtain complete drawdown datasets for a minimum of 24 hours (Kruseman and de Ridder, 2000). These tests potentially give insight in well skin behaviour (degree of resistance) and increase the amount of data from which subsurface parameters can be derived.

- Hydraulic conductivity infiltration bed
The hydraulic conductivities of the infiltration beds are unknown. Since these conditions are decisive in the ASR systems sustainable performance, future research should focus on the infiltration bed. The desired data can for example be gathered by the performance of tension-infiltrometer tests.
- Research locations in northern Ghana
The performed aquifer tests were done at five northern Ghana ASR systems, commissioned by Conservation Alliance (CA) in 2016. The results obtained in data analysis are representative of the local hydrogeology. If the same geological formation is present at any other location in northern Ghana, it is potentially possible to extrapolate these results. Nonetheless, when more detailed information on these untested locations is desired, it is advised to apply aquifer tests locally.

Data analysis

- Model fitting
The research lacks adequate geological information. In the data analysis, simplified model stratifications are applied (based on borehole log-sheets (Appendix A)). The results show that the local hydrogeology is only represented by these models to a certain extent. This can partially be attributed to the process of parameter derivation. The model layer(s) are provided with initial parameter conditions based on values taken from literature. These chosen values undeniably affect the outcomes of the optimizations to determine optimal parameter values. Due to the application of the simplified models and the adopted initial conditions, there is some uncertainty in the geohydrological parameter results.
- Additional research
The results obtained through the analysis of the pumping tests seem to yield plausible estimates of subsurface characteristics. However, the models are not able to closely match the observations in all cases. Additional research could be done to expand the models to include processes that were left out in this analysis, e.g. inflow from the infiltration bed and irregularities (sudden additional decrease) in the drawdown time-series. Methods to deal with missing data (gaps in time series) could also be improved upon. And more generally, it is recommended to gather more data to understand the subsurface better.

Transmissivity (T) & storativity (S) bandwidth definition

- The upper and lower bandwidth of parameters applied in the models do not represent local conditions. The bandwidth predominantly acts as an input for scenario modelling in the subsequent parts of this research. The quantitative outcomes of these scenarios include significant uncertainty, but can be used to interpret the impact of ASR system improvements within northern Ghana.

5.2.2. ASR system - Improvements & sensitivities

Representation of hydrogeology

- General model definition
The (base) model does not represent a single research location (presented in Figure 2.1). Certain approximations were made while setting up the ASR system model that are likely not representative of reality. For example, the research results are influenced by the model assumption of a single homogeneous aquifer. And in reality, the wet-season inundation levels will likely fluctuate over time, and groundwater withdrawal is probably not constant but dependent on daily conditions and choices made by the farmers. Nonetheless it is expected that this base model is useful as a tool to examine the impact of certain design choices or changes in operation for the ASR system.
- Discharge bound
The research explores several types of ASR system improvements. All improvements are focused on the general goal, higher water quantities for the supply of dry season agriculture. Nonetheless, the simple improvement of raising the discharge rate is ignored. The maximum discharge is bounded by a limit in drawdown (maximum Δh of 14 m), so that the well screen (perforation) remains below the groundwater table (GWT) at all times. This is a situation that should be pursued in daily practice, to avoid undesired (chemical, aerobic) subsurface clogging processes and to make sure that the pump remains submerged.
- ASR system infiltration bed
As mentioned above, the hydraulic conductivities of the ASR system infiltration beds are undetermined. As a consequence, the bed (resistance) is ignored in the ASR system simulations. The inclusion of a bed resistance can lead to different results (recharge, discharge and Recovery ratio). Future research into infiltration bed resistance is key to determine the maximum sustainable capacity of an ASR system.

MODFLOW

- Combination of radial scaling and MNW2-CWC
The 'Cell-to-Well hydraulic conductance' (CWC) of a MODFLOW MNW2 well is standard calculated by Equation E.1 (Appendix E.1.3). The CWC equation consists of (amongst other things) an A- and $CQ_n^{(P)}$ -term. The A-term represents the linear aquifer-loss coefficient, while the $CQ_n^{(P)}$ -term accounts for non-linear head losses due to turbulent flow near the well. These terms are understandable in the case of an unmodified (Cartesian geometry) rectangular grid MODFLOW model. However, simulation is performed in a radial scaled model, according to the principles as stated by Langevin (2008). The well cell width perfectly aligns with the radius of the well. It is therefore no longer known how to interpret the A- and $CQ_n^{(P)}$ -term. To work around this issue, the research well conductances are calculated by the Equations 3.1 - 3.4 (Section 3.1.2) and implemented as CWC values manually. Future research is needed to determine the correct use of the MNW2-CWC equation in combination with a radial scaled MODFLOW model. More information on this topic can be found in Appendix F.
- Well skin resistance
The research lacks information on well skin resistances of the northern Ghana ASR systems. As mentioned above, by doing more extensive pumping tests the skin resistance can potentially be measured. In this research the resistances are based on the Equations 3.1 - 3.4. In these equations, parameter

assumptions are implemented. As stated by Konikow et al. (2009), the skin hydraulic conductivity (K_{skin}) is typically expected to be lower than the aquifer hydraulic conductivity (K_h). The research base model gravel-pack hydraulic conductivity (K_{gp}) is assumed to be 20% of the K_h . This definition shows, the well hydraulic conductances are soil scenario dependent. This was not the original intention within this research but was inevitable due to MODFLOW (and time) limitations. The standard MODFLOW solver 'failed to meet the solver convergence criteria' if CWC values are defined too high. The upper solving limits are found to be dependent on the hydraulic conductivity of the soil (in the model). Dependent on the soil conditions, solving appears to be possible when CWC values are maximally about forty times higher than the soil hydraulic conductivities (K_h). Additional research is needed to further specify the MODFLOW solver criteria to allow the gravel pack to be simulated with larger hydraulic conductivities.

5.2.3. ASR system - Business case

The business case is included in the research to offer a rough understanding of the financial feasibility of an operational ASR systems. The case does not give a full financial perspective of an ASR system. As stated below, the business case contains strong simplifications and assumptions. The financial results are only qualitatively indicative.

- Crops of interest

The research crops of interest (Tomato and Groundnut) do not by definition suit the northern Ghana conditions, but are included for research purposes. By the application of the (simple) water utilization efficiencies and wholesale prices, the correctness of the calculated financial yield is uncertain. The crop-specific revenues are influenced by the market (fluctuations) and should only be interpreted as indicative.

- Irrigation efficiency

The determination of irrigation type is based on site visits. Subsequently, the assumed irrigation efficiency is adapted to the statements on drip irrigation described by van de Giesen (2013). The assumptions are rough and future research is needed to gather more detailed information on the irrigation efficiency of a northern Ghana ASR system.

- Pump operation

The use of the Pedrollo 4" submersible pump in simulations is based on the study site aquifer tests. The acquired pumping efficiencies are not by definition realistic. It is for example highly unlikely that in ASR system practice multiple pumps are placed in parallel operation (in the well). Moreover, the generator (pumping) fuel costs are based on multiple rough assumptions (e.g. generator and transmission efficiencies, generator power capacity, fuel consumption and diesel prices). Therefore, the calculated costs contain some uncertainty. The elaborated efficiencies and operation costs serve as an indication. If more details on pumping costs are desired, additional research is needed.

- Additional research

The business case contains simplifications, uncertainties and is far from complete. Multiple additional components in CAPEX and OPEX can be added. It is unknown to what extent ASR system components are eligible for funding by foreign aid. For a more detailed financial feasibility of an ASR system implemented in northern Ghana, future financial research is needed.

6

Conclusions

This chapter shortly discusses the individual research questions. Subsequently, an answer to the main research question is formulated. This report aims to answer the following research question:

How can Aquifer Storage and Recovery (ASR) systems be improved to increase the availability and sustainable use of groundwater for small-scale agriculture in northern Ghana?

Which range of values for transmissivity (T) and storativity (S) can be obtained from aquifer tests at multiple study sites in northern Ghana?

The research is provided with local geohydrological data by performing in-well aquifer tests at northern Ghana study sites in: Bingo, Nungo, Nyong Nayili, Janga and Ziong. The TTim analytic element modelling environment is used to analyse the groundwater drawdown data and derive parameters for subsurface characteristics. TTim allows for the inclusion of additional model parameters such as borehole storage, well skin resistance and multiple model layers. TTim is a useful tool for deriving subsurface parameters and, in this research, TTim outperforms a simple analytic method such as the Theis equation. Despite the differences in absolute parameter size, this research demonstrates that the `Fmin-RMSE` and `Calibrate` (TTim built-in) optimization functions are both applicable for the determination of suitable T and S values. Based on the results of the Root-Mean-Square-Error objective function, a single layer aquifer (most simplistic model) can adequately represent local conditions. Nonetheless, there is some uncertainty in the derived subsurface parameters due to aspects as the performance of only short duration single aquifer test at each well, the presence of large gaps in drawdown data, and the lack of groundwater measurements in the vicinity of the discharge wells. As a consequence, the aquifer (single layer) transmissivity range is determined by the values found in data analysis and some factor of safety, while the definition of the storativity values is based on more commonly found values in literature. As an answer to this research question, plausible values for transmissivity and storativity are suggested to be present in the ranges of respectively 1 to 100 (m^2/d) and $1\text{e-}3$ to $1\text{e-}2$ (-).

How can ASR system design and operation be improved to increase water supply, while maintaining sustainable system use?

To answer this research question, a base model is presented which represents ASR system performance in northern Ghana. The simulations show that the volumes obtained in eight months of daily (four hour) dry season pump operation, with a discharge bounded by a maximum drawdown (Δh of 14 m), do not exceed the gravity based recharge volumes caused by four months of constant inundation (Δh is 8 m). Higher total extraction volumes can be acquired by an extension of the dry season daily pumping time. However, this does not impact recharge rates and means that if the the pumping time is increased to beyond 6-7 hours per day it is possible to extract more water than is infiltrated. To increase both discharge and recharge volumes (and Recovery ratios), the ASR system can be improved by the enlargement of the borehole cross-sectional dimension and the reduction of the well skin resistance. Within the modifications scope ($r_w = 0.0635\text{-}0.3175$ m and $k_{gp} = 0.2\text{-}1.8 * K_h$ m/d), the obtained base model volumes are more than doubled. The

effects of a change in well radius and well skin resistance are non-linear with respect to the total capacity of the ASR system. The first increase in well radius and reduction in well skin resistance is more efficient than the subsequent enlargements/reductions. The recharge and discharge rates are also affected by the ASR systems active screen length. In the scope (10 - 30 m) of this modification type a nearly linear relationship is found between active screen length and volume capacities. Furthermore, the ASR system's sensitivity to the natural conditions of its surroundings is taken into account. The volumes recharged are (for the the research time-span) by approximation linear related (positively) to the duration of the constant level flooding (range 1 - 4 months) and the depth of the inundation level (Δh range 2 - 8 m). The research demonstrates that recharge is normative in the sustainable performance of an ASR system.

How will the ASR system improvements impact the financial yields and pumping costs?

To deal with this question, the dry season simulation is subdivided into a tomato and a groundnut cropping season. While water (withdrawn by ASR system) is approximately evenly distributed, the tomato revenues clearly exceed the financial yield of groundnut (15-20 times higher). The ASR system financial yield is dependent on the cultivated crop type. And on its own, the crop-specific revenues are strongly dependent on aspects as crop quality, shelf life and market conditions. The research lacks access to this uncertain financial data. No distinctive conclusions can be drawn upon the revenues. The yields are compared to the ASR system pumping costs. The system operational costs are not only dependent on the absolute water quantities, also the withdrawal efficiencies are normative. The pump efficiencies of the Pedrollo pump show that this pump is not ideal for all modelled conditions. Pump selection should ideally be tuned to the expected discharge and head difference that needs to be overcome. The selection of a pump that is tuned to local conditions can be beneficial for the operational costs of an ASR system. When maximum pump efficiencies are considered, the fuel costs are approximately 2% of the tomato revenue and 45% of the groundnut revenue at current market prices.

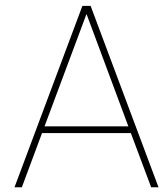
To answer the main research question, the results in this report show that it is indeed possible to sustainably increase the recharge and discharge water quantities (and Recovery ratios) by ASR system modifications. The overall performance of an existing ASR system can be improved by system cleaning. Well maintenance is key to maintain the active well screen length (borehole cleaning). The infiltration and extraction volumes are approximately linearly related to the active well-screen length. Higher inflow and outflow volumes can be obtained by the reduction of the well skin resistance (skin cleaning). The capacity of new ASR systems can be increased by an enlargement of the borehole diameter. The construction of a proper permeable well skin (screen and gravel-pack) positively contributes to the total recharge and discharge volumes. Despite the imposed options in system modifications, the geographic position remains of utmost importance for an ASR system. The ASR system's (sustainable) performance is dependent on the availability of infiltration water and local geohydrological conditions. By the inclusion of soil scenarios, the research demonstrates that the ASR system performs significantly better in regions with higher transmissivity (T) values. Due to a lack in bandwidth-space, the research storativity (S) scope is insufficient to draw further conclusions on desired storativity values. Furthermore, the research gives some insight into financial aspects related to the implementation of an ASR system. A definitive conclusion on whether an ASR system is a sound investment cannot be given. The system revenues are dominantly affected by the choice in crop cultivation. Still, the system modifications can potentially more than double the systems capacities and revenues. It is clear that the performance of an ASR system is positively affected by the improvements explored.

Bibliography

- Bakker, M. (2010). Radial Dupuit interface flow to assess the aquifer storage and recovery potential of salt-water aquifers. *Hydrogeology Journal*, pages 107–115.
- Bakker, M. (2013a). Analytical Modeling of Transient Multilayer Flow. In *Advances in Hydrogeology*, chapter 5, pages 95–114. Springer Science+Business Media, New York, NY.
- Bakker, M. (2013b). Semi-analytic modeling of transient multi-layer flow with TTim. *Hydrogeology Journal*, pages 935–943.
- Bakker, M. and Anderson, E. I. (2011). Mechanics of Groundwater Flow. In *Treatise on Water Science*, pages 115–134. Academic Press, Oxford, United Kingdom.
- Bloomberg (2018). GHS-USD Cross rate currency. Retrieved from <https://www.bloomberg.com/quote/GHSUSD:CUR> Accessed: 2018/07/07.
- Bot, B. (2016). *Grondwaterzakboekje Gwz2016*. Bot Raadgevend Ingenieur, Rotterdam.
- Bruggeman, G. A. (1999). *Analytical solutions of geohydrological problems*. Elsevier Science, Amsterdam, The Netherlands, first edition.
- Canadian International Development Agency (2011). *Hydrogeological Assessment Project of the Northern Regions of Ghana (HAP)*, volume I. SNC Lavalin international, Montreal (Quebec).
- Dillon, P., Pavelic, P., Page, D., Beringen, H., and Ward, J. (2009). *Managed aquifer recharge: An Introduction. Waterlines report*, volume 13. Australian Government - National Water Commission, Canberra, Australia.
- Fitts, C. R. (2012). *Groundwater Science*. Academic Press, Oxford, United Kingdom, second edition.
- Food and Agricultural Organisation of the United Nations (2018a). Crop information - Groundnut. Retrieved from <http://www.fao.org/land-water/databases-and-software/crop-information/groundnut/en/> Accessed: 2018/07/08.
- Food and Agricultural Organisation of the United Nations (2018b). Crop information - Tomato. Retrieved from <http://www.fao.org/land-water/databases-and-software/crop-information/tomato/en/> Accessed: 2018/08/02.
- Food and Agricultural Organisation of the United Nations (2018c). FAOSTAT - download data - crops [Data file]. Retrieved from <http://www.fao.org/faostat/en/#data/QC> Accessed: 2018/07/08.
- Food and Agricultural Organisation of the United Nations (2018d). How close are we to #ZeroHunger? - The state of food security and nutrition in the world 2017. Retrieved from <http://www.fao.org/state-of-food-security-nutrition/en/> Accessed: 2018/07/28.
- Ghana-made (n.d.). Groundnut. Retrieved from <http://ghana-made.org/market-sectors/groundnut/> Accessed: 2018/07/07.
- GlobalPetrolPrices (2018). Ghana diesel prices, liter. Retrieved from https://www.globalpetrolprices.com/Ghana/diesel_prices/ Accessed: 2018/07/07.
- Harbaugh, A. W. (2005). MODFLOW-2005, The U.S. Geological Survey Modular Ground-Water Model — the Ground-Water Flow Process. In *Book 6, Modeling techniques*, chapter A16. U.S. Geological Survey, Reston, Virginia.

- Harbaugh, A. W., Banta, E. R., Hill, M. C., and McDonald, M. G. (2000). *MODFLOW-2000, The U.S. Geological Survey modular Ground-Water model — User guide to modularization concepts and the groundwater flow process*. U.S. Geological Survey, Reston, Virginia.
- Houben, G. J. (2015). Review: Hydraulics of water wells—head losses of individual components. *Hydrogeology Journal*, 23:1659–1675.
- Konikow, L. F., Hornberger, G. Z., Halford, K. J., and Hanson, R. T. (2009). Revised Multi-Node Well (MNW2) Package for MODFLOW Ground-Water Flow Model. In *Book 6, Modeling techniques*, chapter A30. U.S. Geological Survey, Reston, Virginia.
- Kruseman, G. and de Ridder, N. (2000). *Analysis and evaluation of pumping test data*. International Institute for Land Reclamation and Improvement (ILRI), Wageningen, The Netherlands, second edition.
- Langevin, C. D. (2008). Modeling axisymmetric flow and transport. *Ground Water*, 46(4):579–590.
- Martin, N. (2008). Development of a water balance for the Atankwidi catchment, West Africa – A case study of groundwater recharge in a semi-arid climate. Technical report, Cuvillier Verlag, Gottingen.
- Ministry of Foreign Affairs, Ministry of Agriculture, and Wageningen UR (2018). Small Business Innovation Research (SBIR) call - Food security in Sub-Saharan Africa - Background note. Technical report.
- Modern Ghana (2018). Esoko market Wholesale Prices [Data file]. Retrieved from https://cdn.modernghana.com/images/content/report_content/esoko_market_watchweek_ending_march_22nd1.pdf Accessed: 2018/07/07.
- Niswonger, R. G., Panday, S., and Motomu, I. (2011). MODFLOW-NWT, A Newton Formulation for MODFLOW-2005. In *Book 6, Modeling techniques*, chapter A37. U.S. Geological Survey, Reston, Virginia.
- Owusu, S., Cofie, O. O., Osei-Owusu, P. K., Awotwe-Pratt, V., and Mul, M. L. (2017). Adapting aquifer storage and recovery technology to the flood-prone areas of northern Ghana for dry-season irrigation (IWMI Working Paper 176). Technical report, International Watermanagement Institute (IWMI), Colombo, Sri Lanka.
- Owusu, S., Mul, M., Ghansah, B., Awotwe-pratt, V., and Osei, P. K. (2015). Identification and selection of suitable sites for Bhungroo and Pave Irrigation Technologies. Technical report, International Watermanagement Institute (IWMI), Accra, Ghana.
- Strack, O. D. L. (1989). *Groundwater Mechanics*. Prentice Hall, Englewood Cliffs, New Jersey.
- TS24 (2018). KIPOR KDE6700T DIESEL GENERATOR. Retrieved from https://www.ts24.nl//product_info.php/info/398/Kipor-KDE6700T-Diesel-Generator/ Accessed: 2018/07/07.
- United Nations (2014). International Decade for Action 'WATER FOR LIFE' 2005-2015 - Water and food security. Retrieved from http://www.un.org/waterforlifedecade/food_security Accessed: 2018/07/28.
- United Nations (2018). Sustainable Development Goal 2: End hunger, achieve food security and improved nutrition and promote sustainable agriculture. Retrieved from <https://www.un.org/sustainabledevelopment/hunger/> Accessed: 2018/07/28.
- van de Giesen, N. (2013). Dictaat CTB2120 Waterbeheer. Technical report, Delft University of Technology, Delft, The Netherlands.
- Ward, J. D., Simmons, C. T., and Dillon, P. J. (2007). A theoretical analysis of mixed convection in aquifer storage and recovery: How important are density effects? *Journal of Hydrology*, 343:169–186.
- Wood, T. N. (2013). Agricultural Development in the Northern Savannah of Ghana. Technical report, University of Nebraska, Lincoln, Nebraska.

Appendices



Borehole log-sheets

In 2016, Conservation Alliance (CA) commissioned the construction of multiple boreholes in northern Ghana. Some of these boreholes are in this research used for the performance of aquifer tests. Pumping tests are performed at the boreholes located in Bingo; Nungo; Nyong Nayili and Janga. At the location Ziong a borehole is used for the monitoring of the practical use of an ASR system. A geographic overview of the research locations is presented in Figure 2.1 (Chapter 2). During the construction of the boreholes, valuable information is gained regarding local soil stratification. The information is recorded in the original borehole log-sheets, which can be found in this appendix. Besides the local soil stratification, these log-sheets contain information on individual applied well structures. A depth dependent distinction is made in plain versus screened well skin (perforations). These borehole log-sheets are used as a starting point in aquifer test data analysis (theoretical model definition) and as input for the synthetic model design of an ASR system.

CONSERVATION ALLIANCE- THE PAVE PROJECT						BH status:	Successful	✓	
BOREHOLE LOG SHEET									
Community		Bingo	District	Talensi	Borehole ID		BH B1		
Coordinates - Latitude (N) :				Longitude (W)					
Drilling contractor			Drill rig	Method		ROTARY AIR			
Drilling start date		6-8-2016	Compl. date	6-8-2016	Operator				
TEST PUMPING				Date:		Conductivity			
Dynamic WL *		m	Pump type		Total Iron	mg/l	Top of screen *	0 m	
Static WL *		m	Pumping rate (Q)	m ³ /h	Manganese	mg/l	Potential drawdown	m	
Drawdown (s)		m	Duration	h	Nitrate	mg/l	Potential yield	25 l/min	
* Levels to ground level datum		Specific capacity (Q/s)		m ³ /h/m	Fluoride	mg/l	Depth of borehole *	48 m	
BIT SIZE & TYPE	Temporary CASING	SCALE	PROFILE	TIME/DEPTH M/MIN	WATER ZONES CUMULATIVE Q (l/min)	WELL DIAGRAM			
10"			Light brown clay						
Clay cutter		5						5	
		10						10	
		15	Highly weathered light brown sandstone mixed with shaly materials					15	
		20						20	
6.5" hammer bit		25						25	
		30						30	
		35			15			35	
		40	Moderately weathered brownish sandstone					40	
		45						45	
		50			55			50	
Gravel for gravel pack			48	LM	Remarks and stoppages:				
Screen Length			30	LM					
Casing length			18	LM					
Installation of grout seal				M					
Cleaning & development			2	HRS					
Centralisers fitted				No	Prepared by:				
Safety cap fitted			Yes	/	No	Approved:			
Backfill aband. BH			Yes	No	/				
Cement for grout				KG					
Platform construction date									
Distance from last BH				KM					

CONSERVATION ALLIANCE- THE PAVE PROJECT						BH status: Successful	<input checked="" type="checkbox"/>
BOREHOLE LOG SHEET						Dry	
Community		Nungo	District	Talensi	Borehole ID	BH N100	
Coordinates - Latitude (N) :			Longitude (W)				
Drilling contractor			Drill rig	Method		ROTARY AIR	
Drilling start date			6-8-2016	Compl. date	6-8-2016	Operator	
					Kwaku		
TEST PUMPING			Date:		Conductivity	us/cm	Top of screen *
Dynamic WL *		m	Pump type		Total Iron	mg/l	Static WL *
Static WL *		m	Pumping rate (Q)		Manganese	mg/l	Potential drawdown
Drawdown (s)		m	Duration		Nitrate	mg/l	Potential yield
* Levels to ground level datum		Specific capacity (Q/s)		m ² /h/m	Fluoride	mg/l	Depth of borehole *
							42 m
BIT SIZE & TYPE	Temporary CASING	SCALE	PROFILE	TIME/DEPTH M/MIN	WATER ZONES CUMULATIVE Q (l/min)	WELL DIAGRAM	
10"	Clay cutter	5	Highly weathered light brown sandstone			<p>18m PVC Plain</p> <p>42m Gravel pack</p> <p>6m PVC Plain</p> <p>18m PVC Screen</p> <p>1m Bail Plug</p>	
6.5"	hammer bit	10	Moderately weathered light grey sandstone mixed with shaly materials (at 18m, 21-24m)				
		15					
		20					
		25	Light grey sandstone	55			
		30					
		35					
		40					
		45		80			
		50					
Gravel for gravel pack		42	LM	Remarks and stoppages:			
Screen Length		36	LM				
Casing length		6	LM				
Installation of grout seal			M				
Cleaning & development		2	HRS				
Centralisers fitted			No	Prepared by:			
Safety cap fitted		Yes	No	Approved:			
Backfill aband. BH		Yes	No				
Cement for grout			KG				
Platform construction date							
Distance from last BH			KM				

CONSERVATION ALLIANCE- THE PAVE PROJECT						BH status: Successful		<input checked="" type="checkbox"/>
BOREHOLE LOG SHEET								
Community		Nyong Nayili		District	Karaga		Borehole ID	BH NN1
Coordinates - Latitude (N) :				Longitude (W)				
Drilling contractor			Drill rig		Method		ROTARY AIR	
Drilling start date			31/05/2016		Compl. date		31/05/2016	
			Operator		Kwaku			
TEST PUMPING				Date:		Conductivity		us/cm
Dynamic WL *		m		Pump type		Total Iron		mg/l
Static WL *		m		Pumping rate (Q)		Manganese		mg/l
Drawdown (s)		m		Duration		Nitrate		mg/l
* Levels to ground level datum		Specific capacity (Q/s)		m ² /h/m		Fluoride		mg/l
								Depth of borehole *
								54 m
BIT SIZE & TYPE	Temporary CASING	SCALE	PROFILE		TIME/ DEPTH M/MIN	WATER ZONES CUMULATIVE Q (l/min)	WELL DIAGRAM	
10"			Clay					
Clay cutter		5					5	
6.5" hammer bit		10	Highly weathered chocolate brown sandstone				10	
		15					15	
		20					20	
		25					25	
		30					30	
		35					35	
		40					40	
		45	Moderately weathered chocolate brown sandstone				45	
		50					50	
		55					55	
Gravel for gravel pack		54		LM		Remarks and stoppages:		
Screen Length		33		LM				
Casing length		21		LM		Prepared by:		
Installation of grout seal				M				
Cleaning & development		2		HRS		Approved:		
Centralisers fitted				No				
Safety cap fitted		Yes		/		No		/
Backfill aband. BH		Yes				No		/
Cement for grout				KG				
Platform construction date								
Distance from last BH				KM				

CONSERVATION ALLIANCE- THE PAVE PROJECT						BH status: Successful		<input checked="" type="checkbox"/>	
BOREHOLE LOG SHEET									
Community		Janga 1		District		West Mamprusi		Borehole ID BH J1	
Coordinates - Latitude (N) :		0°ju		Longitude (W)					
Drilling contractor		6-3-2016		Drill rig		Method		ROTARY AIR	
Drilling start date		6-3-2016		Compl. date		6-3-2016		Operator	
								Kwaku	
TEST PUMPING									
Dynamic WL *		m		Date:		Conductivity		us/cm	
Static WL *		m		Pump type		Total Iron		mg/l	
Drawdown (s)		m		Pumping rate (Q)		Manganese		mg/l	
* Levels to ground level datum				Duration		Nitrate		mg/l	
				Specific capacity (Q/s)		Fluoride		mg/l	
								Top of screen * 0 m	
								Static WL * m	
								Potential drawdown m	
								Potential yield 35 l/min	
								Depth of borehole * 48 m	
BIT SIZE & TYPE	Temporary CASING SCALE	PROFILE			TIME/DEPTH M/MIN	WATER ZONES CUMULATIVE Q (l/min)	WELL DIAGRAM		
10" Clay cutter	5	Highly weathered light brown sandstone (Very loose formation)							
6.5" hammer bit	10						48m Gravel pack		
	15						48m PVC Screen		
	20						1m Bail Plug		
	25								
	30	Moderately weathered grey shale			15				
	35								
	40								
	45								
	50				35				
Gravel for gravel pack		48		LM		Remarks and stoppages:			
Screen Length		48		LM					
Casing length				LM		Prepared by:			
Installation of grout seal				M					
Cleaning & development		2		HRS		Approved:			
Centralisers fitted				No					
Safety cap fitted		Yes		/		No		/	
Backfill aband. BH		Yes		/		No		/	
Cement for grout				KG					
Platform construction date									
Distance from last BH				KM					

CONSERVATION ALLIANCE- THE PAVE PROJECT						BH status: Successful	<input checked="" type="checkbox"/>	
BOREHOLE LOG SHEET						Dry		
Community		Ziong	District	Savelugu Nanton	Borehole ID	BH Z1		
Coordinates - Latitude (N) :				Longitude (W)				
Drilling contractor		Drill rig		Method		ROTARY AIR		
Drilling start date		27/05/2016	Drill date		27/05/2016	Operator		
TEST PUMPING				Date:	Conductivity	us/cm	Top of screen *	
Dynamic WL *		m	Pump type		Total Iron	mg/l	Static WL *	
Static WL *		m	Pumping rate (Q)		Manganese	mg/l	Potential drawdown	
Drawdown (s)		m	Duration		Nitrate	mg/l	Potential yield	
* Levels to ground level datum		Specific capacity (Q/s)		m ³ /h/m	Fluoride	mg/l	Depth of borehole *	
BIT SIZE & TYPE	Temporary CASING	SCALE	PROFILE	TIME/ DEPTH M/MIN	WATER ZONES CUMULATIVE Q (l/min)	WELL DIAGRAM		
10"			Reddish brown laterite			<p>3m PVC Screen</p> <p>12m PVC Plain</p> <p>48m Gravel pack</p> <p>33m PVC Screen</p> <p>1m Bail Plug</p>		
Clay cutter		5			5			
		10			10			
		15	Highly weathered light brown sandstone mixed with shaly materials		15			
		20			20			
		25			25			
6.5" hammer bit		30			30			
		35			35			
		40	Moderately weathered brownish sandstone		40			
		45			45			
		50			50			
Gravel for gravel pack		48	LM	Remarks and stoppages:				
Screen Length		36	LM					
Casing length		12	LM					
Installation of grout seal			M					
Cleaning & development		2	HRS					
Centralisers fitted			No	Prepared by:				
Safety cap fitted		Yes	/	No	Approved:			
Backfill aband. BH		Yes	/	No				
Cement for grout			KG					
Platform construction date								
Distance from last BH			KM					

B

Aquifer test - Equipment

The northern Ghana aquifer tests (and local geohydrological data collection) would not have been possible without the interference of Conservation Alliance (CA). The NGO did not only provided the research with aquifer test locations (ASR systems), but additionally took care of the necessary test facilities. CA provided the transport, an interpreter and aquifer test equipment. The section below contains detailed information on the equipment applied. In the description a distinction is made between the equipment used for the aquifer tests and the actual groundwater measurements. Moreover small equipment as pliers, screwdrivers, gloves and robes are ignored. Purposes and use of these tools are taken for granted.

B.1. Aquifer test

- Pump: Pedrollo 4" submersible pump; Type 4SR4/18

The research aquifer tests are performed by the use of a 2 HP pump. The pump can for example be used for the supply of water to irrigation fields. While pumping, the water should preferably not exceed 35 °C and should not contain too many particles; no more than 150 g/m³. The pump can be submerged in water up to 100 meters. When installed in the right way, the pump can deliver 20-100 l/min with an head difference of 112-45 m. More specific information about the pump can be found on the webpage below and/or Appendix I.



Figure B.1: Comparable example of the submersible pump used in aquifer test practise
(source: <https://www.pedrollo.com/en/4sr-4-submersible-pumps/150>)

- Generator & power converter: Kipor diesel generator - 5 kVA

A mobile generator is used as a in-field pump power source. The Kipor generator is a relatively small model, easy to handle and meets the pump requirements by the use of the 230 V connection. A power converter (transmission) is positioned between the generator and the pump to manually switch on and off the pump. To facilitate a flawless transfer between generator and pump one should be aware

the cables and connections towards the pump should be waterproof. Moreover these power cables should be of a decent length, to allow the pump to submerge.



Figure B.2: Comparable example of the generator used in aquifer test practise
(source: <https://www.kipor-power.eu/winkel/kipor-kde6700t-diesel-generator-5-kva/>)

- Hose:

During the aquifer tests a flexible water hose is attached to the pump. The withdrawn water is transported and discharged at the head-end of this line. The hose is manufactured in Polyethylene, has an external diameter of 1^{1/4}" and is approximately 100 m long.



Figure B.3: The hose & bucket used in aquifer test practise

- Bucket:

As a rough estimation for discharge an plastic bucket is used. This oversized measuring cup stores volumes up to 50 l and contains 5 l level indicators.

B.2. Water table monitoring

- Pressure sensor data loggers:

- Van Essen; TD-Diver Type DI801 (2x) & Baro-Diver Type DI800 (1x):

TD-Divers and Baro-Divers are applied for the measuring and recording of time dependent fluctuations in (ground)water levels, atmospheric pressures and temperatures. The TD-Divers can record a water-column up to 10 m. The Baro-Divers can be used to measure atmospheric pressures and shallow water levels, approximately up to a range of 0.9 m. Based on the internal memory these devices can store up to 72.000 measurements per parameter (e.g. date & time, pressure, temperature). Measurement logging can be programmed by the use of a USB-Unit and the Diver-Office software. With a battery life of 10 years, long and/or short term measurements can be applied with a sample interval of 0.5 seconds to 99 hours. Moreover the sample interval can be linear or logarithmic.



Figure B.4: Comparable examples of Van Essen TD- & Baro-Divers used in aquifer test practise
(source: <https://www.vanessen.com/images/PDFs/TD-Diver-DI8xx-ProductManual-nl.pdf>)

- In-Situ; RuggedTROLL100 (2x) & BaroTROLL (1x):

The Rugged TROLL 100 and BaroTROLL divers are applied for the measuring and recording of time dependent fluctuations in (ground)water levels, atmospheric pressures and temperatures. The RuggedTROLL100 divers function in a pressure range up to 9 m water-column. The BaroTROLL divers can be used for the measurement of atmospheric pressures, up to 1 bar. The internal memory of 2.0 MB accommodates the storage of 120.000 data records. A single record contains a set of three items; date & time, pressure and temperature. The internal battery has a lifetime of approximately 10 years. By the use of the Rugged TROLL docking-station and the Win-Situ 5 software, linear logging can be programmed. Fastest logging rate is 1 log per second for the Rugged TROLL 100 divers and 1 log per minute for the BaroTROLL divers. Optionally it is possible to display the pressure in units of Psi, Bar, Pascal or water-column (mH₂O).



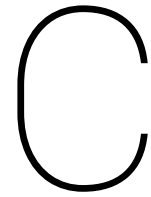
Figure B.5: Comparable examples of In-Situ TD- & Baro-Divers used in aquifer test practise
(source: <https://in-situ.com/product-category/water-level-monitoring/level-temp-data-loggers/>)

- Hand measurement device: Heron water tape

The water tape is applied to hand measure static water levels (GWT) and verify drawdown water levels during the pumping tests. The water tape has a length of 300 ft (100 m). A water level sensing probe is attached to the tail of the tape. The probe to water contact results in an instant auditory signal, after which the depth can be determined by eye. More specific product specifications can be found on the Heron webpage presented below.



Figure B.6: Comparable example of the water tape used in aquifer test practise
(source: <https://envirotechonline.com/water-level-interface-meters/the-heron-water-tape.html>)

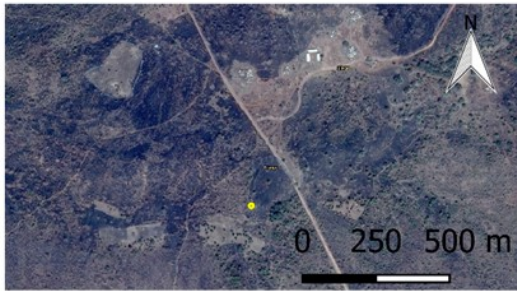


Aquifer test - Factsheets measurement results

The northern Ghana aquifer tests (and local geohydrological data collection) would not have been possible without the interference of Conservation Alliance (CA). Spread over the Upper East (UER) and Northern Region (NR), the NGO holds multiple ASR systems. In consultation with CA, five research pumping tests are performed at ASR systems located in Bingo, Nungo, Nyong Nayili and Janga (2x). By the use of a fifth ASR system, located in Ziong, the system practical use by farmers is monitored for the duration of a week. The aquifer tests are all applied in November-December 2017, shortly after the transition from wet season to dry season. The general aquifer test set-up (as presented in Figure 2.2a, Chapter 2) is implemented at the boreholes located in Nungo; Nyong Nayili and Janga. While the simplified set-up (Figure 2.2b, Chapter 2) is applied at the boreholes located in Bingo and Ziong. The aquifer tests performances and results (e.g. site specific info, test configuration, results and remarks) are individually summarized in the fact-sheets of the Figures C.1 - C.6.

Bingo

Site Specific info



District:	Talensi	<u>Well</u>	
Well coordinates:	N10 36.925	Height:	0.38 m
	W0 40.040	Diameter:	0.127 m

Infiltration bed

Height:	0 m	<u>Borehole depth</u>	
Diameter:	1.55 m	Initial:	48 m
		Measured:	40.50 m

* Lengths relative to surface

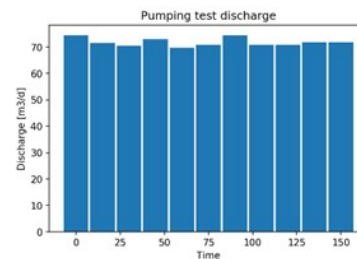
Pumping test configuration

Date: 27-11-17

Positioning

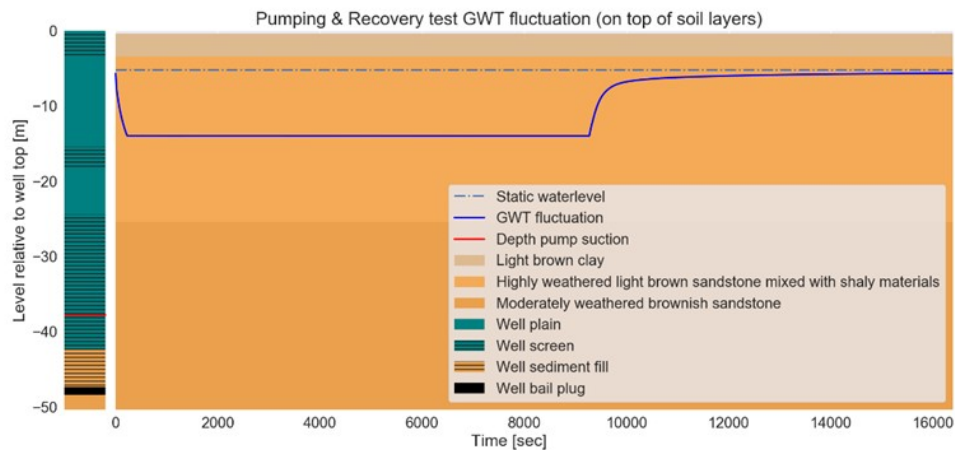
Diver 1:	13.99 m	Time start:	12:44:40
Diver 2:	21.50 m	Time off:	15:17:50
Diver 3:	-	Time stop:	17:18:10
Diver 4:	-		

Static water table	Pump duration:	02:33:10 h
Initial: 5.21 m	$Q_{average}$:	72 m ³ /d
At start: 5.68 m	Suction depth:	37.80 m



* Lengths relative to well top

Result



Remarks

Study site

- Sloping landscape, some rocks at surface
- Area dominated by bush fires, charred vegetation abundant, agricultural field not ready for use
- Although Volta river not far (on map), no river, water flow or ponds seen in direct surroundings
- Wet season floodings caused by rain and 'popping up' out ground, labeled as 'neigh' (1-2m) and disappears in days

Well characteristics

- At walking distance from nearest community
- Steel lid, no tube perforations above surface level

Pumping test

- Start delayed due to malfunctioning power converter
- Tangled rope: Position lowest diver undesirably high & hand measurements not completely possible, result: big gap in data
- Recovery test started at an early stage

Figure C.1: Factsheet of the aquifer test - location Bingo

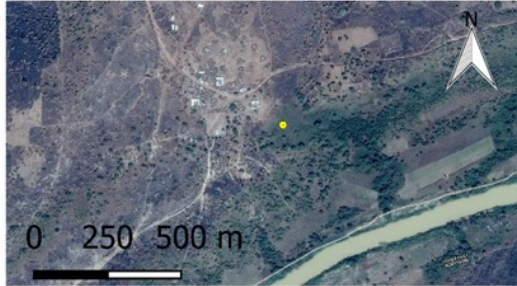
Nungo			
Site Specific info			
			
District:	Talensi		
Well coordinates:	N10 33.419		
	W0 38.990		
<u>Infiltration bed</u>			
Height:	-0.35 m		
Diameter:	1.50 m		
<u>Borehole depth</u>			
Initial:	42 m		
Measured:	9.80 m		
* Lengths relative to surface			
Pumping test configuration			
Date: 28-11-17			
<u>Positioning</u>			
Diver 1:	9.05 m	Time start:	09:45:00
Diver 2:	17.90 m	Time off:	11:00:00
Diver 3:	25.05 m	Time stop:	11:15:00
Diver 4:	-		
<u>Static water table</u>		Pump duration:	01:15:00 h
Initial:	3.02 m	$Q_{average}$:	< 5 m ³ /d
At start:	3.00 m	Suction depth:	31.20 m
Pumping test aborted			
* Lengths relative to well top			
Result -			
Pumping test aborted			
Remarks			
<u>Study site</u>			
<ul style="list-style-type: none"> - Mildly sloped till flat landscape - Vegetation abundant, agricultural field present but not ready for use - Volta river in close range (approximately 400 m) - Wet season floodings caused by riverbank overtopping; labeled as extreme (>3m) and constant; duration as long as wetseason 			
<u>Well characteristics</u>			
<ul style="list-style-type: none"> - At short walking distance from nearest community - No lid, and tube perforations present above surface level 			
<u>Pumping test</u>			
<ul style="list-style-type: none"> - Pump hard to descend in well; well clogged due to combination of clay, sand and water - Discharge rates very low during test - To improve discharge, test multiple times applied with increased position of pump suction - No drawdowns perceived, pumping test aborted 			

Figure C.2: Factsheet of the aquifer test - location Nungo

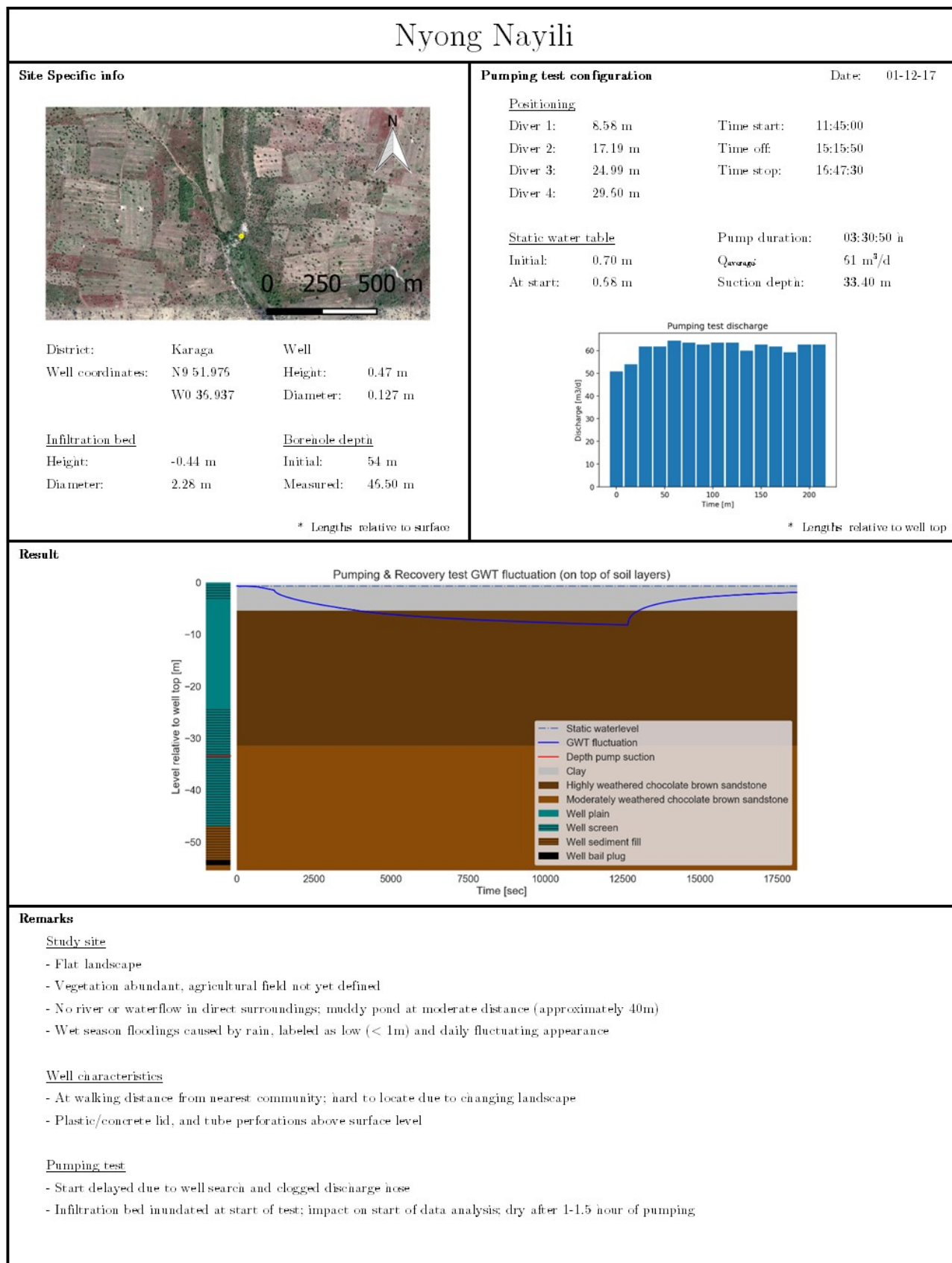


Figure C.3: Factsheet of the aquifer test - location Nyong Nayili

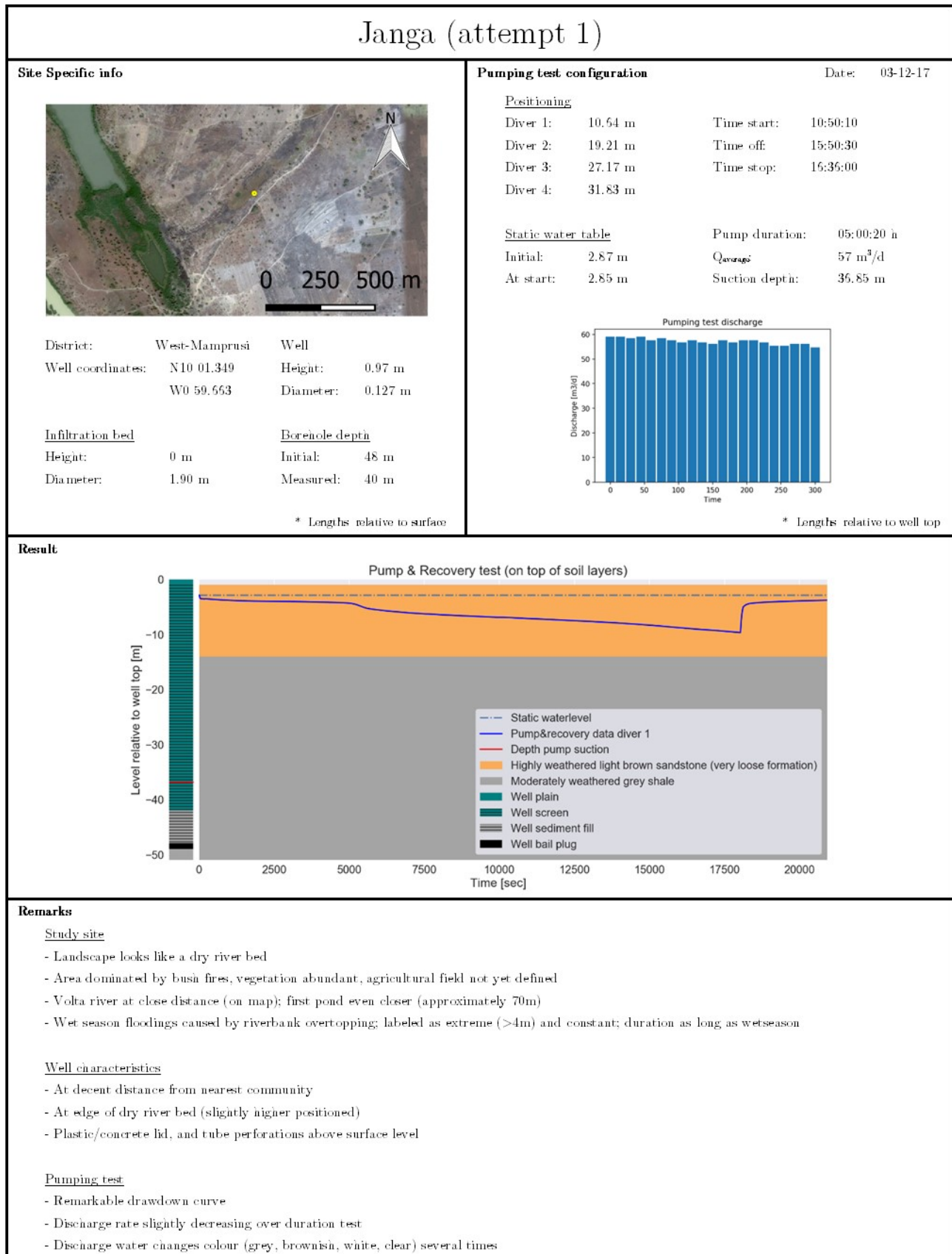


Figure C.4: Factsheet of the aquifer test - location Janga (1/2)

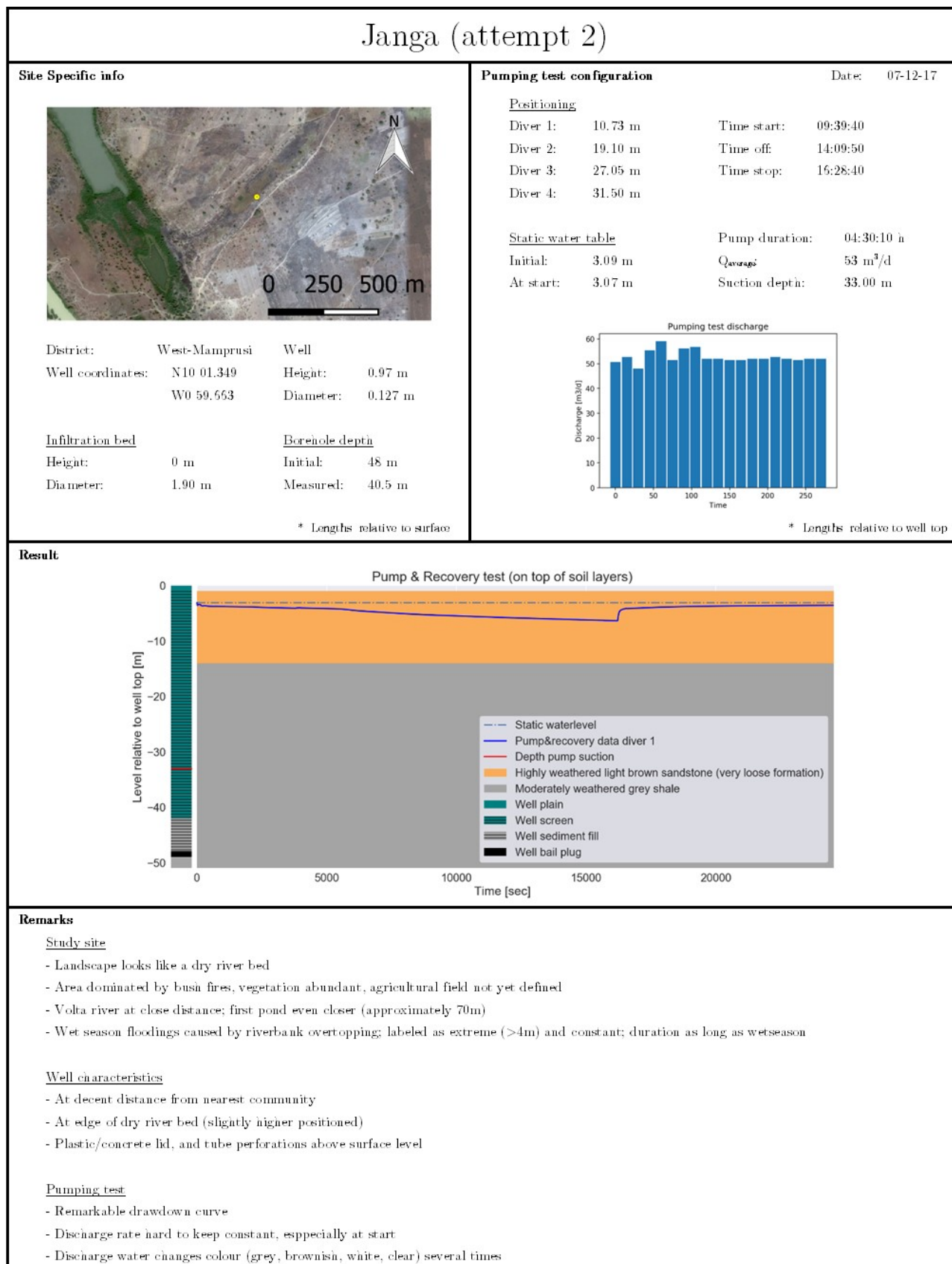


Figure C.5: Factsheet of the aquifer test - location Janga (2/2)

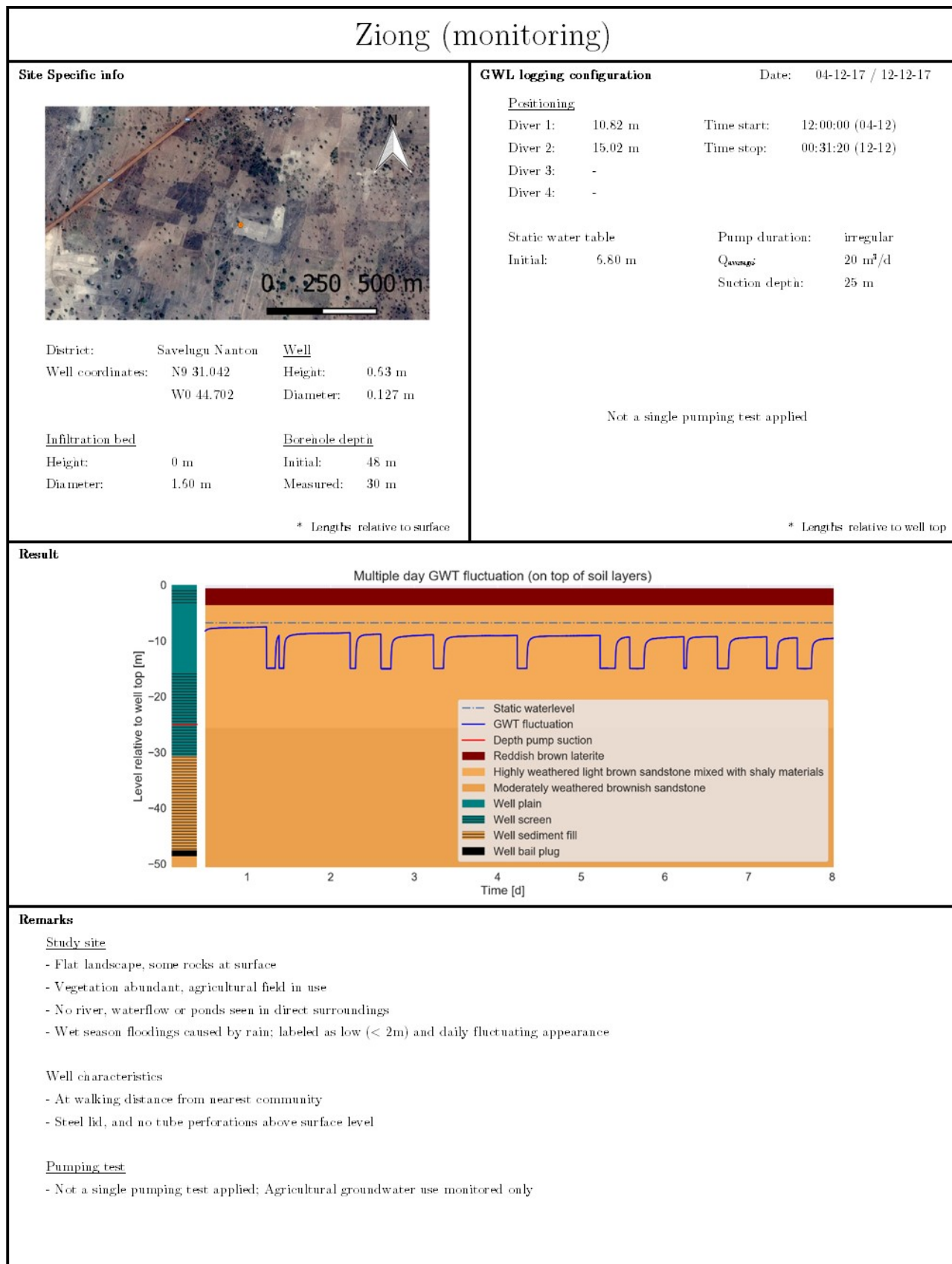


Figure C.6: Factsheet of the aquifer test - location Ziong (monitoring ASR system practical use)



Aquifer test - Data analysis overview

This appendix presents detailed information (location specific) regarding the aquifer test data analysis. Section D.1 contains several distinctive python script applied in the data analysis. An all-encompassing overview of the obtained geohydrological parameter values (T and S) can be found in Section D.2.

D.1. Example Python scripts

Example Python script - Theis's method

The Python implementation of the analytical Theis's method is presented below. The script describes the drawdown development of the groundwater table (GWT) over time, a development caused by a single pumping test (drawdown and recovery process).

```
def drawdown(t, T, S):  
    s = Q / (4 * np.pi * T) * exp1(r**2 * S / (4 * T * t))  
    s[t > toff] -= Q / (4 * np.pi * T) * exp1(r**2 * S / (4 * T * (t[t>toff] - toff)))  
    return s
```

Where s (m) is the drawdown at distance r (m) from the well, Q (m^3) is the constant well discharge, KD (m^2/d) is the aquifer transmissivity ($KD = T$), S (-) is the aquifer storativity, t (d) is the time measured from the start of pumping and $\exp1$ is the exponential integral. The drawdown measurements in this research are limited to in-well measurements. The distance r in Theis's equation is assumed to be the length of the well radius (0.0635 m).

Example Python script - Fmin-RMSE optimization

An example Python implementation of Fmin optimization is given below. It shows an optimization of a two layered model, containing five parameters (T and S values for two model layers and well skin resistance).

```
def optimTTim_Qvar(params, t, meas):  
    kaq = np.zeros(2)  
    Saq = np.zeros(2)  
    kaq[0] = params[0]  
    kaq[1] = params[1]  
    Saq[0] = params[2]  
    Saq[1] = params[3]  
    res = params[4]  
    s = drawdownTTim_Qvar(t, kaq, Saq, res)  
    error = np.sqrt(np.mean((s-meas)**2))  
    return error  
  
xopt = fmin(optimTTim_Qvar, x0=[10, 10, .01, .001, 0.1], args=(to[mask], do[mask]),  
           xtol=1e-4)
```

Where $kaq[0]$ and $kaq[1]$ (m/d) are respectively the hydraulic conductivities of the first and second layer, $Saq[0]$ and $Saq[1]$ (-) are the storativities of the first and second layer, res (d) is the well skin resistance, s (m) is the modelled (optimal) drawdown, $error$ (m) is the RMSE objective function and $x0$ contains the ordered initial parameter conditions. The $to[mask]$ and $do[mask]$ arguments are defined to make sure the time and drawdown data of an observed gab (measured) is not taken into account.

Example Python script - TTim Calibrate optimization

In the Python script below, an example of the TTim Calibrate function is given. In terms of content the script contains the same example as mentioned in the Fmin optimization above.

```
cal = Calibrate(mlc)
cal.parameter(name='kaq0', layer=0, initial=10, pmin=0)
cal.parameter(name='kaq1', layer=1, initial=10, pmin=0)
cal.parameter(name='Saq0', layer=0, initial=.01, pmin=0, pmax=0.3)
cal.parameter(name='Saq1', layer=1, initial=.001, pmin=0, pmax=0.3)
cal.parameter(name='res', par=wc.res, initial=0.1)
cal.series(name='obs3', x=ro, y=0, layer=[0,1], t=to[mask], h=-do[mask])
cal.fit()
```

Where ' $kaq0$ ' and ' $kaq1$ ' (m/d) are respectively the hydraulic conductivities of the first and second layer, ' $Saq0$ ' and ' $Saq1$ ' (-) are the storativities of the first and second layer, ' res ' (d), x (or y) (m) is the radius of the well, $layer$ contains the layer numbers of the 'active' connected layer, $initial$ is the initial parameter condition and $pmin$ and $pmax$ are the predefined 'allowed' minimum and maximum values for the particular parameter.

D.2. Data analysis overview

The individual GWT drawdown datasets (obtained in aquifer tests) are analysed by multiple simulations. The simulations are distinctive in: theoretical model (single layer, double layer and double layer with partial penetration of the well), method (analytical Theis's method (single layer only), TTim) and optimization function (Fmin-RMSE and TTim Calibrate). In the TTim analysis an additional distinction is made in well design definition of: (a) an actual borehole storage and no well resistance, (b) an optimal borehole storage and no well resistance, (c) an actual borehole storage and optimal well resistance, (d) an optimal borehole storage and optimal well resistance. Summarized, the location specific datasets are subjected to 25 different approaches in analysis; analytical (1x), Fmin-RMSE (3x4 = 12x) and TTim Calibrate (3x4 = 12x). An overview of the simulation approaches in aquifer test data analysis is presented in Table D.1. All obtained results (T and S values) can be found in the Figures D.1 - D.10.

Table D.1: Schematic overview of the distinctive simulation approaches in aquifer test data analysis

		Actual borehole storage	Optimal borehole storage	Optimal well resistance
Analytical		-	-	-
Fmin-RMSE	a	x	-	-
	b	-	x	-
	c	x	-	x
	d	-	x	x
TTim Cal	a	x	-	-
	b	-	x	-
	c	x	-	x
	d	-	x	x

Where the different approaches of the Fmin-RMSE and TTim Calibrate (a-d) are subsequently analysed in combination with a theoretical model defined by: a single layer system (1), a double layer system (2) and a system with a two layers and partial penetration of the well (2pp).

D.2.1. Location: Bingo

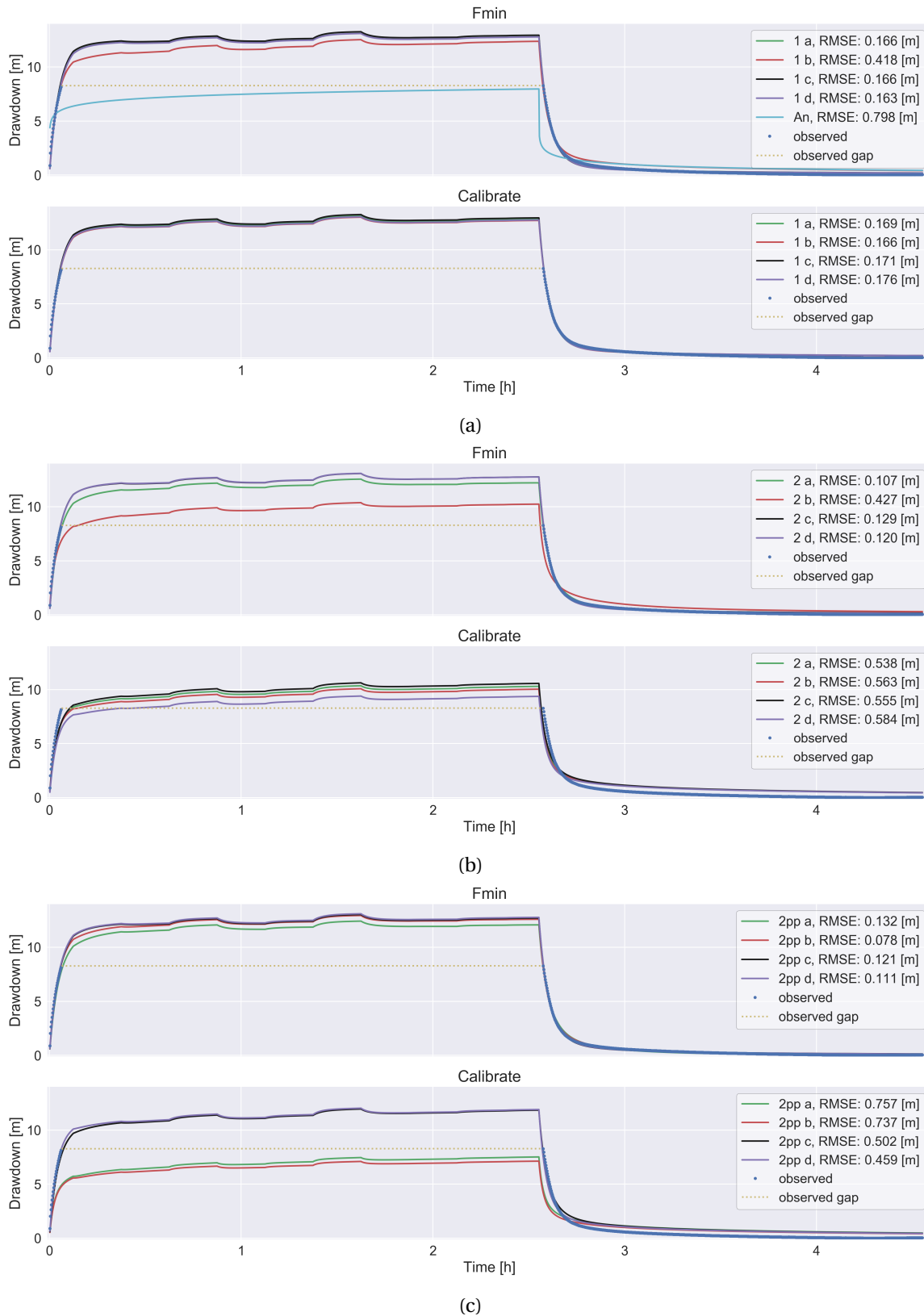


Figure D.1: Bingo - overview of the aquifer test data curve fitting analysis by the optimization fmin-RMSE method and the TTim calibrate method for (a) a single layer system, (b) a double layer system, and (c) a system with two layers and partial penetration of the well

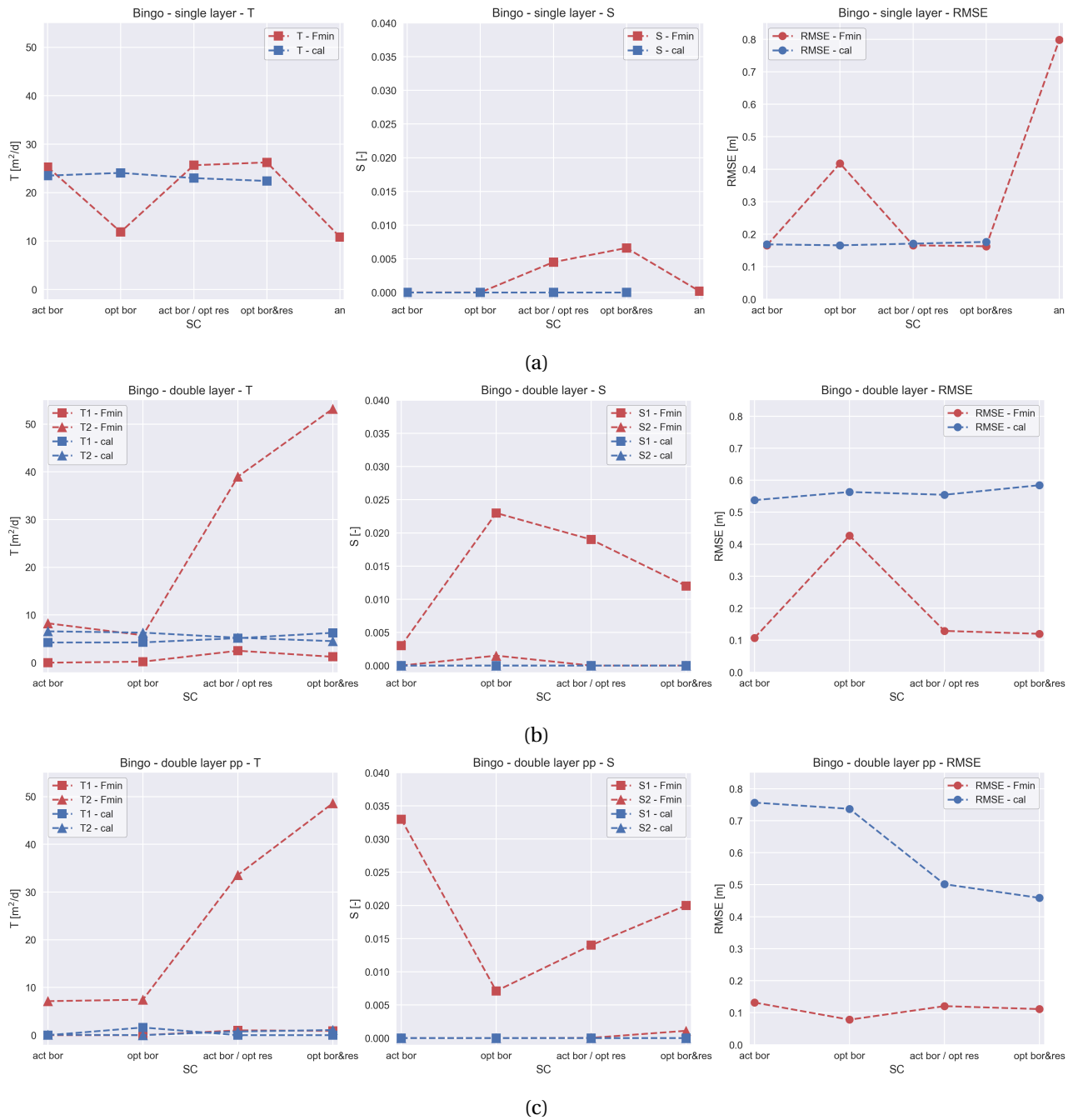


Figure D.2: Bingo - overview of the derived optimal geohydrological parameter values (Fmin and Calibrate) for (a) a single layer system, (b) a double layer system, and (c) a system with two layers and partial penetration of the well

D.2.2. Location: Nungo

The obtained aquifer test data at the location Nungo is not sufficient for the analysis and derivation of the geohydrological parameter values (T and S).

D.2.3. Location: Nyong Nayili

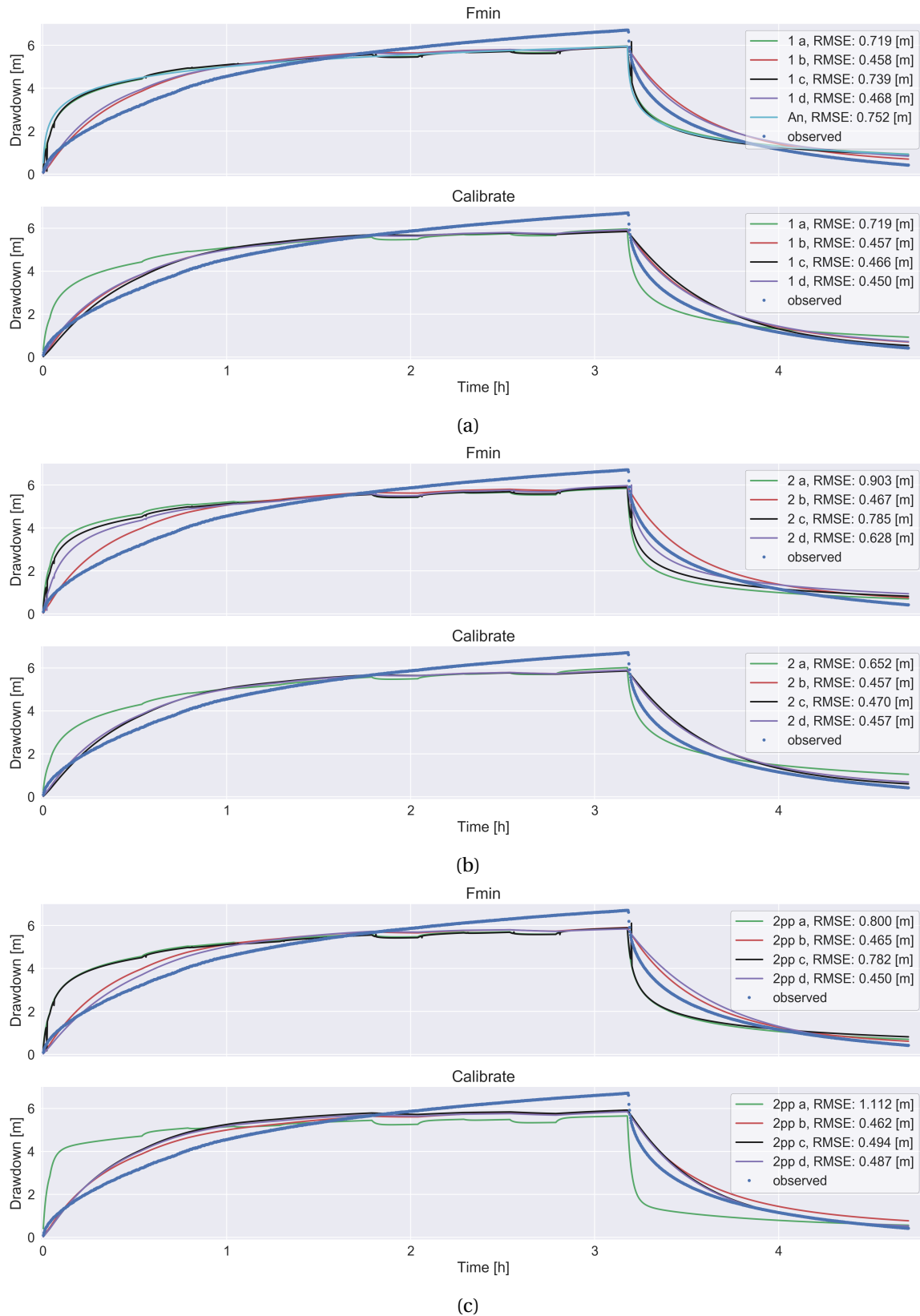


Figure D.3: Nyong Nayili - overview of the aquifer test data curve fitting analysis by the optimization fmin-RMSE method and the TTim calibrate method for (a) a single layer system, (b) a double layer system, and (c) a system with two layers and partial penetration of the well

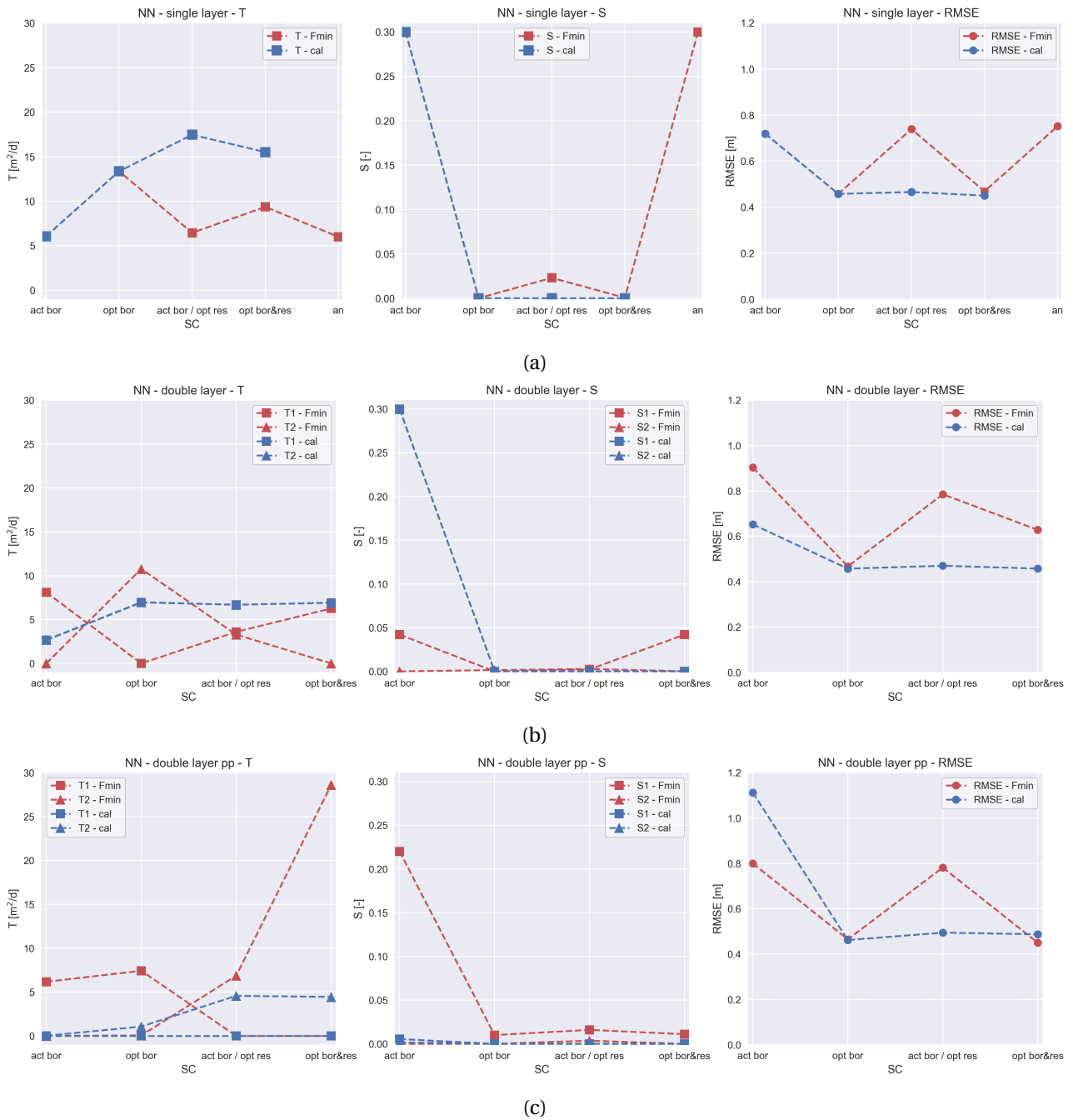


Figure D.4: Nyong Nayili - overview of the derived optimal geohydrological parameter values (Fmin and Calibrate) for (a) a single layer system, (b) a double layer system, and (c) a system with two layers and partial penetration of the well

D.2.4. Location: Janga (1/2)

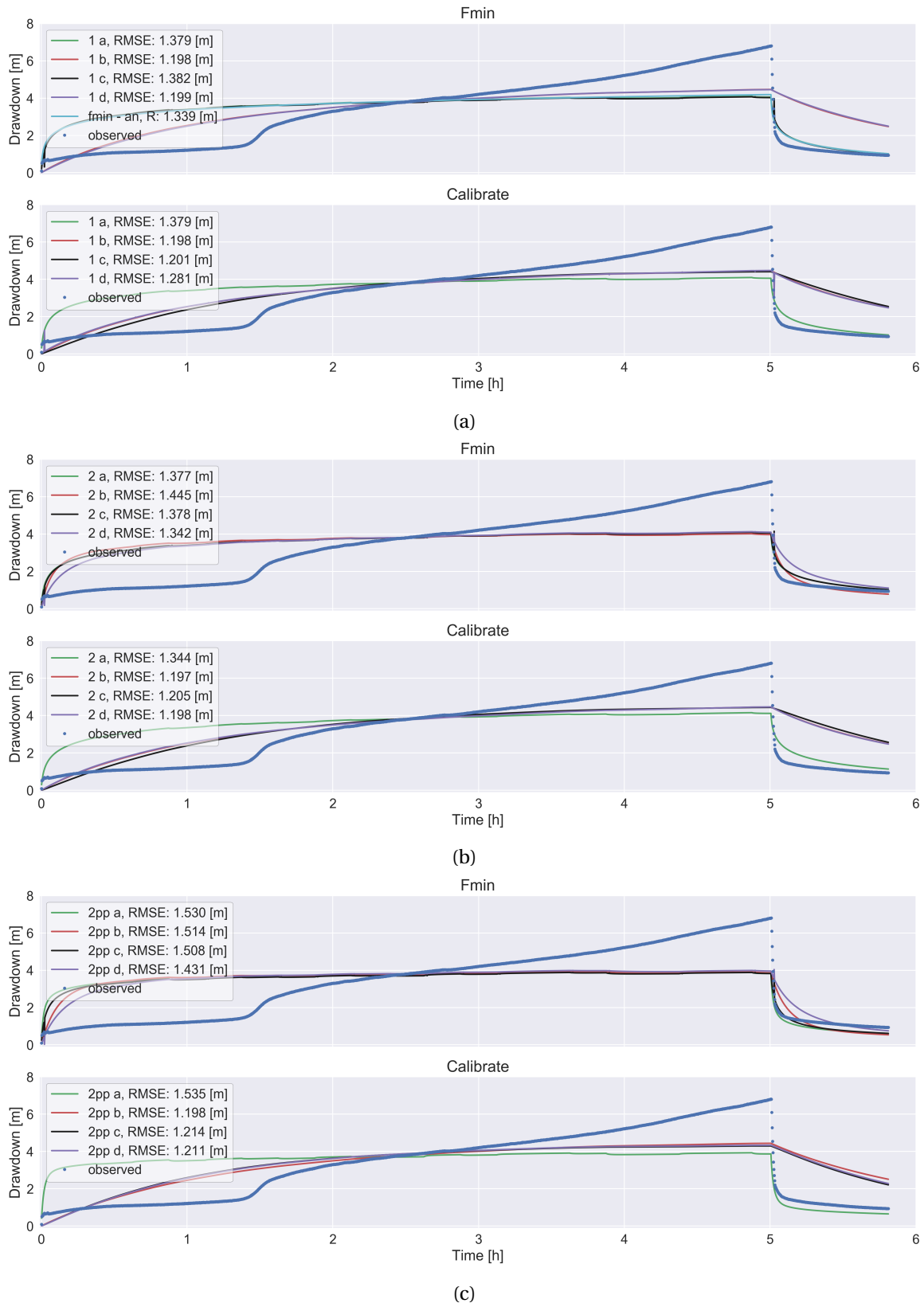


Figure D.5: Janga (1/2) - overview of the aquifer test data curve fitting analysis by the optimization fmin-RMSE method and the TTim calibrate method for (a) a single layer system, (b) a double layer system, and (c) a system with two layers and partial penetration of the well

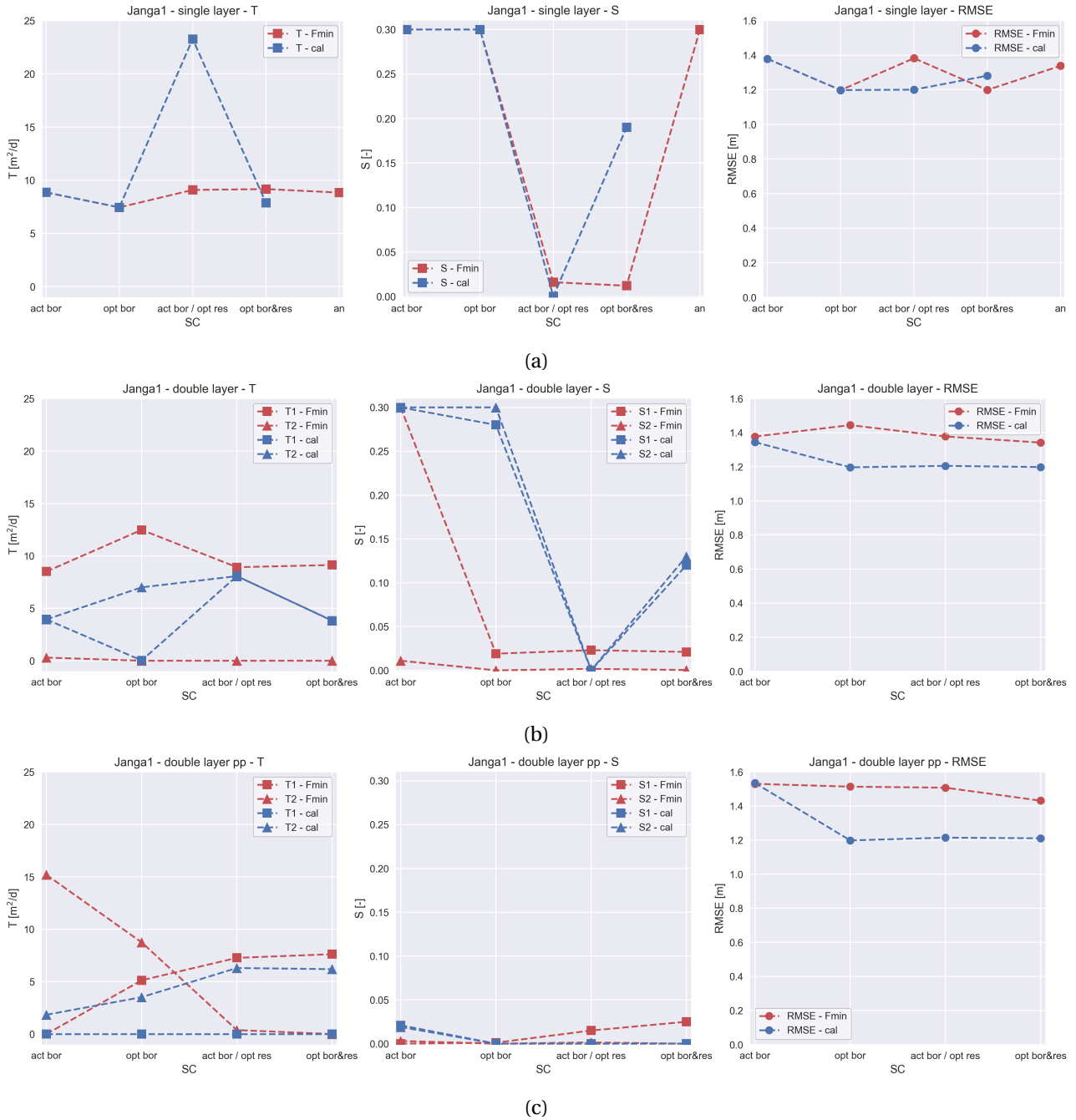


Figure D.6: Janga1 (1/2) - overview of the derived optimal geohydrological parameter values (Fmin and Calibrate) for (a) a single layer system, (b) a double layer system, and (c) a system with two layers and partial penetration of the well

D.2.5. Location: Janga (2/2)

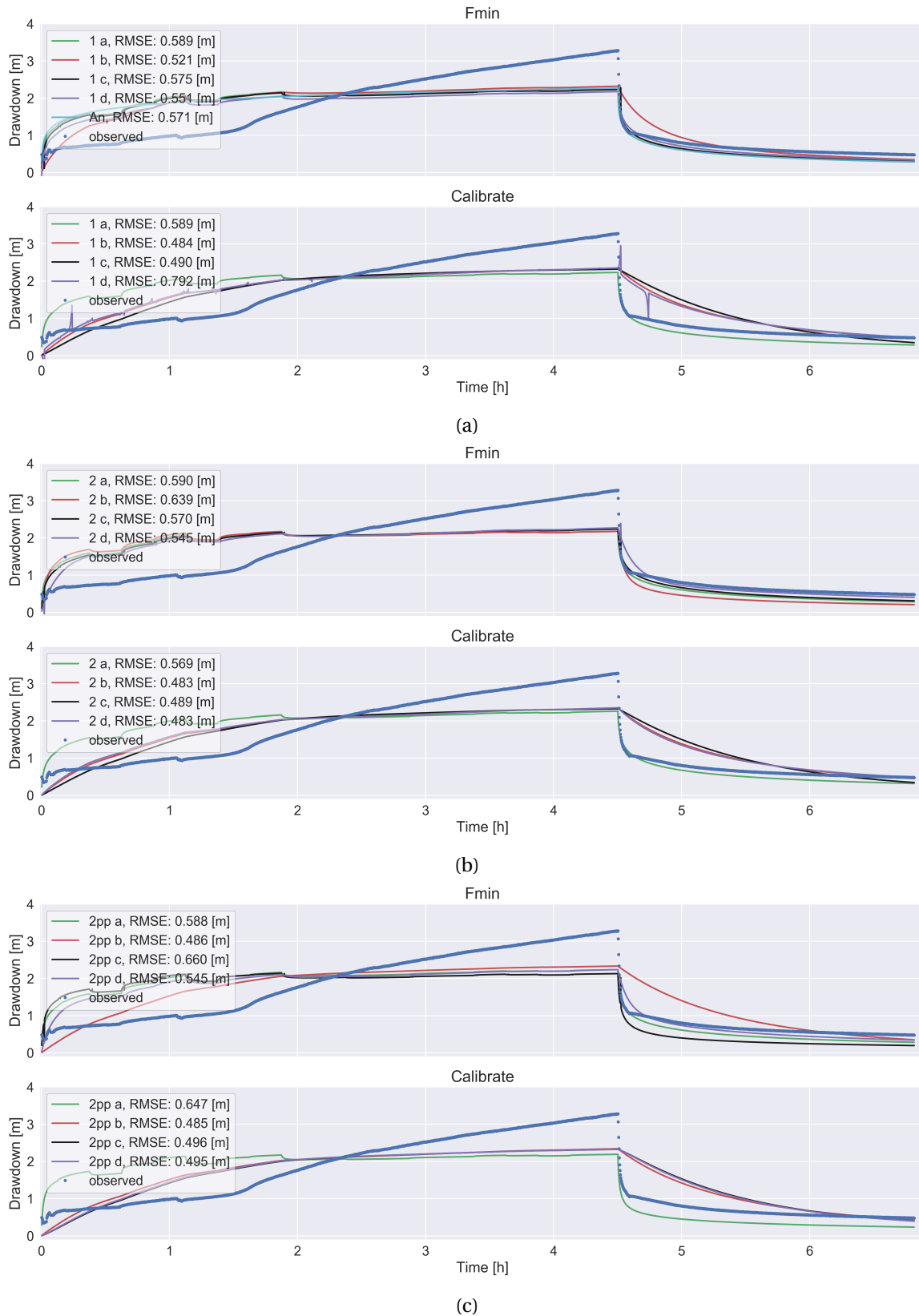


Figure D.7: Janga (2/2) - overview of the aquifer test data curve fitting analysis by the optimization fmin-RMSE method and the TTim calibrate method for (a) a single layer system, (b) a double layer system, and (c) a system with two layers and partial penetration of the well

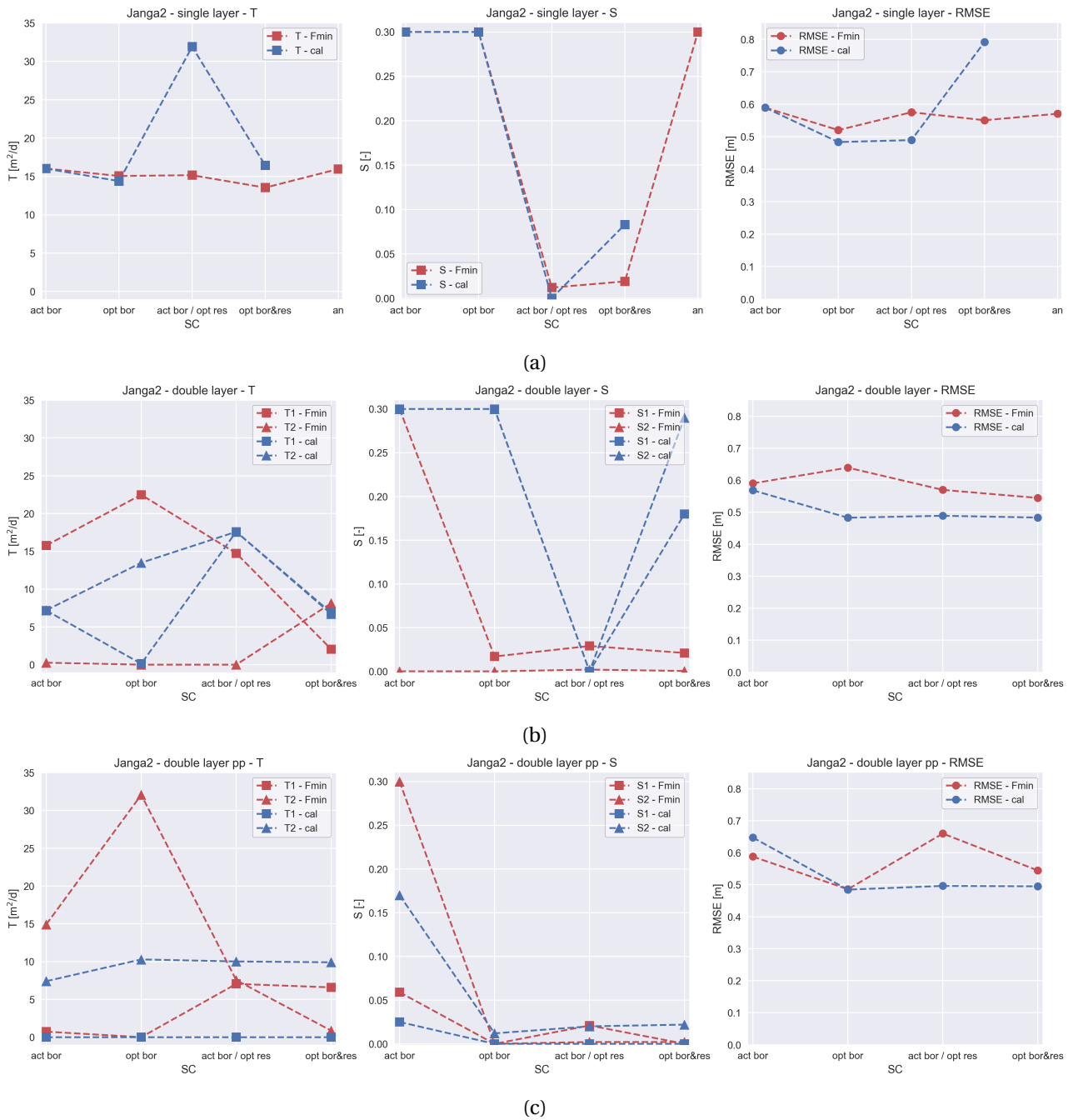


Figure D.8: Janga (2/2) - overview of the derived optimal geohydrological parameter values (Fmin and Calibrate) for (a) a single layer system, (b) a double layer system, and (c) a system with two layers and partial penetration of the well

D.2.6. Location: Ziong

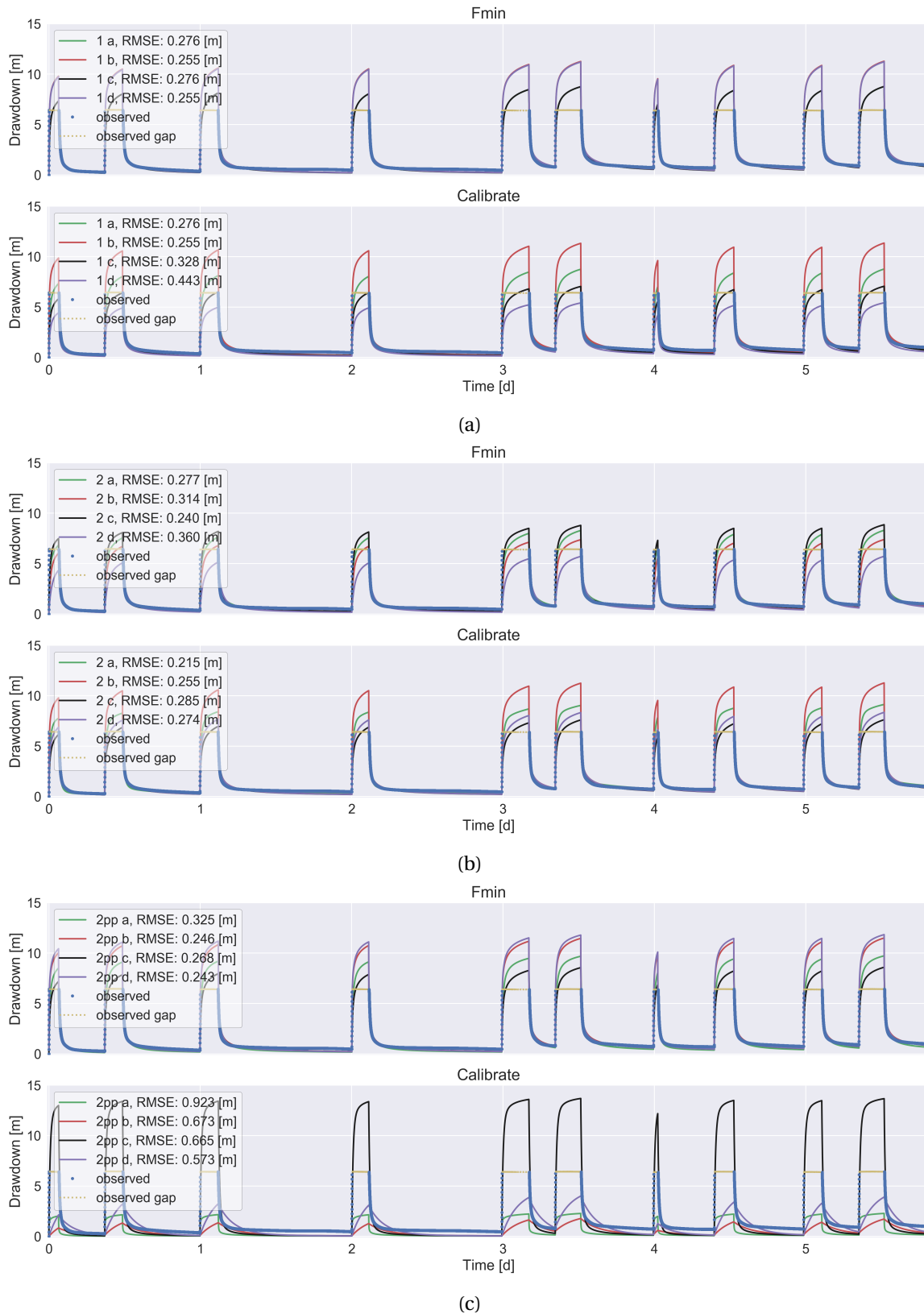


Figure D.9: Ziong - overview of the aquifer test data curve fitting analysis by the optimization fmin-RMSE method and the TTim calibrate method for (a) a single layer system, (b) a double layer system, and (c) a system with two layers and partial penetration of the well

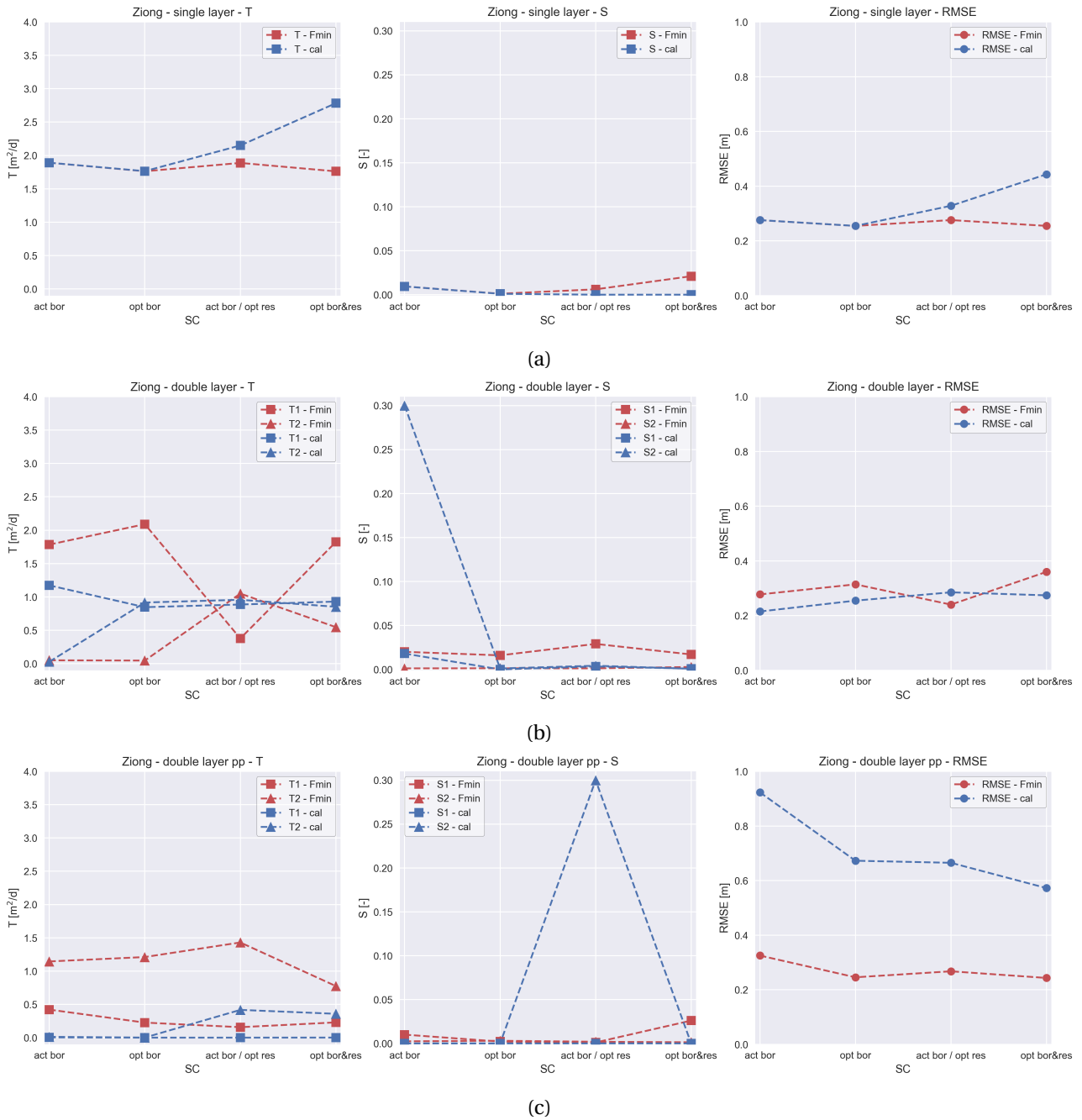
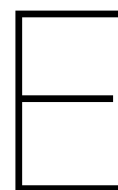


Figure D.10: Ziong - overview of the derived optimal geohydrological parameter values (Fmin and Calibrate) for (a) a single layer system, (b) a double layer system, and (c) a system with two layers and partial penetration of the well



MODFLOW - Radial conversion

The general thesis topic is pointed at the performance of a single ASR system in northern Ghana. Due to seasonal circumstances, the same ASR system acts both as an extraction and injection well. The direction of groundwater flow is alternately pointed towards and away from the well. This phenomenon can be simulated straightforward by the use of the standard USGS's modular groundwater flow model; MODFLOW. To generate adequate results in groundwater fluctuations, high model accuracies are desirable. The rectangular model preferably accommodates a fine-meshed grid (especially at close well range). This can be done by the implementation of a multitude of rows and columns. As a consequence, model run times will last long. A more sophisticated research approach that works around this issue is potentially more suitable in this case. The groundwater flow around a single well can be approached as a phenomenon of radial symmetry. The radial conversion of parameter can reduce the number of dimensions in the MODFLOW model. A modification that reduces model run times substantially (Langevin, 2008). Section E.1 contains a detailed description of the MODFLOW model radial scaling of subsurface parameters. These specific conversions are included in the models applied in this research. In Section E.2, three fictive well simulation examples are presented to validate and compare the performance of a radial scaled MODFLOW model.

E.1. Theoretical method of radial scaling a MODFLOW model

MODFLOW is originally based on a geometry consisting of rectangular cells. By the concatenation of multiple cells, a MODFLOW model grid is defined as being (multi layered) rectangular. The rectangular model shape is not eminently applicable on the situation of a single well simulation. Under the assumption of subsurface conditions to be homogeneous and the absence of elements disturbing the regional hydraulic gradient, it is possible to interpret the groundwater flow around a well as a phenomenon that is strictly cylindrical. In this way, one can define an axially symmetric model that simulates the single well performance (Figure E.1).

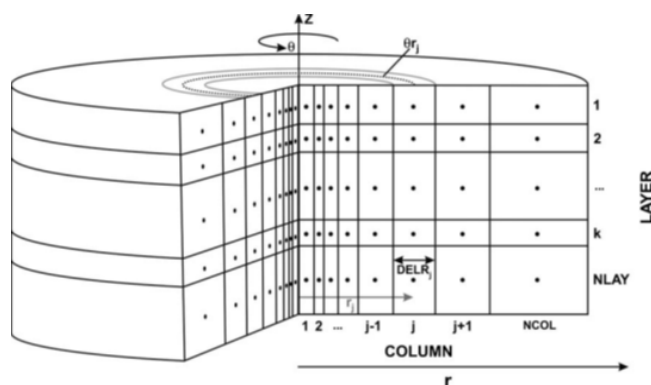


Figure E.1: Schematic of an axially symmetric model (Langevin, 2008)

The cylindrical model approach of a single well can be simulated in MODFLOW (rectangular geometry) by a specific definition of the grid structure. The model grid should accommodate one or more layer(s), one row only and multiple columns. In this single row MODFLOW model it is assumed the well is included in the first column (absolute left). Moreover, the single row should act as the representation of a subsurface slice. This is achieved by the radial modification of multiple parameters. The radial parameter scaling guaranties the conversion of a rectangular (single row) MODFLOW model into a fictive radial model. Elaborating on the explanation of Langevin (2008) the following model parameters become radial dependent:

$$K_h \rightarrow K_{h,j}^* = K_{h,j} \theta r_j \quad (\text{E.1})$$

$$K_v \rightarrow K_{v,j}^* = K_{v,j} \theta r_j \quad (\text{E.2})$$

$$S_s \rightarrow S_{s,j}^* = S_{s,j} \theta r_j \quad (\text{E.3})$$

$$S_y \rightarrow S_{y,j}^* = S_{y,j} \theta r_j \quad (\text{E.4})$$

$$n \rightarrow n_j^* = n_j \theta r_j \quad (\text{E.5})$$

Where K_h and K_v represent the horizontal and vertical hydraulic conductivity, S_s is the specific storage, S_y is the specific yield (phreatic storage) and n is the porosity. The radial scaled (modified) parameters are highlighted by the introduction of the superscript *. As visible by the subscript j the parameters hereby become column (radial) dependent. r_j is the radial distance between column j and the well (absolute left column) and θ is the angle of the representing slice. For the purpose of radial scaling a well, θ covers a complete ring; θ equals 2π .

The main advantage of the implementation of the radial parameter conversion is the reduction in model dimensions. At local scale (close well range) the model can contain a detailed meshed-grid without the emergence of excessive model run times. Moreover, the parameter conversion is applied within the common modelling program MODFLOW itself, no specialized programs are required. However, it should be mentioned that the circular model approach can only be applied under the specific assumptions of radial symmetry (Langevin, 2008).

E.2. Validation of a radial scaled MODFLOW model

To test the radial scaled MODFLOW model performance, three test exercises are presented in this part. These examples do not apply to the simulation of a northern Ghana ASR system. The examples are fictive well presentations and are purely included in the report to validate the model performances. In these exercises a comparison is made between the radial scaled MODFLOW model (Figure E.2c) and two rectangular based MODFLOW models. The standard rectangular MODFLOW grid (Figure E.2a) is included in the most straightforward model. Due to the squared shape, deviations in model outcome are expected (compared to radial scaled model). Whereas the rectangular round MODFLOW model (Figure E.2b) is manually circularized. This model accommodates for the gradual increase in flow area in the radial direction of the well. By the interpretation of the descriptions stated by Langevin (2008), it can be expected that the results of the rectangular round model should more closely approximate the radial model performances.

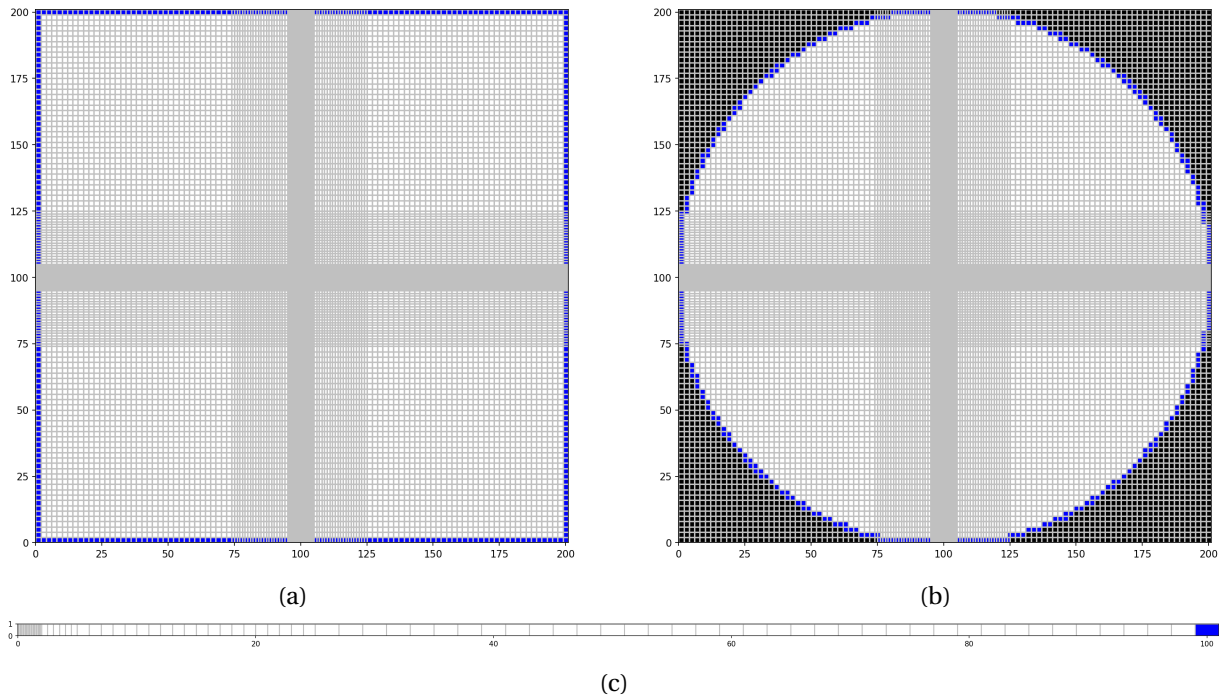


Figure E.2: A top view visual impression of the test example grid structures for: (a) a rectangular MODFLOW model, (b) a rectangular round MODFLOW model and (c) a radial scaled (single row) MODFLOW model (grey = cell boundary, red = well position, blue = boundary condition, black = inactive cell)

The test exercises applied in this research deliberately show strong similarities with the first two test problem cases described by Langevin (2008). In terms of content the exercises are designed with the same set of parameters, making it possible to validate the results in general. As an exception, a deviation is applied in terms of grid definition. In the exercises of this research, the cell sizes increase (grouped) stepwise and are based on an increasing (radial) distance from the well. By the use of the cell sizes 0.1 (20x), 0.5 (6x), 1.0 (20x) and 2.0 m (38x) a total model length (radial length) of 101 m is simulated. This grid structure is applicable on the single row (radial) model. The rectangular and rectangular round models accommodate a corresponding grid structure, as visible in the MODFLOW model top view grid structures of Figure E.2.

E.2.1. Test 1: Steady flow to a fully penetrating well in a confined aquifer

The steady state solution of a confined aquifer that is fully penetrated by a well, is applied as a first MODFLOW model performance test. The exercise schematic configuration is presented in Figure E.3. The case is characterized by its simplicity, making it an exercise eminently suitable for model performance comparison. The results of the different MODFLOW models are compared with the groundwater table (GWT) drawdowns (and heads) obtained by the analytical solution. The situation can be expressed analytically by both methods below.

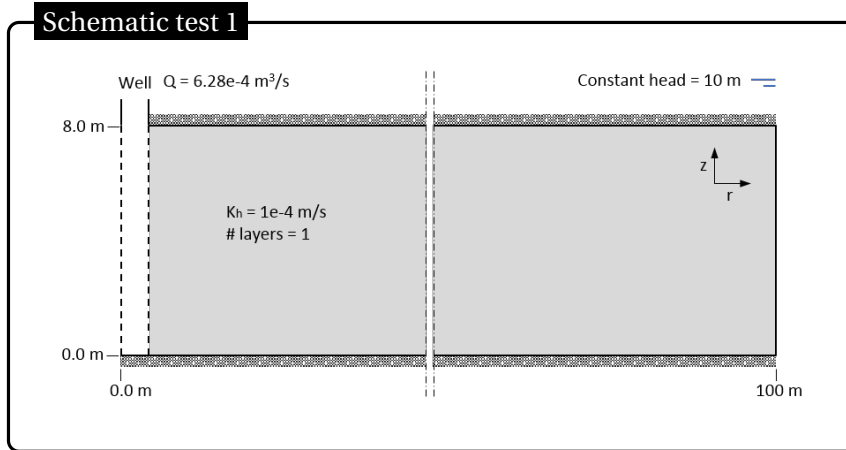


Figure E.3: Schematic test 1

Analytical Thiem's method

The analytical Thiem's method (Equation E.6) can be applied to obtain the steady state drawdown solutions caused by the radial well flow in a confined aquifer (Kruseman and de Ridder, 2000):

$$S_j = \frac{Q \ln\left(\frac{r_2}{r_j}\right)}{2\pi K_{(h)} H} \quad (\text{E.6})$$

Where S_j is the drawdown in column j , Q is the discharge, $r_2 = 100 \text{ m}$ (constant head at a distance of in this case 100 m from the well), r_j is the radial distance between column j and the well (column 1), $K_{(h)}$ is the horizontal hydraulic conductivity and H is the aquifer thickness.

Analytical discharge potential (ϕ)

The decline in groundwater head, due to the presence of a single well in a confined aquifer, can be expressed by the use of the analytical discharge potential (ϕ). The equation for the discharge potential is presented in (Equation E.7). When confined conditions are applicable, it is given that the H equals h_0 (Bakker and Anderson, 2011; Strack, 1989). As a result, the confined aquifer groundwater heads can be determined by the application of equation E.9. The obtained groundwater head values are in correspondence with the drawdowns calculated by the analytical Thiem's method.

$$\phi_j = \frac{Q}{2\pi} \ln\left(\frac{r_j}{R}\right) + \phi_0 \quad (\text{E.7})$$

$$\phi_0 = k_h H h_0 \quad (\text{E.8})$$

$$h_j = \frac{\phi_j}{k_h H} \quad (\text{E.9})$$

Where ϕ_j is the discharge potential at column j , Q is the discharge, $R = 100 \text{ m}$ (constant head (h_0) at a distance of in this case 100 m from the well), r_j is the radial distance between column j and the well (absolute left column), $K_{(h)}$ is the horizontal hydraulic conductivity and H is the aquifer thickness.

Model validation test results

The results of the different Modflow models generally do not deviate much from the (GWT) heads obtained by the analytical solution(s). A close comparison with the outcomes of the analytical solution learns that the rectangular MODFLOW model overestimates drawdowns slightly (modelled heads are slightly lower). This overestimation is present over (almost) the entire radial extent of the model. A difference in outcome that can be explained by the rectangular shape of the model; imposed boundary condition along the model edge (especially the corners) are positioned ‘outside’ the defined radial boundary of 100 m from the well. The rectangular round model works around this inconvenience, and shows more similarities with the results obtained by the analytical solution. Some deviation in the first meter(s) around the well are present, which can potentially be attributed to the cell structure (rectangular grid size). These minor deviations are absent by the application of the radial scaled (single row) model. Regardless the (radial) position (and model solver (LPE, UPW)), the radial converted MODFLOW modelled results in heads and drawdowns are identical to the analytical solution. This is an indication that the radial scaled MODFLOW model is usable for the research purposes.

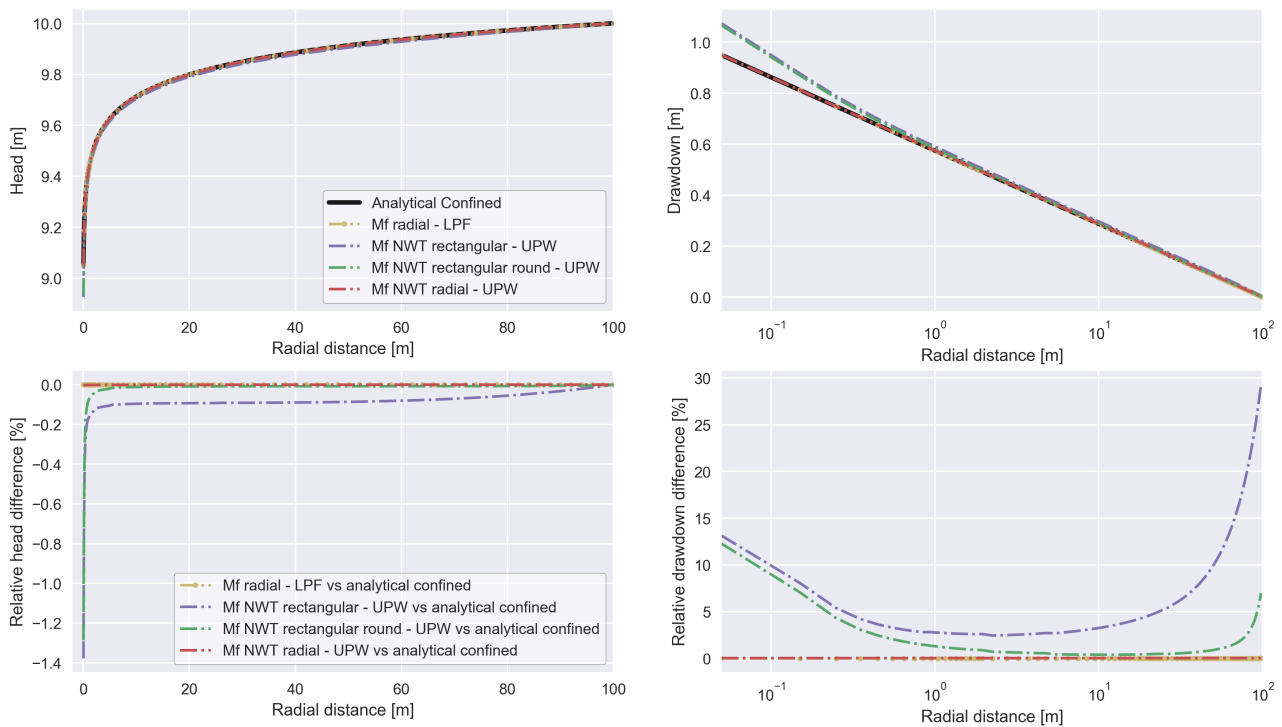


Figure E.4: Results test 1

E.2.2. Test 2: Steady flow to a fully penetrating well in an unconfined aquifer

The example test exercise two (Figure E.5) accommodates almost the same fictive problem as stated in test one (Section E.2.1). As a single exception, the test problem is in this part defined by the presence of a well that is fully penetrating an unconfined aquifer. The conditions are valid to compare the obtained MODFLOW model results with the results of the analytical solution(s). In this example the analytical steady state drawdown solution is presented by the Thiem-Dupuit's method, while groundwater heads can be derived directly by the use of the analytical discharge potential.

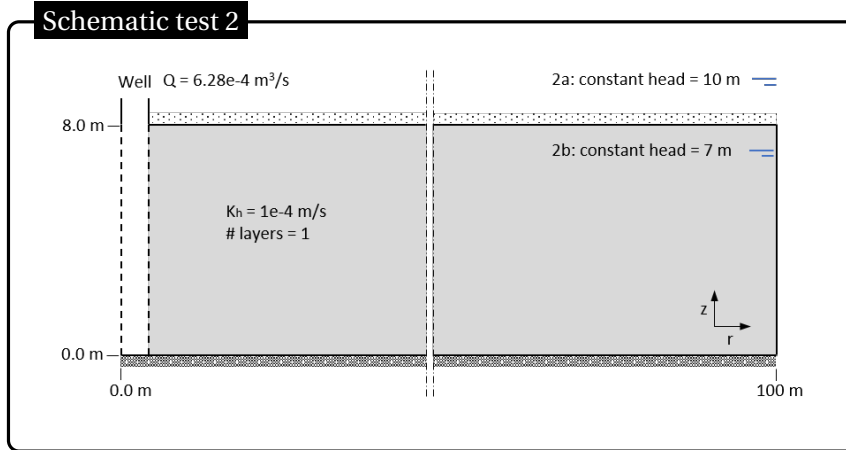


Figure E.5: Schematic test 2

Analytical Thiem-Dupuit's method

The analytical Thiem-Dupuit's method (Equations E.10 and E.11) can be applied to obtain the steady state drawdown solutions caused by the radial well flow in a unconfined aquifer (Kruseman and de Ridder, 2000):

$$S'_j = \frac{Q \ln\left(\frac{r_2}{r_j}\right)}{2\pi K_{(h)} D} \quad (\text{E.10})$$

$$S'_j = S_j - \frac{S_j}{2D} \quad (\text{E.11})$$

Where S'_j is the uncorrected drawdown in column j , S_j is the observed drawdown (to be determined iteratively) in column j , Q is the discharge, $r_2 = 100 \text{ m}$ (constant head at a distance of 100 m from the well), r_j is the radial distance between column j and the well (absolute left column), $K_{(h)}$ is the horizontal hydraulic conductivity and D is the (flow through) thickness between the aquifer bottom and the constant head. For the purposes of this exercise the drawdowns obtained by the analytical Thiem-Dupuit's equations are iteratively determined with a precision of 1×10^{-6} .

Analytical discharge potential (ϕ)

The previously introduced analytical discharge potential (ϕ) (Equation E.12) can also be applied under unconfined aquifer conditions (Bakker and Anderson, 2011; Strack, 1989). Compared to the confined aquifer conditions, the derivation of (GWT) heads deviates slightly when unconfined conditions are applicable. In the situation of an unconfined aquifer, the head is defined by equation E.14. An advantage in the use of the discharge potential, compared to the analytical Thiem-Dupuit's method, is the absence of the iterative head derivation process. The analytical results in (unconfined aquifer) groundwater head are obtained fast and accurate by the application of the discharge potential.

$$\phi_j = \frac{Q}{2\pi} \ln\left(\frac{r_j}{R}\right) + \phi_0 \quad (\text{E.12})$$

$$\phi_0 = \frac{1}{2} k_h h_0^2 \quad (\text{E.13})$$

$$h_j = \sqrt{\frac{2\phi_j}{k_h}} \quad (\text{E.14})$$

Where ϕ_j is the discharge potential at column j , Q is the discharge, $R = 100$ m (constant head (h_0) at a distance of in this case 100 m from the well), r_j is the radial distance between column j and the well (column 1), $K_{(h)}$ is the horizontal hydraulic conductivity and H is the aquifer thickness.

Model validation test results (a) Head at model extent equals 10 m

In relative terms, the results obtained by the MODFLOW rectangular, rectangular round and radial scaled (single row) models deviate substantially from the results obtained by the unconfined analytical derivation method (discharge potential method). A performance that can be justified by the definition of an ‘unconfined’ aquifer in the MODFLOW-NWT environment. In MODFLOW-NWT this test problem situation is simulated by the definition of a ‘convertible’ layer type. In the case of a predefined GWT that exceeds the aquifer height, it is actually the aquifer height itself that becomes normative. The MODFLOW-NWT model simulates the heads (drawdowns) by the use of a flow through area (height) that equals the aquifer thickness (difference between aquifer top and bottom (8m)). An interpretation that is confirmed by comparing the radial scaled MODFLOW-NWT results to the results of the confined analytical solution.

The results obtained by the more common applied MODFLOW-2005 (LPF solver) show more similarities in performance with respect to the analytical unconfined solution. Nonetheless, the radial converted MODFLOW model results (in heads and drawdowns) are not identical to the analytical solution (discharge potential method). A performance that can be assigned to the MODFLOW-2005 definition of an ‘unconfined aquifer’. Here, the flow through area (height) is spatially fixed and defined as the difference between the position of the constant head and the aquifer bottom (10m). As a result, the obtained heads are slightly overestimated (drawdowns underestimated). An interpretation that is confirmed by comparing the radial scaled MODFLOW (LPF solver) model results to the results of the quasi unconfined analytical solution (uncorrected Thiem-Dupuit’s method).

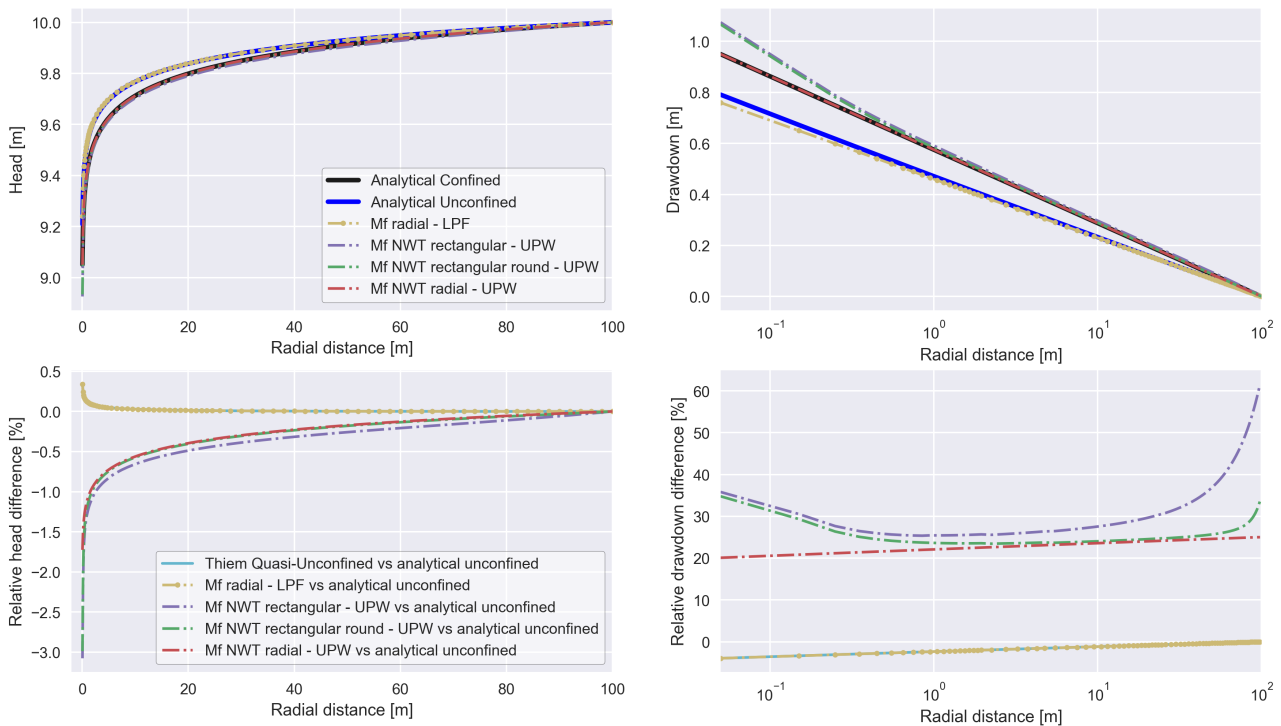


Figure E.6: Results test 2a

Model validation test results (b) Head at model extent equals 7 m

In addition, the case of test two (unconfined aquifer) is subjected to a situation in which the constant head at the model extent (tail) is defined at an elevation of 7 m (GWT head defined below the top of the aquifer). Under these conditions, the MODFLOW-2005 (LPF solver) performance is not substantially changed, while the heads (and drawdowns) obtained by the MODFLOW-NWT models show more similarities with respect to the results of the unconfined analytical solutions (discharge potential method). When the GWT remains below the top of the aquifer, the performances of the MODFLOW-NWT models are comparable to the previously obtained performances in the example of test case one (Section E.2.1). Compared to the analytical unconfined solution, the drawdowns obtained by rectangular and the rectangular round MODFLOW models are slightly overestimated (especially at close well range). Meanwhile, the radial converted MODFLOW-NWT model results (in heads and drawdowns) are identical to the results obtained by the unconfined analytical solution. These performances show the advantageous of the use of a radial scaled MODFLOW-NWT model that accommodates a ‘convertible’ layer type (Figure E.7).

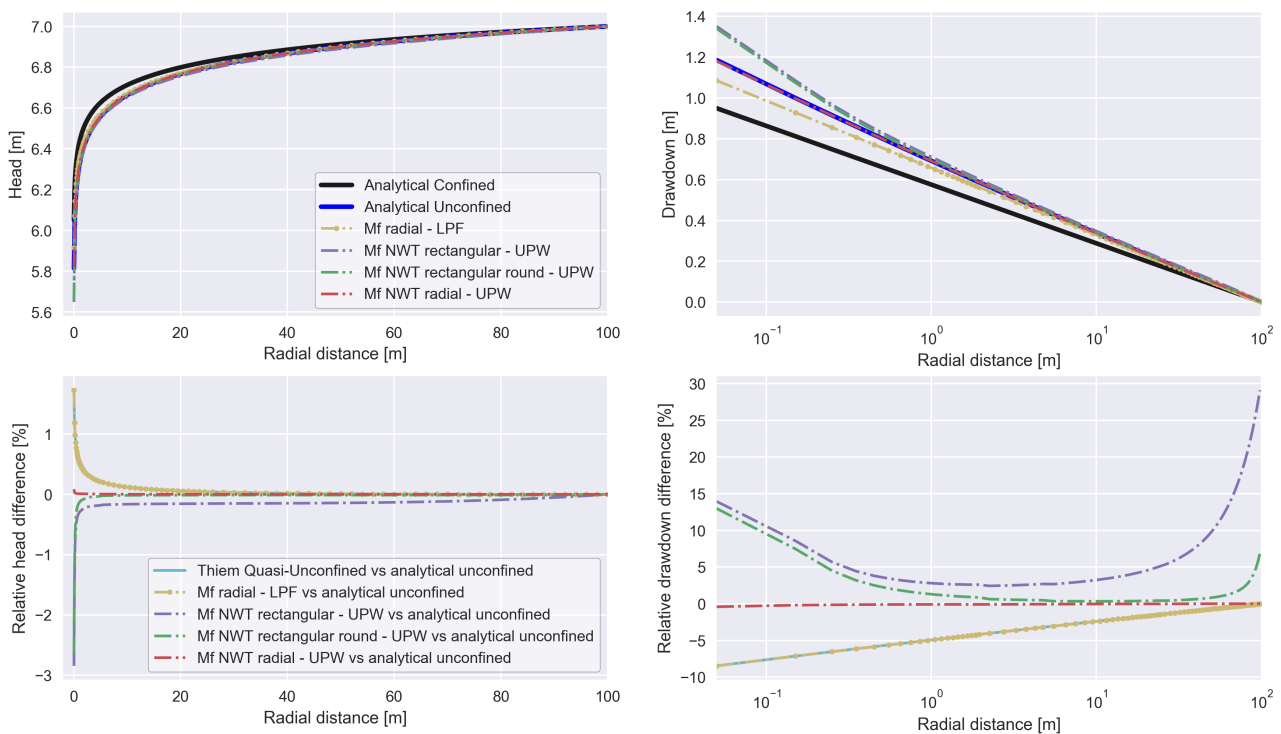


Figure E.7: Results test 2b

E.2.3. Test 3: Unsteady flow to a partially penetrating well in a confined/unconfined aquifer

As a final exercise the different MODFLOW models are subjected to a more complicated case (Figure E.8). The specific exercise (test 3) includes all model parameters which are dependent on radial scaling. In this way, the overall radial model performance is tested. The test problem consists of a well which is partially penetrating the aquifer, making it a multi-layered problem. By summing up the fractional discharges of the penetrating model layers (48-72), the total well discharge is obtained. Moreover, the exercise is time dependent. The modelled results are obtained after one day of groundwater withdrawal.

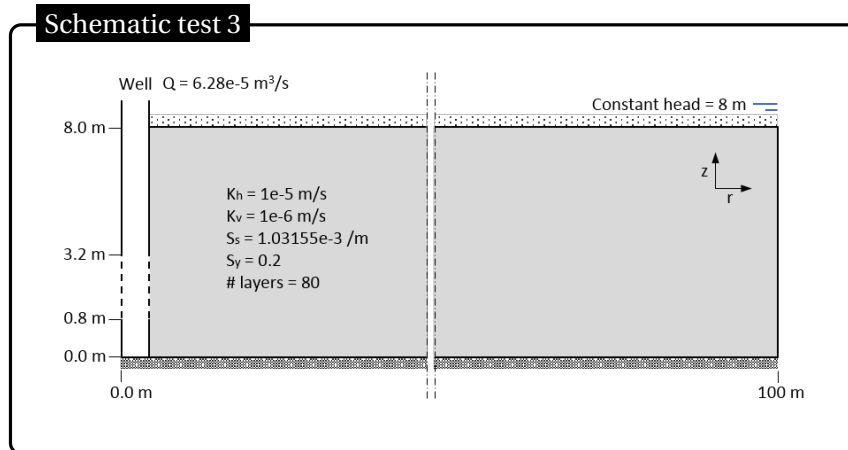


Figure E.8: Schematic test 3

The performance of the radial scaled (single row) MODFLOW-NWT model is visualized by the head contour plot in figure E.9. The figure illustrates the well discharge impact on heads in the first 20 m of the radial surroundings (within the aquifer). The different MODFLOW models (rectangular, rectangular round, radial NWT and radial LPF) are mutual compared by the head results at an height of 2.0 m (relative to aquifer bottom) along the entire radial extent of the aquifer (Figure E.10). The outcome of the comparative study is a scaled (single row) radial MODFLOW model (MODFLOW-NWT and MODFLOW-2005) which performs as expected. With the exception of the first meter(s) around the well, absolute differences in heads between the rectangular and the rectangular round models versus the radial MODFLOW models are negligible. The deviations at close well range can be attributed to the chosen grid structure. Due to the absence of reference material (e.g. an analytical solution not included) no further conclusions can be drawn upon this test exercise model performance. The correctness of the obtained head (and drawdown) values is undetermined.

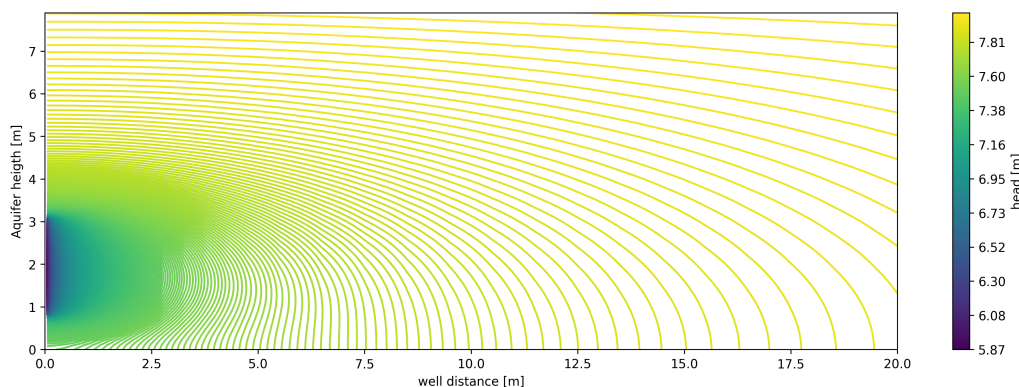


Figure E.9: Results test 3: Cross-sectional head contour plot after 1 day of pumping

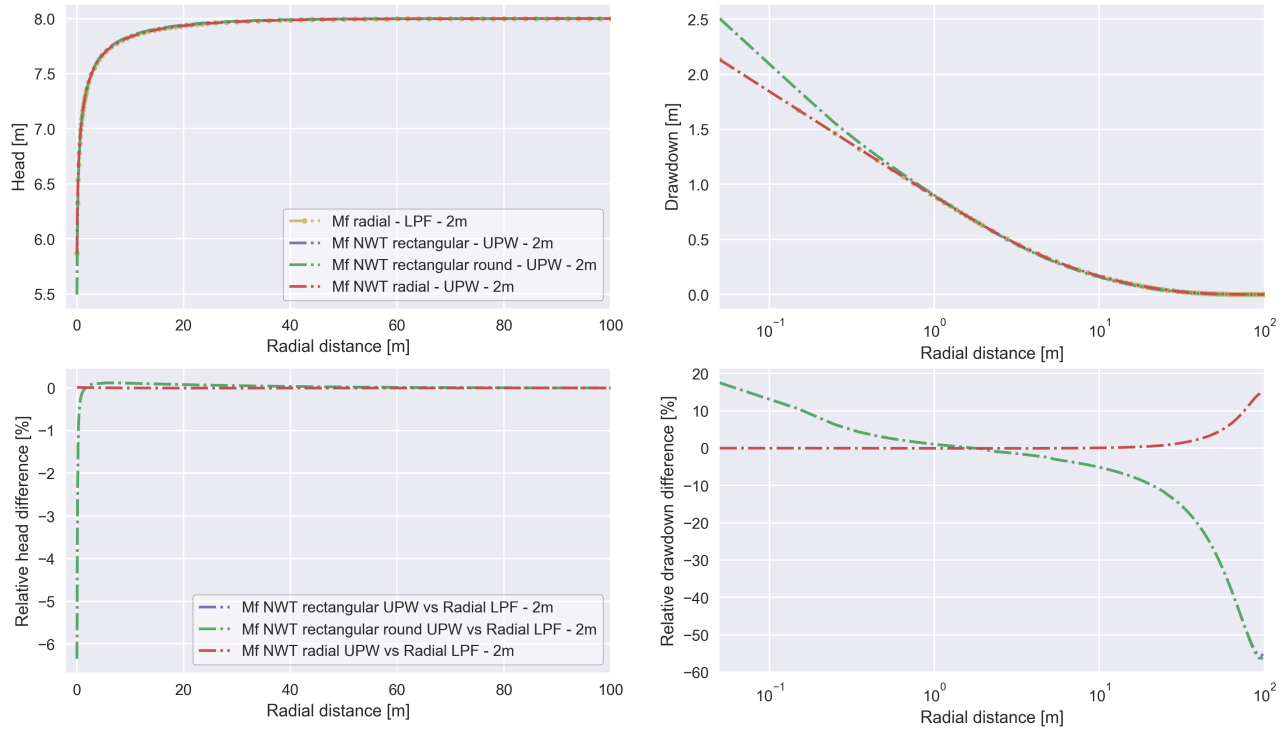
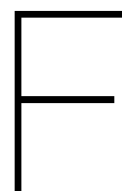


Figure E.10: Results test 3: Head after 1 day of pumping at 2.0 m (relative to aquifer bottom)



MODFLOW - Model definition

The computational modelling of the northern Ghana synthetic ASR system is in this research done by the use of a Modular Ground-Water Flow Model; MODFLOW. MODFLOW is a finite difference model environment for groundwater flow, developed and written by US Geological Survey (USGS). It is stated to be the international standard (most convenient) open source computer program for the simulation of groundwater flow. In MODFLOW it is possible to simulate a variety of aquifer features by the introduction of (free available) packages. In this research, input files (needed by MODFLOW) are created by the use of Python and the FloPy package ((Harbaugh, 2005; Niswonger et al., 2011)). The background definitions of the MODFLOW model (year-round ASR system simulation) are described in this Appendix.

F.1. Model design

The unmodified versions of MODFLOW uses Cartesian geometry. The simulations are standard performed in a (single or multi layer) rectangular grid model. These models can simulate the three-dimensional ASR-system performance accurately. However, it requires disadvantageous large computational power. In this particular case the single well simulation is approached axially symmetric. As prescribed by Langevin (2008), the rectangular model structure is radially scaled by the adjustment of several input parameter. The radial design is advantageous for the model precision and run times. A detailed description of radial scaling of a MODFLOW model can be found in Appendix E.

Due to the applied MODFLOW radial scaling the defined grid consist of a single row (1 m width) and multiple columns. The well is located in the (left) first cell (column 0, row 0). The width of the columns increases (grouped) stepwise, and is based on the (radial) distance between the specific column and the well. By the use of the cell sizes 0.0635 m (40x), 0.1 m (25x), 0.5 m (20x), 1.0 m (25x), 2.0 m (30x) and 5.0 m (10x) a total (radial) length of 150 m is simulated. An extent assumed to be sufficient for the purposes of this research (Appendix F.2). The vertical (third) dimension is added to the model by a total of 50 layers (thickness of 1.0 m each).

The one year model timespan is divided into an abundance of logarithmic time frames. Higher temporal resolutions is added to the moments at which fluctuation in head are expected. The design of four months infiltration contains a single logarithmic time frame of 200 steps. While, every single day in dry season (243 days) contains a 4 hour logarithmic time frame for pumping (8 steps) and a subsequent 20 hour logarithmic time frame for recovery (10 steps). This puts the year-round total number of model time steps on 4574.

F.1.1. MODFLOW-NWT

Due to the set initial model conditions and expected strong temporal variations in groundwater tables (GWT), cells may fall dry and become wet again over time. Model simulation is therefore performed through the use of MODFLOW-NWT: The Newton-Raphson formulation for the (more convenient) MODFLOW-2005 program. As stated by Niswonger et al. (2011), MODFLOW-NWT is intended for solving problems involving drying and re-wetting non-linearities of the unconfined groundwater-flow equation. MODFLOW-NWT

requires a combined use with the Upstream Weighting (UPW) package for calculation conductances between cells (instead of the BCF, LPF or HUF packages, applicable in combination with MODFLOW-2005). The UPW package keeps dry cells active, while water outflow of the cell is not allowed. Moreover, if applicable inflow to a dry cell automatically flows further down to the adjacent (non-dry) cell in the layer below (Niswonger et al., 2011). In correspondence with the use of MODFLOW-NWT the (own) NWT solver is used for model simulation (instead of the more convenient PCG solver).

F.1.2. General Head Boundary package (GHB)

The simulated wet season infiltration due to flooding is included the model design by the use of the General Head Boundary (GHB) package. For as long as the wet season (stress periods), GHB cells are specified through stress period data. The General Head Boundaries are added to the well cells (row 0, column 0) in the predefined layers of penetration (layer 20-46). The GHB stress period data requires an additional definition of stage and cond (conductance) (Harbaugh et al., 2000). The stage equals the constant flood inundation level ($h^* = 2$ m). For the purposes of this research conductances are aligned with the CWC (Cell-to-Well hydraulic conductance). More information on the CWC can be found in Section F.1.3.

F.1.3. Revised Multi-Node Well package (MNW2)

The synthetic ASR system consists of a well which is partially penetrating a single aquifer. And the MODFLOW model depth (including aquifer) is defined by multiple (50) model layers. A model set-up causing the convenient MODFLOW Well package to be insufficient. For a solid simulation the more extended Multi-Node-Well2 (MNW2) package is used. The MNW2 well houses several additional options (e.g. bounded drawdown, addition of well skin resistances and pump related adjustments in discharge). Thence, the definition of an abundant list of parameters is required (within the node data and the stress period data) (Konikow et al., 2009). Several parameters are by default correct, some however need a specification. The well penetration interval (screen) is recorded by the definition of z_{top} (-20 m) and z_{botm} (-47 m). The MNW2 well assigns the screen to the model nodes (the well cells in the corresponding layers). The in-well GWT preferable does not drop below the elevation of -20 m, a desire guaranteed by the definition of H_{lim} . The flag of a q_{limit} that equals 1 activates the defined H_{lim} . The moments (stress-periods) of pump operation are set by an ITMP flag that equals 1. At the contrary, the ITMP is set to 0 at all other moments (stress-periods) to simulate pump inactivity. Furthermore, the MNW2 well requires the input of a desired discharge (q_{des}) and a specification of Cell-to-Well hydraulic conductance (CWC), topics highlighted below.

Desired discharge (q_{des})

Based on a predefined desired discharge, the MNW2 well determines a model layer dependent discharge iteratively. As long as the head bound (H_{lim}) is not restrictive, the summed layer discharges equal (approximately) the desired discharge. In the context of this research, the predefined desired discharges are based on the criteria of sustainable system use. The dry season (total) discharge volume should not exceed the wet season (total) recharge volume. The desired discharge (q_{des}) is defined in such a way, that this condition is always met.

The Python FloPy package is used for the reading of the MODFLOW binary output files. The results of the year-round simulated recharges and discharges are obtained by reading the `binaryfile.CellBudgetFile`.

Cell-to-Well hydraulic conductance (CWC)

Due to the MNW2 well package application, a deviation between the head in the well and the head in the model (well)cell is present. Multiple model elements contribute to the head difference. The total head difference is dependent on the expression of the Cell-to-Well hydraulic conductance (CWC), presented in Equation F.1 (Konikow et al., 2009).

$$CWC_n = [A + B + CQ_n^{(P-1)}]^{-1} \quad (F.1)$$

Where CWC_n (m^2/d) is the n^{th} Cell-to-Well hydraulic conductance, A is the linear aquifer-loss coefficient resulting from the well having a smaller radius than the horizontal dimensions of the cell in which the well is located, B is the linear well-loss coefficient accounting for head losses that occur adjacent to and within

the borehole and well screen (skin effects) and $CQ_n^{(P)}$ accounts for non-linear head losses due to turbulent flow near the well (Konikow et al., 2009). The derivation of these CWC components can be carried out by means of the Equations F.2 - F.4:

$$A = \frac{\ln(r_o/r_w)}{2\pi b\sqrt{K_x K_y}} \quad (\text{F.2})$$

$$r_o = 0.14\sqrt{\Delta x^2 + \Delta y^2} \quad (\text{F.3})$$

$$B = \frac{SKIN}{2\pi b\sqrt{K_x K_y}} \quad (\text{F.4})$$

$$SKIN = \left(\frac{bK_h}{b_w K_{SKIN}} - 1\right) \ln\left(\frac{r_{skin}}{r_w}\right) \quad (\text{F.5})$$

Where r_o (m) is the effective external radius of a rectangular finite-difference cell for isotropic porous media, r_w (m) is the well radius, r_{skin} (m) is the well radius plus the thickness of improved soil around the well, b (m) is the saturated thickness of the cell(layer), b_w (m) is the saturated (active) length of the borehole in the cell(layer) (in the purposes of this research equal to b (1 m)), K_h (m/d) is the horizontal (non-radial scaled) hydraulic conductivity (equals K_x and K_y due to the assumption of horizontal anisotropy), Δx (m) is the grid spacing in the x-(column-)direction and Δy (m) is the grid spacing in the y-(row-)direction (Konikow et al., 2009).

As stated, the aquifer-loss coefficient (A) accounts for the difference in dimensions between the well (cross-section) and the (well)cell. A difference perfectly understandable in the case of an unmodified (Cartesian geometry) rectangular grid MODFLOW model. However, this research simulation is performed in a radial scaled MODFLOW model. According to the principles as stated by Langevin (2008), the well cell width perfectly aligns the radius of the well. Therefore, the A-term can perhaps be ignored. But the precise interpretation of the term is in this manner no longer known. The same applied for the implementation of the $CQ_n^{(P)}$ term. Further research should be done on the implementation of the MNW2 Cell-to-Well hydraulic conductance in combination with a radial scaled MODFLOW model. In this research the CWC values are specified manually. The applied conductances are calculated by the Equations 3.1 - 3.4 (Section 3.1.2).

F.2. Model extent - Leakage factor (λ)

The leakage factor, or characteristic length, is a measure that represents the degree of groundwater flow interaction between an aquifer and an aquitard (Kruseman and de Ridder, 2000). The extent of the synthetic MODFLOW model is in this research based on the double layer leakage factor. The analytical solution for the double (aquifer) layer leakage factor (λ) is presented in equation F.6 (Bruggeman, 1999; Fitts, 2012).

$$\lambda = \sqrt{\frac{c * T_0 * T_1}{T_0 + T_1}} \quad (\text{F.6})$$

where λ is the leakage factor (m), c (d) is the resistance of the leaky layer (aquitard) between aquifer one and two and T_0 and T_1 are the transmissivities of respectively aquifer one and two.

The optimal geohydrological parameter values (T_0 , T_1 and c) determined in the aquifer test data analysis are used as input. More precisely, it concerns the parameter values obtained by the TTim Fmin optimization function in combination with the theoretical model defined by; a double layer system and a system with a double layer and partial penetration of the well. In TTim Model3D, the soil stratification is not characterized by a regular sequence of alternately aquifers and leaky layers; TTim Model3D houses an accumulation of aquifers. The resistance (c) of the fictive leaky layer is computed from the middle of first layer to the middle of the second layer (Bakker, 2013a,b). For the determination of the leakage factor a vertical anisotropy of

0.25 (-) is assumed. An overview of the obtained leakage factors (λ) can be found in Table F.1.

Table F.1: An overview of the obtained leakage factors (λ) (m)

	Bingo		Nyong Nayili		Janga (1/2)		Janga (2/2)		Ziong	
	2 layer	2 layer pp	2 layer	2 layer pp	2 layer	2 layer pp	2 layer	2 layer pp	2 layer	2 layer pp
a	31.11	31.11	33.94	33.94	51.51	17.01	51.95	20.10	35.25	32.31
b	31.27	31.11	36.77	33.96	52.33	34.56	52.33	17.01	35.27	31.82
c	31.38	31.25	35.32	36.77	52.33	51.15	52.33	38.37	32.29	31.56
d	31.21	31.20	33.94	36.77	52.33	52.33	27.97	49.54	34.42	32.13

A MODFLOW radial model extent of 3 to 4 times the leakage factor (characteristic length) is desirable. In correspondence with this approach, it can be expected that 95-99% of the actual water flow is taken into account by the model. Moreover, the head at the model tail is by approximation no longer affected by the (centrally positioned) well performance. The assumption of a constant head at the model tail becomes valid (Bot, 2016; Fitts, 2012). The obtained leakage factors are generally in close range of the, 36.74 m, average leakage factor (Table F.1). To comply with the above mentioned requirement, a total radial extent of 150 m is implemented in the MODFLOW model.

G

MODFLOW - TTim model validation

The synthetic ASR system simulations are performed by the use of MODFLOW (finite difference environment). The results obtained by the MODFLOW simulations are validated by the use of analytic element modelling environment of TTim. A comparable synthetic ASR system model is defined in TTim. The validation solely examines the results of the total inflow volumes. Except from the 'Extension of daily pumping time' (not applicable on wet season inflow) all types of ASR system improvements and sensitivities are included. The comparison is only performed for the wet season total inflow results of soil scenario 3.

The simulation results of the different model environments are presented in the Figures G.1 - G.5. Small (MODFLOW-TTim) deviation are present in absolute water infiltration quantities. But more importantly, in all simulated types of ASR system improvements and sensitivities the performance is qualitatively comparable. Herewith, the overall research results are more trustworthy.

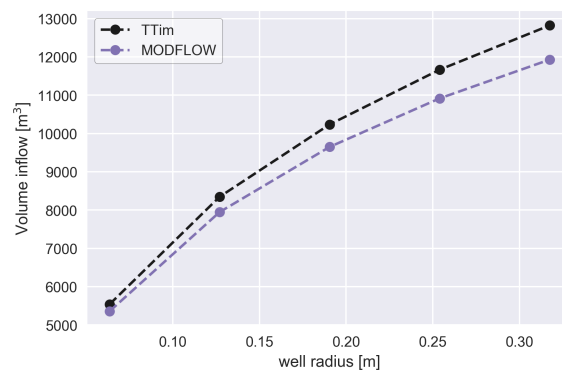


Figure G.1: TTim validation of the ASR system MODFLOW model infiltration results for soil scenario 3 - Enlargement well diameter

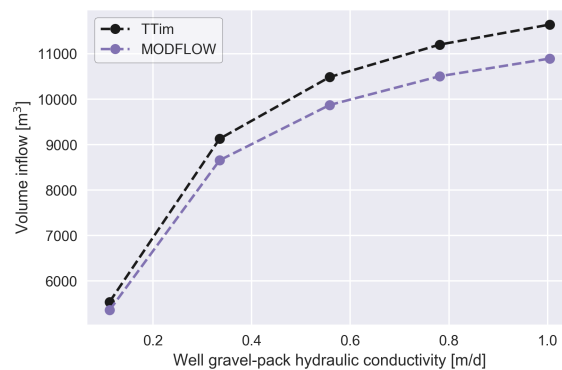


Figure G.2: TTim validation of the ASR system MODFLOW model infiltration results for soil scenario 3 - Reduction well skin resistance

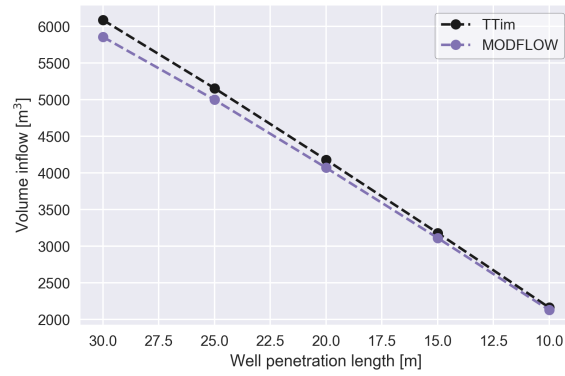


Figure G.3: TTim validation of the ASR system MODFLOW model infiltration results for soil scenario 3 - Degradation well depth by clogging

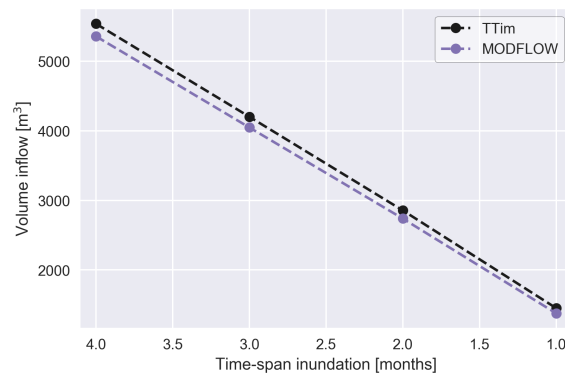


Figure G.4: TTim validation of the ASR system MODFLOW model infiltration results for soil scenario 3 - Shortening the wet season inundation time

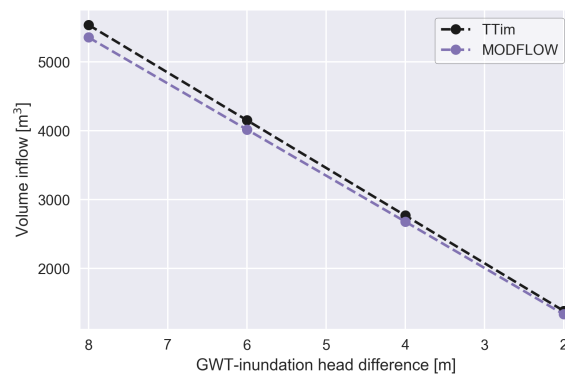
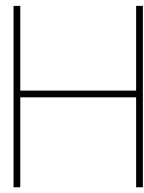


Figure G.5: TTim validation of the ASR system MODFLOW model infiltration results for soil scenario 3 - Reduction wet season inundation level



Additional model results

H.1. ASR system base model performance

Figure H.1 illustrates the precise impact of flood based ASR-system infiltration on soil scenario 3 groundwater heads in several representative (model) layers. It is worth-mentioning that the groundwater level increase is already limited at relative short radial distance (60 - 80 m) (steep groundwater cone).

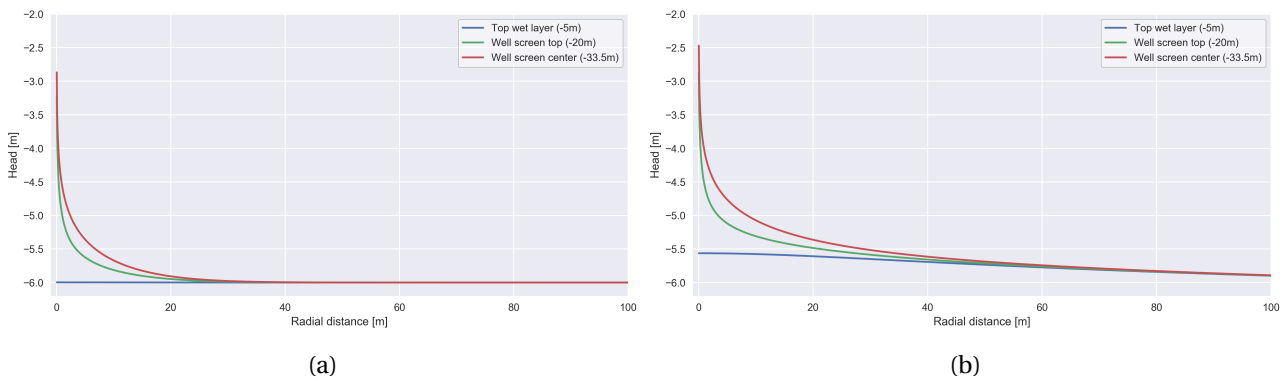


Figure H.1: Base ASR system model infiltration performance for soil scenario 3 - Head in representative layers after (a) five days and (b) 122 days of infiltration

Figure H.2 presents the precise impact of discharge on soil scenario 3 groundwater heads in several representative (model) layers. After the first day of pumping the transition from wet (recharge) to dry season (discharge) is still of influence. Most definitely in the higher model layers (close to surface) the increased heads (Above initial GWT of -6 m) remain active for some time. Towards the end of dry season this impact is no longer present.

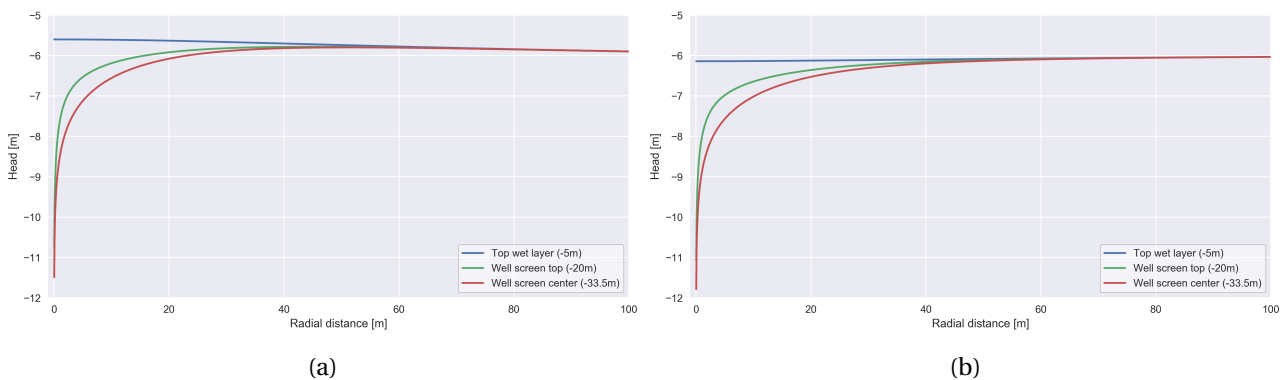


Figure H.2: Base ASR system model extraction performance for soil scenario 3 - Head in representative layers after four hours of pumping on (a) the first day (day 123) and (b) the last day (day 365) of dry season

H.2. ASR system improvements

The Figures H.3 - H.5 present the relative recharge, discharge and recovery ratio results for the three types of ASR system improvements. Instead of the original results (Chapter 3.3), the outcomes are relative to the base model ASR system performance. As a consequence, all graphs start (left) at the dimensionless value one. The figures emphasize on the impact magnitude of the system improvements.

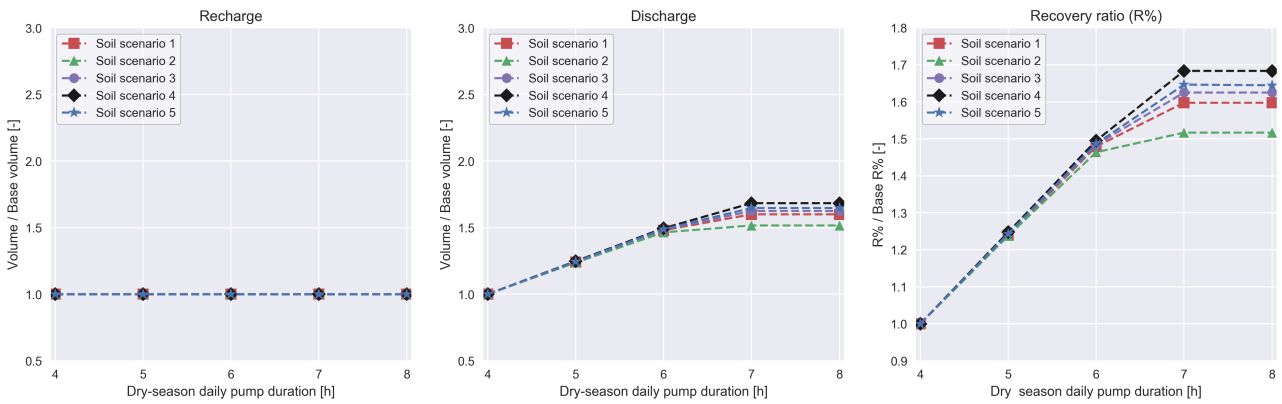


Figure H.3: Results of the ASR system year-round performance (total inflow, outflow and recovery ratio) by the extension of the daily pumping time - relative to the base ASR system

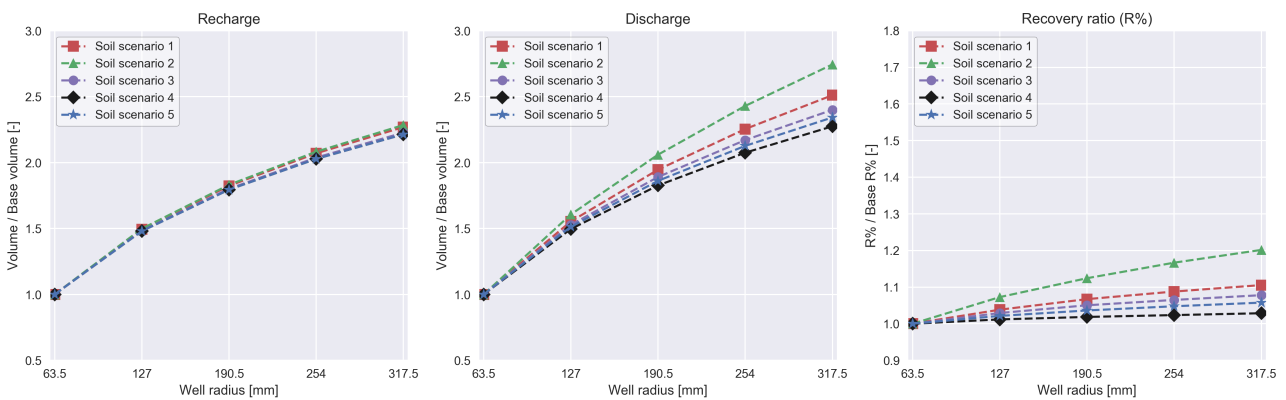


Figure H.4: Results of the ASR system year-round performance (total inflow, outflow and recovery ratio) by the enlargement of the well diameter - relative to the base ASR system

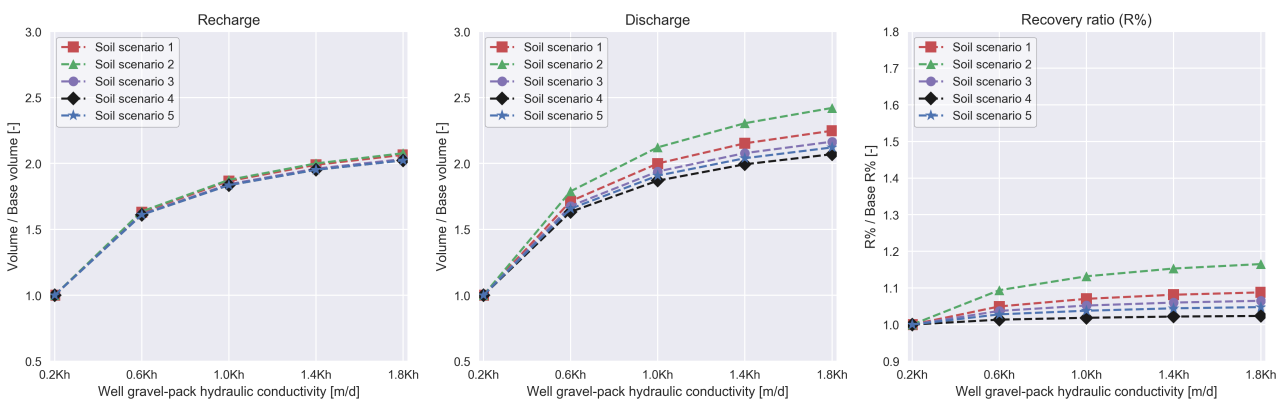


Figure H.5: Results of the ASR system year-round performance (total inflow, outflow and recovery ratio) by the reduction of the well skin resistance - relative to the base ASR system

Note, in these figures the dimensionless recovery ratios above one do not represent unsustainable system use. The recovery ratios are also values relative to the base model performance.

H.3. ASR system sensitivity

The Figures H.6 - H.8 present the relative recharge, discharge and recovery ratio results for the three types of ASR system improvements. Instead of the original results (Chapter 3.4), the outcomes are relative to the base model ASR system performance. As a consequence, all graphs start (left) at the dimensionless value one. The figures emphasize on the impact magnitude of the system sensitivities.

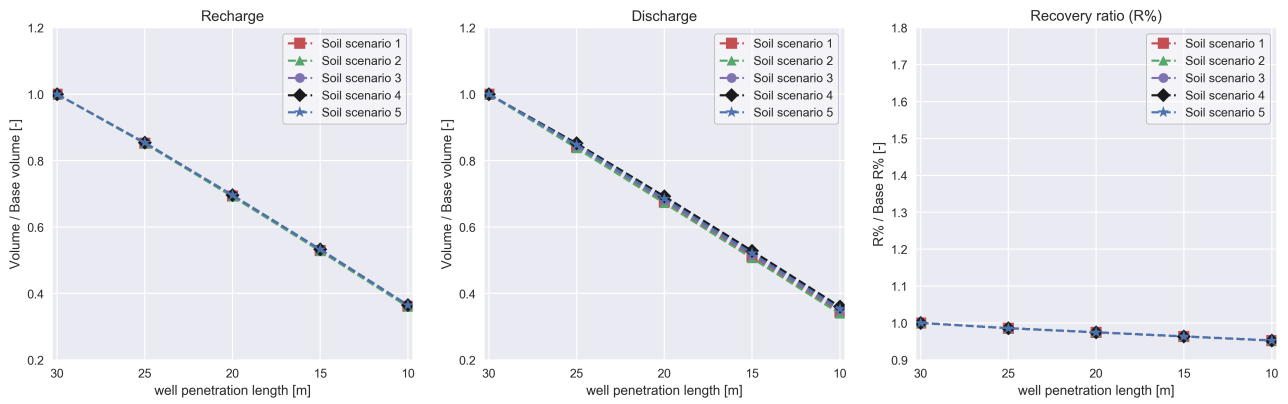


Figure H.6: Results of the ASR system year-round performance (total inflow, outflow and recovery ratio) by the degradation of the well depth - relative to the base ASR system

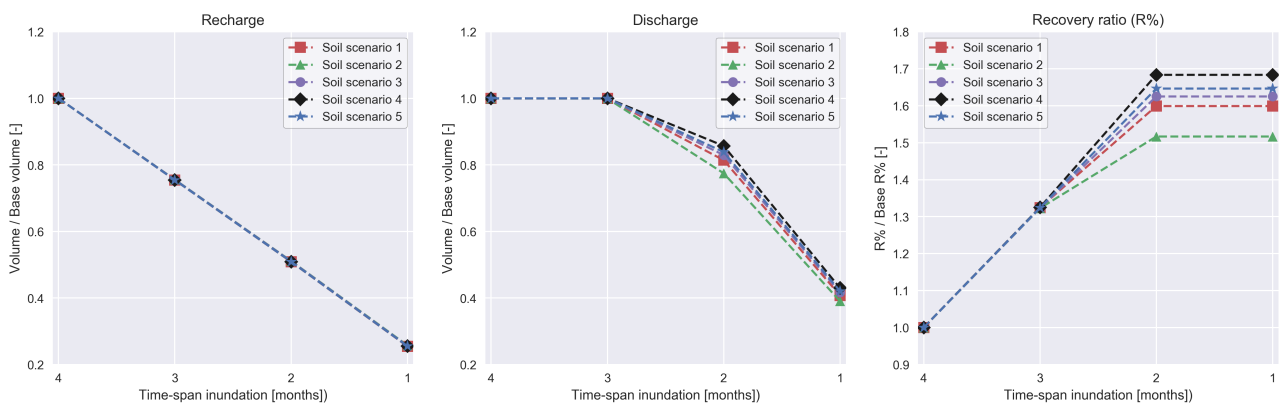


Figure H.7: Results of the ASR system year-round performance (total inflow, outflow and recovery ratio) while shortening the wet season inundation time - relative to the base ASR system

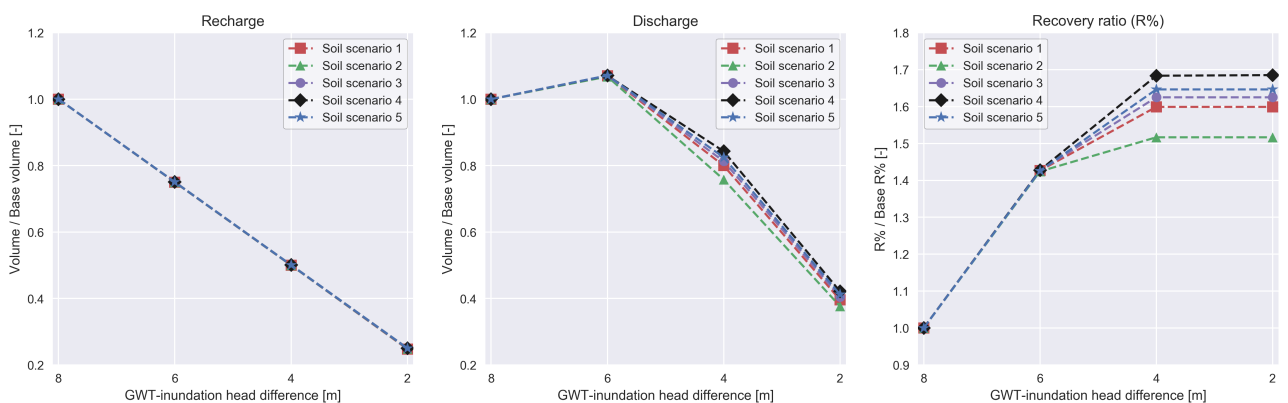


Figure H.8: Results of the ASR system year-round performance (total inflow, outflow and recovery ratio) by the reduction of the wet season inundation level - relative to the base ASR system

Note, in these figures the dimensionless recovery ratios above one do not represent unsustainable system use. The recovery ratios are also values relative to the base model performance.

H.3.1. Degradation of well depth by clogging

The Tables H.1 and H.2 give insight in the slightly non-linear performance in relation to the reduction in well-screen length (borehole clogging). The absolute total inflow and outflow volumes are increasingly negatively affected by a further reduction of the well screen length. In this case soil scenario 3 is used as an example. The ASR system performance is (relatively) comparable for the other soil scenarios.

Table H.1: The ASR system screen average specific recharge and discharge volumes (m^3/m) for soil scenario 3 - when the well depth decreases

Screen length (m)	30	25	20	15	10
Average specific recharge volume (m^3/m)	195.23	199.98	203.57	207.58	212.96
Average specific discharge volume (m^3/m)	121.03	122.67	123.65	124.89	126.85

Table H.2: The ASR system total recharge and discharge volumes specific reduction (m^3/m) for soil scenario 3 - when the well depth decreases

Reduction screen length (m)	5	10	15	20
Total recharge volume specific reduction (m^3/m)	171.47	178.54	182.87	186.36
Total discharge volume specific reduction (m^3/m)	112.84	115.78	117.17	118.12

Figure H.9 shows the precise distribution of the soil scenario 3 recharge volumes over the varying well-screen length. The figure is added to the report to improve the understanding of the infiltration performance of a well that is partially penetrating the aquifer.

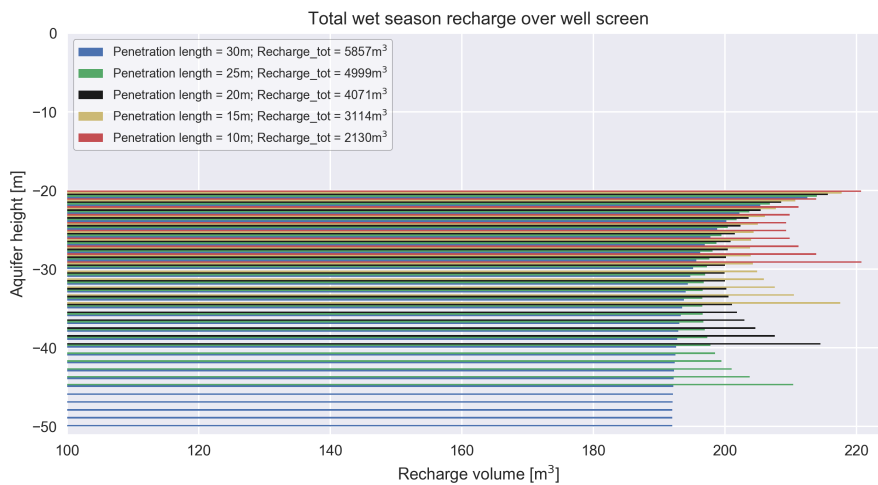


Figure H.9: The ASR system total recharge volume by model layers (1m) for soil scenario 3 - when the well depth decreases

H.3.2. Shortening wet season inundation time

Figure H.10 presents the soil scenario 3 discharge development over time, ranging from 4 months of inundation till 1 month. The base ASR system model performance (4 months of inundation) is visualized by the black line. The figure is an addition to the content of the report Sections 3.2.1 and 3.4.2.

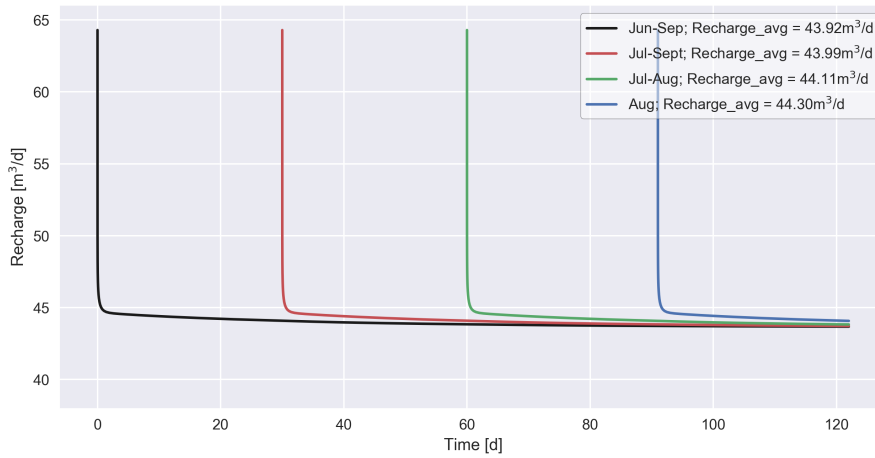


Figure H.10: The ASR system recharge rates over time for soil scenario 3 - while shortening the wet season inundation time

H.3.3. Reduction wet season inundation level

Figure H.11 presents the soil scenario 3 discharge development over time, while the wet season inundation level is reduced. The base ASR system model performance ($\Delta h = 8m$) is visualized by the black line. The figure is an addition to the content of the report Sections 3.2.1 and 3.4.3.

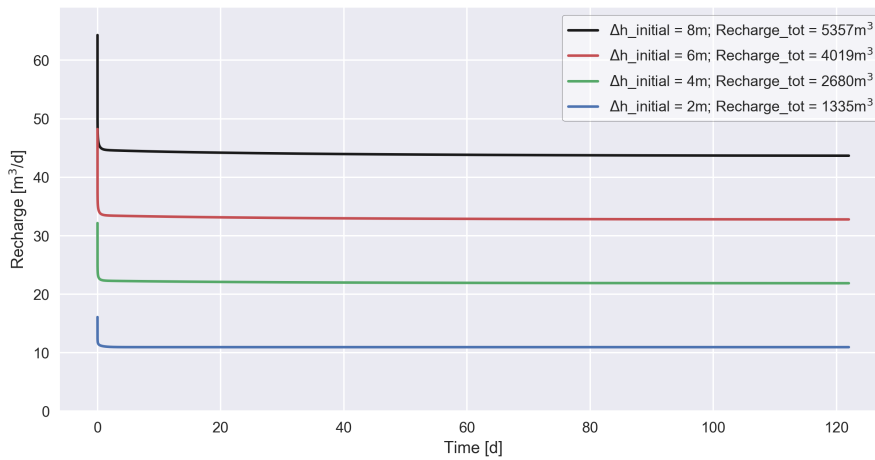


Figure H.11: The ASR system recharge rates over time for soil scenario 3 - while reducing the wet season inundation level

H.4. Business case

Figure H.12 presents an overview of the ‘actual’ net financial returns of a northern Ghana ASR system, for each soil scenario and for each type of system improvement. The results are solely based on the components considered in the business case. The financial returns equal the summed tomato and groundnut yields minus the ‘actual’ operational costs. For these ‘actual’ costs the discharge dependent pump efficiencies of the Pedrollo 4" submersible pump are applied.

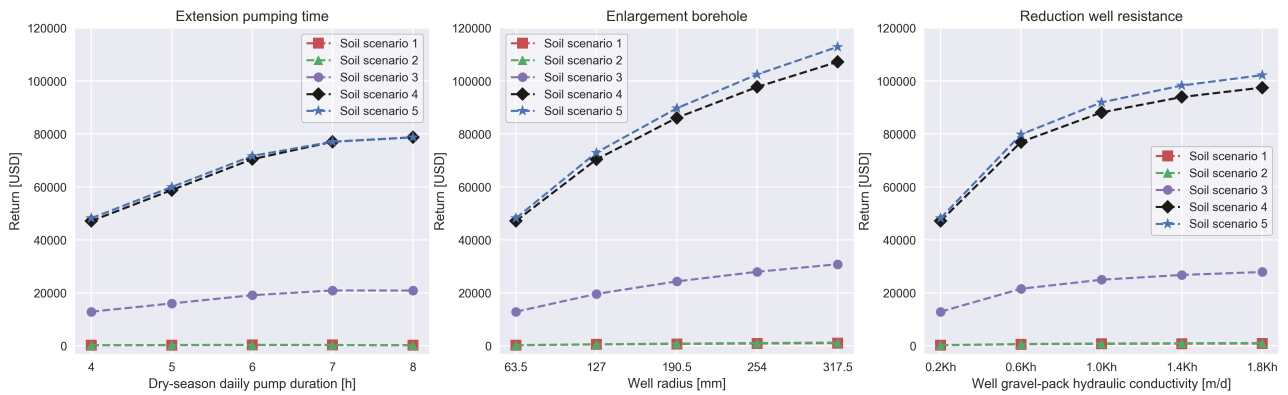


Figure H.12: The ASR system year-round net financial returns for the explored three types of system improvement

Figure H.13 presents an overview of the potential net financial returns of a northern Ghana ASR system, for each soil scenario and for each type of system improvement. The results are solely based on the components considered in the business case. The financial returns equal the summed tomato and groundnut yields minus the (more) optimal operational costs. For these (more) optimal costs a constant maximum pump efficiency of 58% is applied (based on Pedrollo 4" submersible pump).

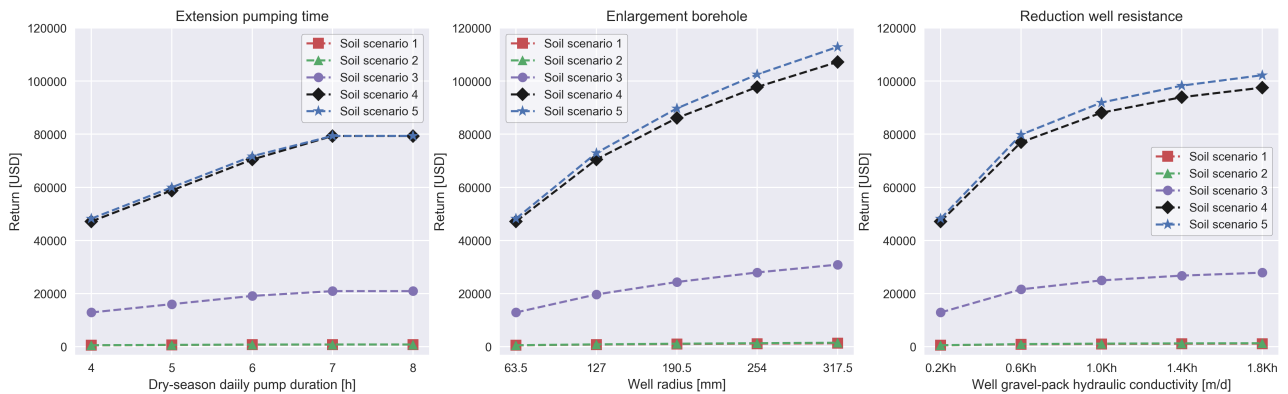


Figure H.13: The ASR system year-round net financial returns for the explored three types of system improvement - while maximum pump efficiency (58%) considered



Pedrollo 4" submersible pump - product specifications

The Pedrollo 4" (4SR4/18) submersible pump serves multiple purposes in this research. During the aquifer tests, the pump is used for the withdrawal of groundwater (Chapter 2). The same pump , i.e. its specifications, is applied to derive the pump energy consumptions and costs of an operational ASR system in northern Ghana. The pump capacities and (optimal) efficiencies are taken into account (Chapter 4). In this report section, the specifications of the Pedrollo 4" submersible pump are presented in detail.

4SR

4" submersible pumps

-  Clean water
(Maximum sand content 150 g/m³)
-  Domestic use
-  Civil use
-  Industrial use



PERFORMANCE RANGE

- Flow rate up to **340 l/min** (20.4 m³/h)
- Head up to **405 m**

APPLICATION LIMITS

- Maximum liquid temperature **+35 °C**
- Maximum sand content **150 g/m³**
- **100 m** immersion limit
- Installation:
 - vertical
 - horizontal, with the following limits:
 - 4SR1 - 4SR1.5 - 4SR2 - 4SR4 up to **27 stages**
 - 4SR6 - 4SR8 up to **17 stages**
 - 4SR10 - 4SR12 - 4SR15 up to **12 stages**
- Starts/hour: **20** at regular intervals
- Minimum flow rate for motor cooling **8 cm/s**
- Continuous service **S1**

CONSTRUCTION AND SAFETY STANDARDS

ELECTRIC MOTOR

- Single-phase 230 V - 50 Hz
- Three-phase 400 V - 50 Hz

Length of power cable:

- for P₂ from 0.37 to 3 kW: **1.7 m** 4SR-PD, **2.0 m** 4SR-PS
- for P₂ from 4 to 7.5 kW: **2.7 m** 4SR-PD, **3.0 m** 4SR-PS

➔ The **4SR-PD** and **4SR-PS** single-phase versions supplied with a capacitor included in the packaging.

EN 60335-1
IEC 60335-1
CEI 61-150

EN 60034-1
IEC 60034-1
CEI 2-3



EU REGULATION N. 547/2012

CERTIFICATIONS

Company with management system certified DNV
ISO 9001: QUALITY
ISO 14001: ENVIRONMENT



INSTALLATION AND USE

Suitable for use with clean water with a sand content of no more than **150 g/m³**. Because of their high efficiency and reliability, they are suitable for use in domestic, civil and industrial applications such as for the distribution of water in combination with pressure tanks, for irrigation, for washing plants and for pressure boosting in fire-fighting sets, etc.

PATENTS - TRADE MARKS - MODELS

- Patent n. EP2419642

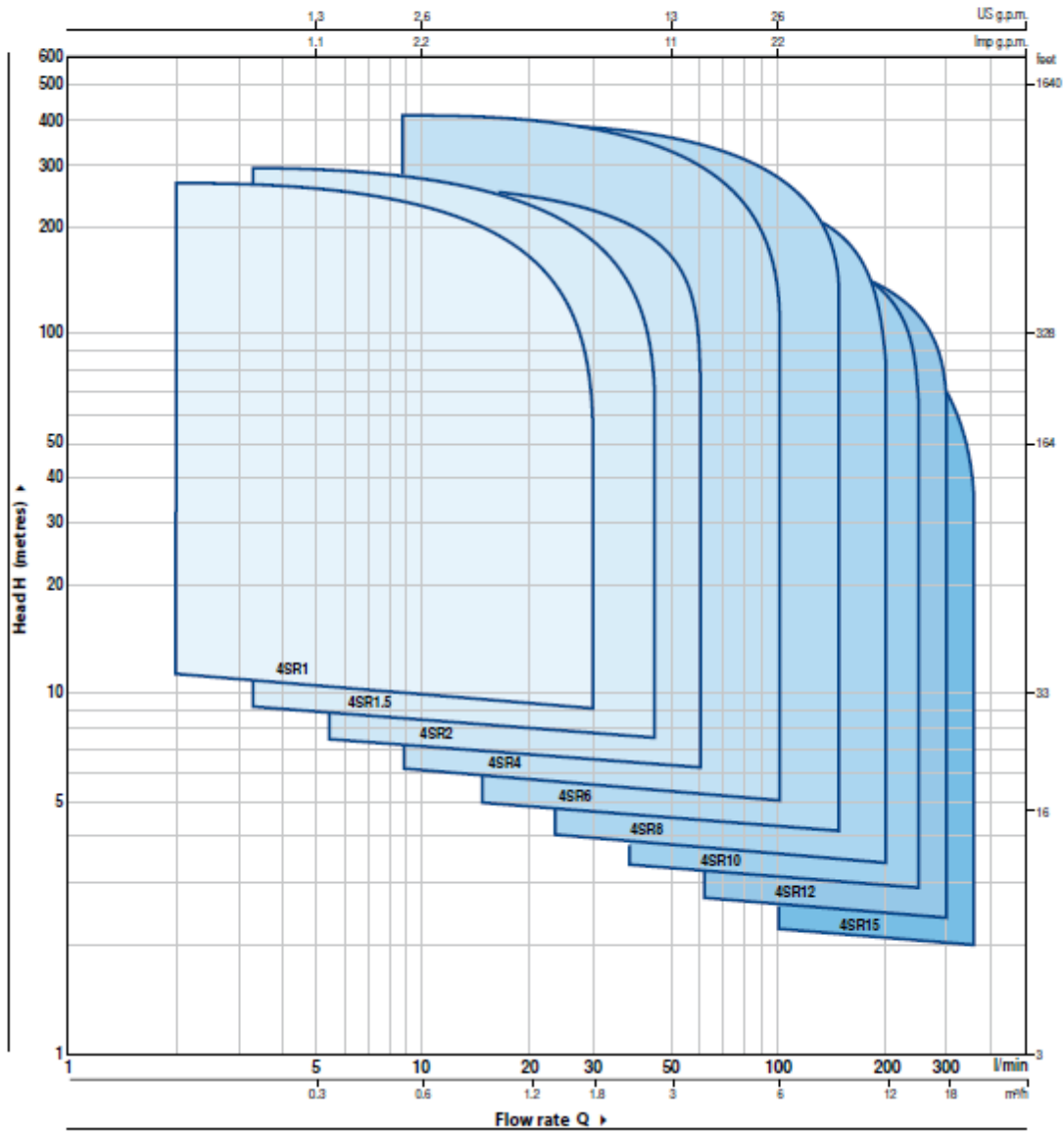
OPTIONS AVAILABLE ON REQUEST

- Other voltages or 60 Hz frequency
- **Kit of cooling jacket complete with filter and supports**



PERFORMANCE RANGE

50 Hz n= 2900 rpm



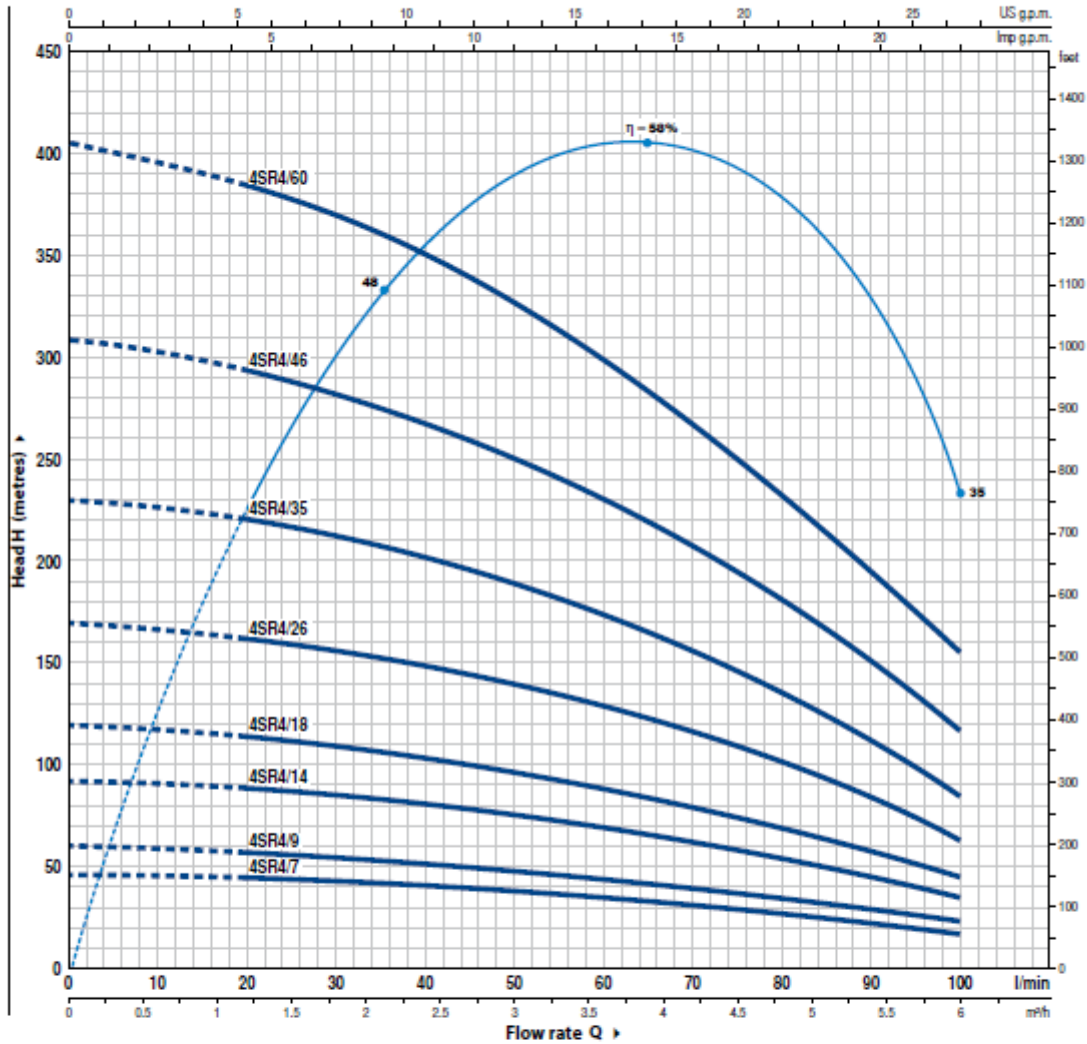
NOMENCLATURE

4 SR 1 m / 13 - PD or PS or HYD

- Borehole diameter in inches _____
- Series _____
- Flow rate in m³/h at the point of highest efficiency _____
- Single-phase motor _____
- Number of stages _____
- PD: pump with "4PD PEDROLLO" motor _____
- PS: pump with "4PS PEDROLLO" motor _____
- HYD: pump without motor _____

CHARACTERISTIC CURVES AND PERFORMANCE DATA

50 Hz n= 2900 rpm



MODEL		POWER (P ₂)		Q	H metres											
Single-phase	Three-phase	kW	HP		m ³ /h	0	1.2	1.8	2.4	3.0	3.6	4.2	4.8	5.4	6.0	
				l/min	0	20	30	40	50	60	70	80	90	100		
4SR4m/7	4SR4/7	0.55	0.75	H metres	46	44	42	40	38	35	32	28	23	17		
4SR4m/9	4SR4/9	0.75	1		60	56	55	52	49	45	40	35	29	23		
4SR4m/14	4SR4/14	1.1	1.5		92	88	85	81	76	70	63	55	45	35		
4SR4m/18	4SR4/18	1.5	2		120	112	109	104	98	90	81	70	58	45		
4SR4m/26	4SR4/26	2.2	3		170	162	157	150	141	130	116	101	84	63		
-	4SR4/35	3	4		230	220	211	202	190	175	157	137	113	85		
-	4SR4/46	4	5.5		308	293	280	269	249	230	205	181	151	117		
-	4SR4/60	5.5	7.5		405	385	370	350	325	300	270	235	195	155		

Q = Flow rate H = Total manometric head

Tolerance of characteristic curves in compliance with EN ISO 9906 Grade 3B.

